The People's Democratic Republic of Algeria
Ministry of Higher Education and Scientific Research
University of Ibn Khadloun-Tiaret, 2018
Faculty of Material sciences

A Dissertation
Submitted in Partial Fulfillment of the Requirements for the
LMD doctorate.

The Study and modeling of nanoparticles' interactions

"influence of physical, morphological, structural, textural and environment properties"

applications to nanotechnology and environmental nanotoxicology

Presented by

DJAFRI YOUCEF

Under the supervision of:
Dr. TURKI Djamel

Members of the jury:

President	M. BELARBI El-Habib	Professor	University of Tiaret
	M. BAGHDAD Rachid	Professor	University of Tiaret
Examiner	M. YANALLAH Khelifa	Professor	University of Tiaret
	M. KHARROUBI Mohamed	Professor	University of Djelfa
supervisor	M. TURKI Djamel	MCA	University of Tiaret

University of Ibn Khaldoun- Tiaret Algeria
2018/2019

To all those who made this possible

AKNOWLEDGEMENTS

Abstract

In the current work, dispersion interactions between nanoparticles and the effects different parameters (size, Geometry, interparticle distance, retardation and many body forces) were investigated. The effect of particles' geometry is studied by comparing three basic shapes: cubic, cylindrical and spherical. The results show that effect of geometry is significant for interparticle distances less than 20% of particles radius. The retarded van der Waals interaction energy is also investigated, and it was shown that this effect is highly dependent on particle' size and shape as well as the distance. A modified model is proposed for extremally small nanoparticles ($R \sim 10$ nm). We used the coupled dipole method and then from the Trace formulism of this model we introduce a new algebraic formula of the interaction energy between identical nanoclusters. Furthermore, A novel representation using graph theory is also used to represent each mode of interaction derived from the new formulism. These graphs were used to derive the formula for m-body interaction energy in a form of a series which was proven to be equivalent to the results developed from more complicated methods such as perturbation theory in quantum mechanics. We also have studied the interaction between two chains of atoms, with two geometrical configurations parallel and colinear. When our result is compared to that which was calculated from the pairwise summation method, we find that many body interactions have a significant effect on the overall interaction.

Keywords: Dispersion interactions; van der Waals forces; many-body forces; Coupled Dipole Method; Nanoparticles**.**

Contents

Liste of table

List of figures

CHAPTER 4

List of symbols

Symbol	Units	Physical Quantity
A_H	(J)	Hamaker constant
$\alpha(i\omega)$	(C m^{2}V^{-1})	Dynamic polarizability
$\alpha/\alpha(0)$	(C m^{2}V^{-1})	Static polarizability
c	m/s	speed of light
d	(m)	The shortest distance between macroscopic objects
e	(C)	charge of the electron
E_{ind}	(J)	Induction interaction "Debye interaction" energy
E_{disp}	(J)	Dispersion "London" energy
E_0^A / E_0^B	(J)	Ground state energies of particles A and B
E_m^A / E_n^B	(J)	Energies of the excited states of particles A and B
ε_i	(F/m)	Permittivity of the medium "i"
ε_0	(F/m)	Permittivity of free space
F_e	(N)	Electrostatic force between particles
F_c	(N)	Capillary force
Γ	//	Gamma function
γ	(N/m)	Surface tension
H	//	The Hamiltonian operator
H_0	//	The Hamiltonian of the unperturbed state.
$\hbar$	(J·s)	The reduced Planck constant

h	(J·s)	Planck constant
I	//	Identity matrix
k_B	(J/K)	Boltzmann constant
λ	(m)	Characteristic wavelength
m_e	(Kg)	Mass of the electron
M	(Kg)	Mass of the nucleus
n_i	//	Refractive index
ω	(Hz)	Characteristic frequency
ω_M	(Hz)	Characteristic microwave absorption frequency
ω_I	(Hz)	Characteristic infrared absorption frequency
ω_U	(Hz)	Characteristic ultraviolet absorption frequency
ω_0	(Hz)	Characteristic frequency of the ground state.
P	(Pa)	Liquid pressure
p	//	Particles momentum operator
ψ_s^A / ψ_r^B	//	The wave functions of the excited individual particles A and B.
ψ_0^A / ψ_0^B	//	Ground state wave functions of particles A and B
q	(C)	Particle's Charge
R	(m)	Particle's radius
R_G	(J / mol. K)	the ideal gas constant
r_{ij}	(m)	the distance between particles i and j
r_m	(m)	The radius of the meniscus in liquid bridges

ρ	(Molecule/m^3)	the number density of the molecules (number per cubic meter)
T	(K)	The absolute temperature
T_{ij}	//	The static dipole-dipole interaction tensor
V	(m^3)	Volume
V(A,B)	//	The electrostatic interaction potential between particles A and B.

INTRODUCTION

One of the most promising aspects of modern material sciences and applied physics is that which involves the study of nanosystems that exhibit unique properties and surprising interdisciplinary applications. Nanoparticles been a simple nanosized material is similarly under the focus of many researchers for various fields, and their applications and presence in our daily lives is inevitable, whether as part of the products which we use or as hazardous unfortunate biproduct of natural phenomena or technological machinery. Therefore, and inspired by these facts, it is highly recognised in the scientific community that there is an urging need to study and understand the dynamics and interactions between nanoparticles and their environment, that is for the aim of better controlling and predicting how these interactions effect their behaviour.

Thus, the first chapter of this dissertation would be dedicated for setting up a prospect on nanoparticles and their different aspects starting from their origins and their applications and their toxicological aspects, where we recognise that these aspects are all influenced by the interactions which take place between particles themselves and between them and the environment. These interactions are defined and classified in the end of this chapter. Since the only interaction mode which is considered in our work is dispersion or van der Waals forces, the second one is a theoretical study of dispersion interaction between molecules thus understanding the origins and different aspects of these forces which are the focus of our work.

The third chapter is a study of these interactions between macroscopic bodies where we survey the existing modelling approaches, then use the simplest of those which is the pairwise summation approach to study the effect of geometry of particles on the intensity of these interactions, and study how the retardation effect is influenced by the different geometrical aspects of nano-particulate materials. And in the last chapter we start from the coupled dipole method and further continue with simple algebraic manipulations in order to develop a model that can help us to study many-body interactions individually and we also attempt to propose an innovative coupling between this physical model and the concepts of graph theory and develop a representation that can be used for both understanding the many-body interactions and calculating them, and study the many body forces for an example of linear chains using the developed model. And thus, complete this modest work with an intention of creating an elegant and meaningful work. We should also emphasise that this work -being a simple effort- presents an initiation to the subject on which other researches shall take place in the future.

CHAPTER 1

Introduction to nanoparticles and nanoparticulate materials

> *"What we have to discover is that there is no safety, that seeking is painful, and that when we imagine that we have found it, we don't like it."*
>
> **Alan Wilson Watts,** *The Wisdom of Insecurity: A Message for an Age of Anxiety.*

1. Definition of nanomaterials:

Nowadays, Nanomaterials is a highly recognized term which is defined by The International Organisation for Standardisation as a 'material with any external dimensions in the nanoscale or having internal structure or surface structure in the nanoscale'. The term 'nanoscale' is defined as the size that ranges approximately from 1 nm to 100 nm (**Fig.1.1**) [1-3]. And the European Commission (EC) in 2011 defined it as "a natural, incidental or manufactured material containing particles, in an unbound state or as an aggregate or as an agglomerate and where, for 50 % or more of the particles in the number size distribution, one or more external dimensions is in the size range 1 nm-100 nm". Yet since both definitions are either ambiguous or too elaborate to some sense, a more precise and concise definition would be as follows "Nanomaterials are materials having at least one characteristic length scale in the range 1–100 nm, and with at least one property is considerably different from that of the bulk counterpart as a result of the nanoscale dimensions", therefore focusing on the importance of the nanosized scale on changing some if not all of the material properties[1].
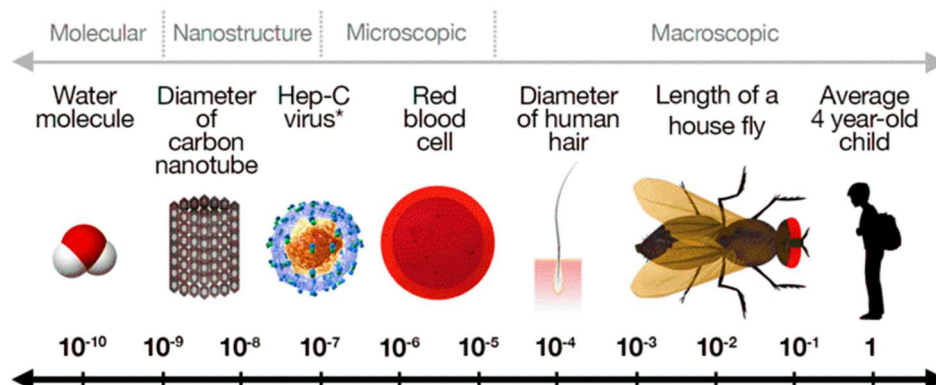
Figure 1.1: The size of nanoparticles compared to biological entities with the definition of the range of "nano" and "micro" sizes **[6]**.

Nanomaterials come in different manifestations and types (bionanomaterials, nanostructured materials, nanoporous materials…), however if the dimensions of such objects are considered, three types are defined [1] :

- **Three-dimensional (3-D)** nano-materials with all dimensions less than 100 nm are mainly called nano-particles or nano-pores if the object is nanoscaled pores embedded in a larger structure.
- **Two-dimensional (2-D)** nano-materials where two of its dimensions are less than 100 nm (nanorods, nanowires, nanotubes).
- **One-dimensional (1-D)** nano-materials that have only one dimension (thickness) less than 100 nm (eg. thin films, nanoplates).

Since the focus of our work is the behaviour of nanoparticles which were defined above, we shall embark on a more elaborate survey on the different aspects and manifestations of these materials. Additionally, it should be stated clearly that; Although this type of materials is considered as a highlight of modern technology and research, yet nanoparticles have been used throughout the history back to the ninth century BC in Mesopotamia where they used similar materials to obtain the glittering effect on the surface of ceramic vessels [7].

2. Classification of nanoparticles:

There are many types of nanoparticles that can be recognized based on different criterions (**Fig.1.2**):

1. **Origin:** even though the term nanoparticles is currently attached mostly for nanoscale particles that have anthropogenic origins (synthesized in lab), there are many nanoparticles that come naturally from geological, cosmic or weather-dependent phenomena, which produce fairly considerable amounts of particulate materials containing nanoscale particles. These nanosized particles are introduced into the ecosystem from volcanic eruptions [8], disintegrating meteorites ingoing earth's atmosphere, gathering cosmic dust or particles boosted in the air by air currents generated by storms or strong winds [7].

2. **Chemical composition:** Where we recognize three major types: **inorganic**, **organic** and **biological** elements. There are also nanoparticles which are composed of different materials. moreover, Synthesized nanomaterials (including nanoparticles) can also be classified based on their composition into various classes including **metals**, **metal oxides**, **carbon and semiconductors nanomaterials** [9].

3. **Morphology:** Where aspect ratio flatness and sphericity are the major characteristics which are considered to classify nanoparticles on the basis of their morphological character. They can be classified into two categories: high and low aspect ratio particles [9].

4. **Uniformity and agglomeration:** Although nanoparticles are intended primarily to be dispersed and suspended in a gas or as colloidal particles, yet the chemical
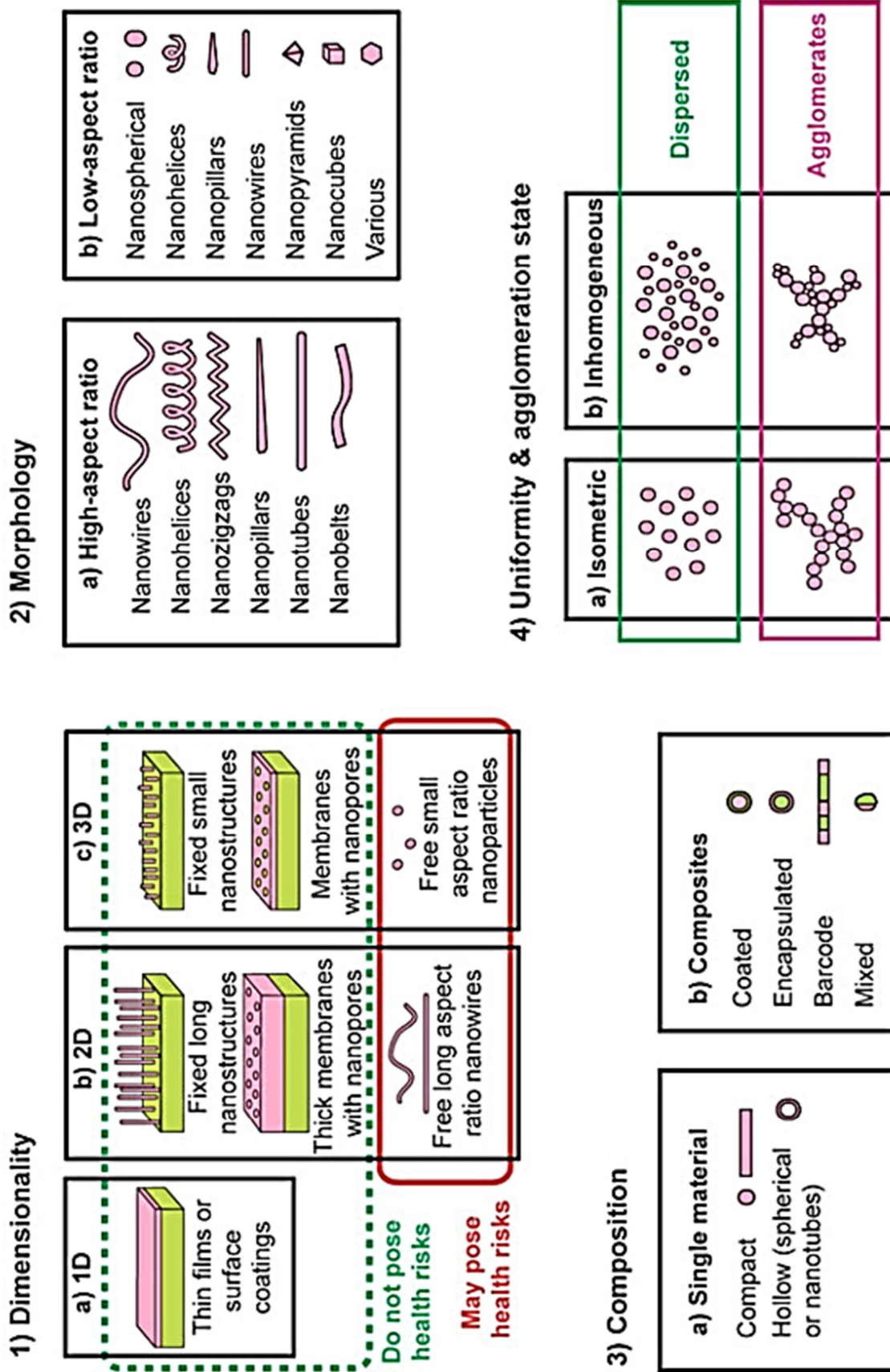
Figure 1.2: classification of nanoparticles [9].

and electromagnetic properties of some of these nanomaterials might lead to the formation of clusters and agglomerates due to the interaction forces exerted between particles [9-11]. For example, magnetic particles tend to form clusters due to their magnetic interaction. This characteristic of nanoparticles and particulate materials, in general, urges the study and understating of the interaction responsible for their agglomeration.

3. The difference between bulk and nanoscale material characteristics:

While bulk materials have size independent and constant physical/chemical properties, nanoparticles show a great different behaviour from its bulk counterpart, with properties more or less dependent on the size of the same material at the nanoscale [7]. There are two major causes behind these dramatic size-dependent changes[12]:

1. **Surface effects**: Since the fraction of atoms at the surface of nanoparticles is higher when compared to it in bulk materials (**Fig.1.3.a**), and having a significantly larger surface area and higher number of particles per unit mass [7, 9], for example a carbon microparticle of 60 μm diameter and with a mass of 0.3 μg has a surface area of 0.01 mm^2, while the same mass of the same material consisting of nanoparticles of diameter of the order of 60nm has a surface area of 11.3 mm^2 along with 10^9 particles. This dramatic increase in contact surface area gives nanoparticles an interesting behaviour where we notice an increase in contact surface-dependent properties like chemical reactivity, optical, electrical and magnetic properties [9]. Moreover, it might lead to radical changes in some of these physical and chemical or mechanical characteristics in a way where we notice the emergence of new properties that did not exist before [9, 12].**Fig.(1.3.b)** shows the change/decrease of Gold melting temperature at the nanoscale[9].
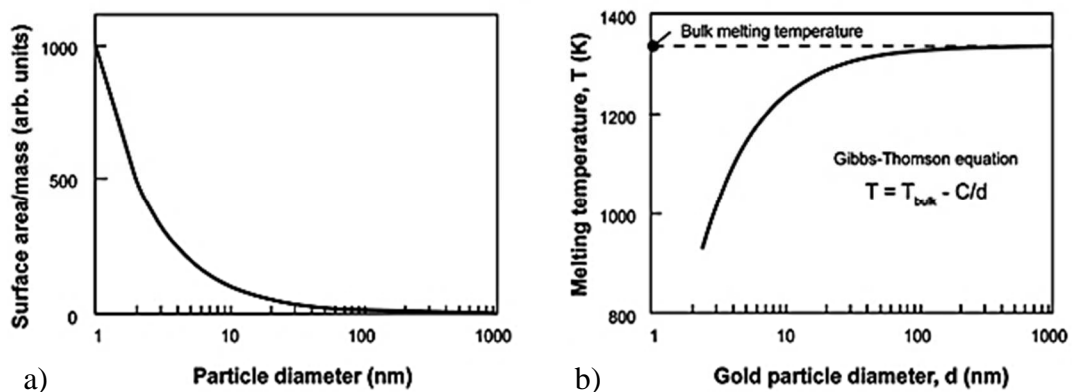
Figure 1.3 : (b) The variation of surface area per mass plotted in function of particles' diameter, (c) the variation of gold melting temperature with respect of particles' diameter **[9]**.

2. **Quantum effects:** Nanoparticles behave like molecules and atoms where due to quantum confinement in materials, they display discontinuous spontaneous physical characteristics [7, 9, 12], such as the discrete energy level structure noticed in the case nanocrystals in **Fig.(1.4)**.
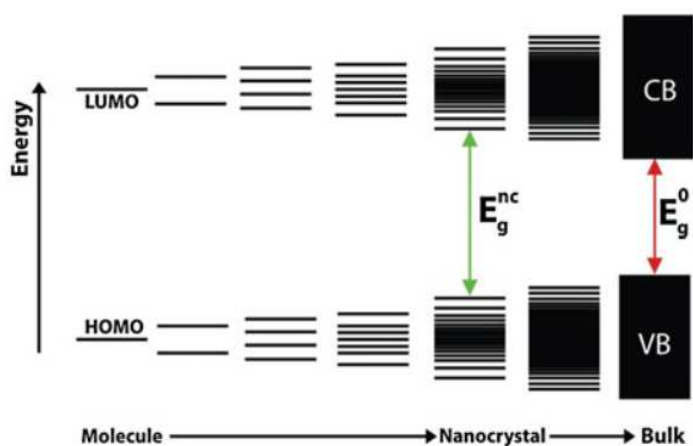
Figure 1.4 : Evolution of the energy level structure from a hypothetical diatomic molecule to a bulk semiconductor. Where E_g^{nc} and E_g^0 indicate the energy gaps for a nanocrystal and a bulk material, respectively (CB = conduction band, VB = valence band). Reprinted from Ref.[4]

Moreover, It has been established repeatedly and conclusively that materials display different physio-chemical properties at the nanoscale then when they are bulk substances, at this nano-level, "it is fairly expectable to say that gold is not gold and platinum is not platinum" and any material is not what we know is [13, 14].

Another remarkable example of the unique properties of nanoparticles which are originated from the quantum confinement effects is the innovative technology of quantum dots where it is remarkably noticed that the electronic behaviour is very similar to single atoms, thus having, for example, discrete quantized energy spectrum [9]. Quantum dots also might present the property of having a magnetic moment, even in materials that are not magnetic in bulk size, this quantum confinement effect also results in the quantification of electrical charge transfer (donate or accept) [12], and many other strange properties from the quantum world [13].

4. Synthesis methods of nanoparticles:

Nanoparticles / Nonmaterial's synthesis can be realized using numerous techniques. Nonetheless, all those techniques have distinctively two approaches that have been used since the ancient times [15]; Top-Down and Bottom-up methods :

Although there are many different methods of synthesising nanoparticles, yet all those methods have the property of obeying certain conditions that should be present for the technique to be efficient. For example, there must be a considerable control of the size, size distribution and shape of produced particles also of crystal structure and composition distribution. lower impurities must be insured in the structure of synthesized particles. there must also be a careful control of the formation of aggregation and agglomerates. And a high mass production, scale-up without forgetting the economical urge of having lower costs.

4.1. Top – Down:

Else know as breakdown method: where a solid is squashed by applying an external mechanical force that breaks it down to smaller particles [15]. Generally, mechanical size reduction methods such as grinding and milling (**Fig.1.5**) have been widely employed to

generate nanoparticles. These methods are the traditional approaches to produce fine particles and they have been able to generate nanoparticles from minerals such as clay, coal and metals. To avoid particle aggregation in the course of the size reduction process, the grinding and milling operations are often carried out with colloidal stabilizers [16, 17].
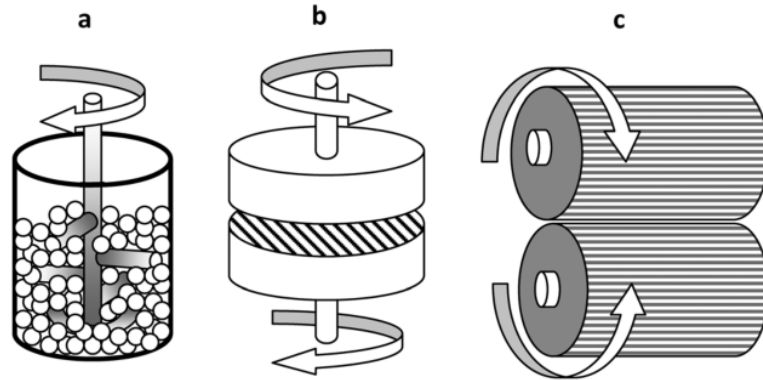
Figure 1.5: Schematic representation of the direct milling equipment: (a) attritor mill, (b) pan mill, and (c) roll mill (the figure is reprinted from [17]).

4.2. Bottom-Up:

Also called the build-up method: here nanoparticles are produced by atomic transformation or condensation of atoms of a fluid phase matter [15]. This approach includes various methods, for example, gas phase synthesis using flame pyrolysis (the mechanism of this method is demonstrated as an example case in **Fig.(1.6)**), high-temperature evaporation, and plasma synthesis, microwave irradiation, physical and chemical vapour deposition processes; colloidal or liquid phase methods in which chemical reactions in solvents form colloidal particles, and molecular self-assembly [16] which is very interesting to our work since it is depends strongly on the intermolecular forces acting between molecules .
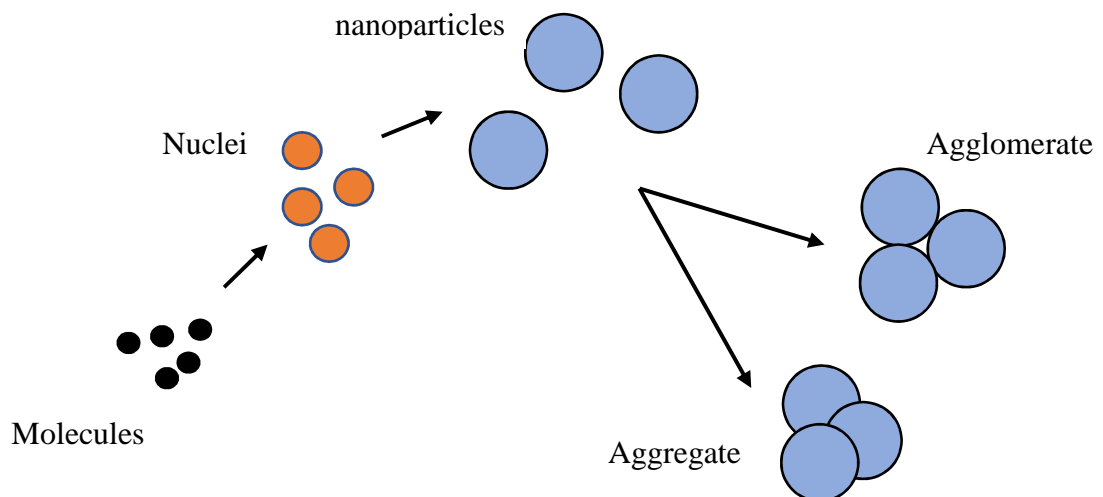
Figure 1.6: Mechanism of nanoparticle production using vapour phase or liquid phase/ colloidal methods, where the starting molecules are generated respectively either by vaporization or by chemical reaction/precipitation. The resulting nanoparticles may form either agglomerate which can be re-dispersed or non-dispersible aggregate clusters[16].

5. Applications of nanoparticles:

Nanoparticles offer tremendously countless possibilities of application in various fields like electronics, biology, medicine, optics, photonics, communication and others [18], and that is due to the peculiar properties that these particles have [18]. It might be impossible to track the entire spectrum on which the nanotechnology can be applied, yet we mention some of the promising fields of applications of nanoparticles:

a. **Nanoelectronics:** nanoscaled/molecular electronics have the same role as conventional electronic devices yet with new features and extreme precision [18-20]. an example of a nanoscale electronic device are nanosensors which principally can translate certain molecular properties into electrical signals. For this aim, many nanoscale materials have been investigated in order to hopefully be used to create novel nanosensors [18, 21, 22]. A very interesting example of nanoelectronic devices demonstrated within scientific literature in many research works is the application Single-wall nanotubes (SWNTs), and multiwall nanotubes (MWNTs) as basic construction blocks of gas, strain or thermal nanosensors [23-27].

b. **Nanobots:** since the publication of Eric Drexler's book "Engines of Creation" in 1986 this term nanobots signifying " microscopic robot used in nanotechnology" as the Webster's New Millennium™ Dictionary of English defines it, this subjected became the highlight of academia, as well as a public debate [28]. The potential applications of these nanoparticles are limitless; as they can be used for the delivery purpose of therapeutic agents, early detectors of and perhaps protectors against diseases.

c. **application in biology and medicine:** the relatively small size of nanoparticles compared to cellular size makes it theoretically suitable for use as probes of biological cellular machinery [29, 30]. And from the list of properties of nanoparticles, it is mostly the optical and magnetic properties that have been applied in biology and medicine [30].

6. Nanoparticulate materials:

Nanoparticles as a discrete amount of matter do not exist individually for most of the cases, rather they exist as a collective ensemble of particles which we call nanoparticulate materials. This type of material can be defined as every material constituted by individual nanoparticles where the collection acts as a fluid in most of the case[31, 32].

We shall consider the following classification which is based on two characteristics, the distance between particles and the medium in which these particles are dispersed, consequently we distinguish that there are three classes of particulate materials defined as follows:

6.1. Nanopowders:

Nano-powders are ultrafine powders which consist of nanoparticles with the distance between neighbouring particles is extremally small. This type of materials is currently receiving an increasing noteworthy attention in a wide spectrum of fields such as micro/nanoelectronics,

materials manufacturing, medicine and biotechnology, energy and the environment [33]. We distinct some of the important current applications found in daily life and they are as follows :

- Catalysts
- Solid Rocket Fuel
- Magnetic tapes & fluid
- Targeted drug delivery

- Metallic paint
- Sintering aids
- Transparent polymers
- Synthetic Bone
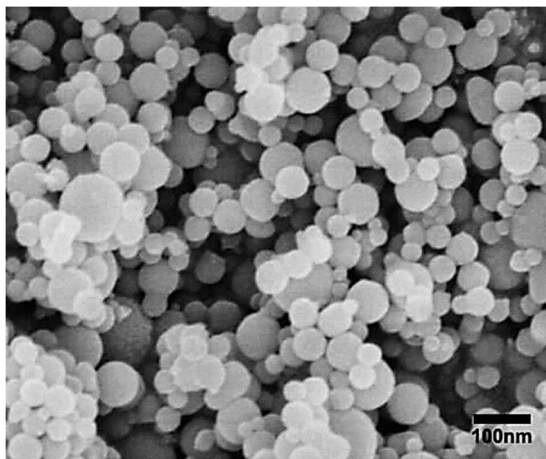
Figure 1.7 : Aluminum Nano powder constituted by spherical nanoparticle with radius ranging from 40 to 60 nm (the picture is taken from www.ssnano.com as a product photo under the product number 0220XH). these powders are used mostly as energetic nanomaterials/Combustive catalyst [5].

6.2. Nano aerosols:

An aerosol is a suspension of fine solid or liquid particles in a gas medium [34]. This type of materials is characterized by a relatively large distance between the constituent particles. Although the definition of aerosols includes liquid particles[34], leading to the generalization of the term nanoparticles to include both soft and hard matter, nonetheless in this work our focus would be mostly on hard nanoparticles.

Aerosols are present in our daily lives whether naturally as dust clouds or as a misfortunate product of the human technological aspects like smoke coming from cars or generally combustion engines. Additionally, these materials have many important and surprising applications; the simplest of those is the application of nanoaerosols and aerosol-science to study and develop drug inhalers which present a very widespread method of drug delivery [35, 36]. Another none evident application of these materials is that they are used by the military as a delivery mechanism of biological warfare agents, such as clouds of toxic dust. The other side of this application in the military is the urge to design filters which will protect military personnel against these toxic clouds of fine particles [34].

6.3. Nano colloid:

The term nanocolloids is relatively recent where it seems to have surfaced in the scientific literature in mid-80s of the past century, with the first mention in a patent was in mid-90s [37]. nanocolloids or Colloids on general can be define as every material that is in particulate form constituted by discrete entities of compounds in the amorphous or crystalline state, either

organic or inorganic, whereby these entities are dispersed/suspended within a fluid medium. This suspension is a result of the net repulsion forces that prevent a macroscopic phase separation (for example sedimentation) during a "practically useful" period of time [37].

Since we are concerned only with materials inside the nano limits, another condition is added to the definition of nanocolloids, where the average particles size is characteristically in the 1-100 nm range. This results in a huge surface-to-volume ratio of nanocolloids as stated before for nanoparticles in general, which ensures contact of a large percentage of the particle's constituent atoms with the surrounding liquid [37, 38].

This type of materials is widely used in various domains especially in pharmaceutics where we find many medical products in the form of colloidal suspensions. thud due to their importance, it is extremely necessary to understand and control the interactions between these particles which are responsible to the stability of such products, that is since these forces if not controlled might lead to the agglomeration of nanoparticles within the medium and thus jeopardizing the quality of these colloidal suspensions [37-40].

7. Nanotoxicology:

Due to the widespread of nanoparticles implementation in every field of our daily life as much as in the research environment, this emerging type of materials became one of the biggest evolving research and economic domains in the modern world [41], which urge the scientific society to inspect the environmental risks and hazard coming from the varying and developing exposure to nanoparticles [42].

7.1. Exposure to nanoparticles:

While nanomaterials embedded in other bulk materials have no considerable risk to be hazardous or even been exposed to at dangerous levels, except for bio-nanocomposites that have tendency towards degradation [43], which might ultimately lead to releasing the embedded nanoparticles into the environment. Accordingly, what is most interesting for nanotoxicological studies are free nanoparticles that have the ability to enter the human body and other ecological entities, and thus present a possible toxicological hazard to those biological systems [43] .

The exposure to nanoparticles can either be in the industrial environment, as the works are exposed to these materials during the manufacturing process that they are involved in. also when these products are introduced to the consumers, they on their turn will be exposed to these dispersed particles in the environment, through air, water or food, the graph below shows different roots of exposure to nanoparticles [43].

When it comes to studying the toxic effects of nanoparticles, most of in vivo studies concentrate on studying mammalians, with a great focus on hazards arising from the exposure to inhaled particles through the respiratory system, yet there are other tracts that should be considered like the skin and the gastrointestinal (GI) tracts [44].
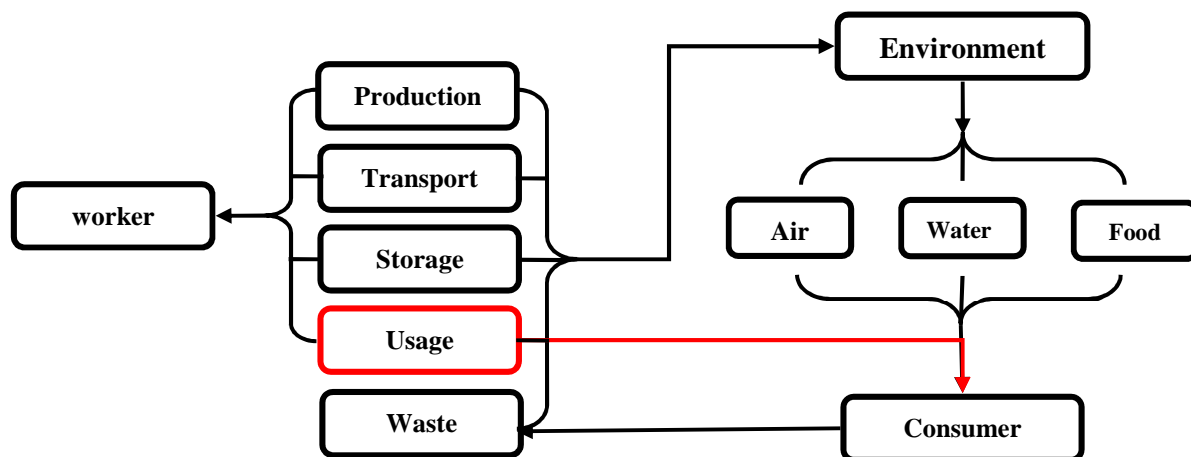
Figure 1.8: Nanoparticles exposure channels from manufacturing to utilization [6, 7].

7.1.1. Exposure through the respiratory system:

When particles are suspended in air they tend to take the easy way inside the human body and enter the respiratory system through mouth and nose [43]. So in the case of the toxicological studies, it is essential to have enough knowledge about the mechanisms and roots of deposition of these particles in the human corps when entering through this tract [44].

Nanoparticles behaviour in the respiratory tract can be summarized in two possibilities they either deposit in the system and thus presenting a hazard to be toxic and produce inflammation or pulmonary dysfunction [44], or they can reach the alveoli (**Fig.1.9**), thereafter the translocation to the respiratory system these particles would be transported to other organs in the human body via the bloodstream [43, 45]. another possibility is that these nano-scaled particles and through olfaction get transported directly to the brain [36, 46].

The mechanisms of deposition of nanoparticles are poorly understood, yet we recognize that the main mechanism is originated from particles diffusion as they collide with air molecules [44]. These mechanisms can be studied using either experimental approach or complex computational simulations [47]. Modelling techniques are more preferable since they are non-invasive, non-destructive and more important they are reproducible and can be replicated as many times as needed [47]. Analytical/numerical models can compute deposition efficiency at a total scale or by region [48-52]. **Fig.(1.9)** shows a simulation result regarding the deposition of particles of different sizes from micronic to nanoparticles, and it demonstrates that whilst large micronic particles tend to deposit the nasal, pharyngeal and laryngeal regions, nanoparticles on contrast are more likely to reach the alveolar capillary bed region and then to the bloodstream [44].

We should also recognise that the recent models are developed to study the flow of particles using the methods of two-phase fluid dynamics, in which the need to incorporate the interactions between particles is crucial to accomplishing more realistic simulations.

11
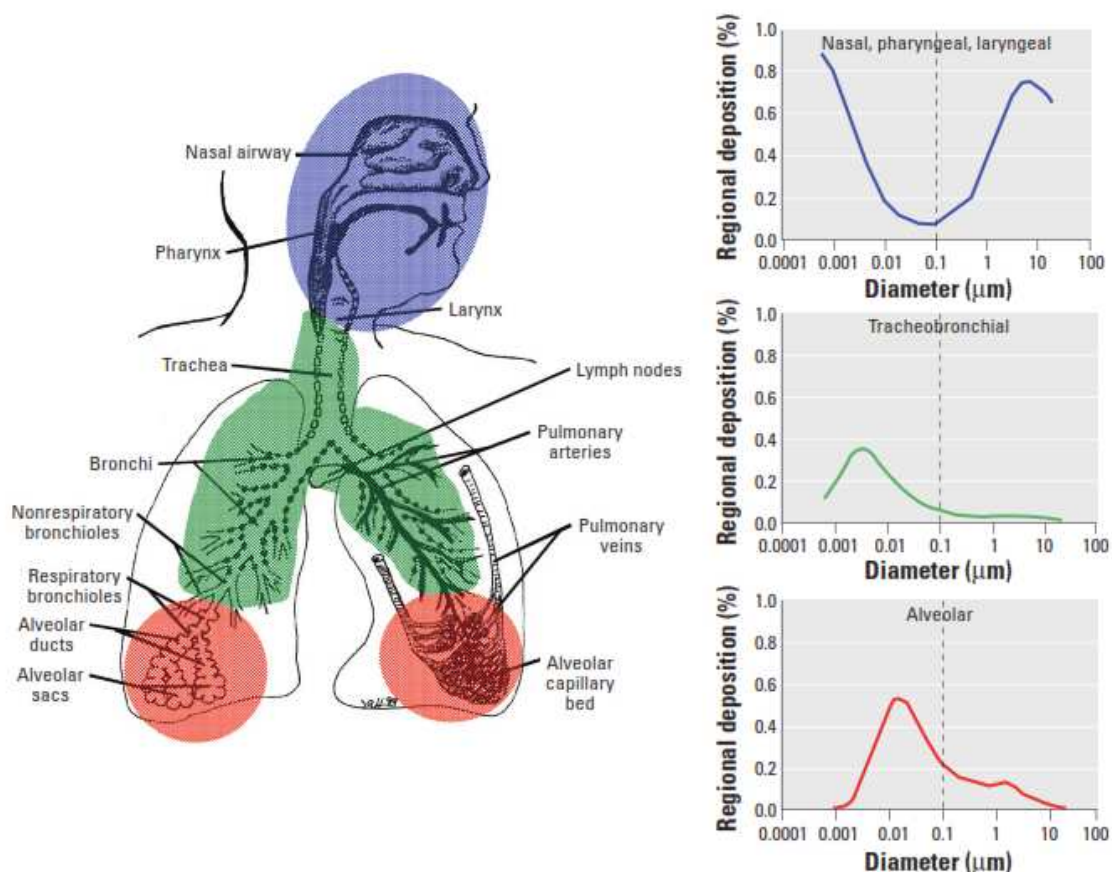
Figure 1.9: Prediction of the deposition of nanoparticles in different parts of the respiratory system during inhalation through the nose [44].

7.1.2. Exposure through the skin and GI tract:

Although the respiratory system present the major source of nanoparticles exposure to the human corps [53], yet the properties of these particles give rise to the possibility that they can penetrate the skin into the internal organs, and thus presenting the likelihood of been hazardous [54, 55]. Although the skin with its composition presents a large defence organ yet several studies have shown a deep penetration of small nanoparticles that ultimately might get transported via translocation to other organs through blood [11].

Nanoparticles that reach the gastrointestinal tract either have the possibility of been originally injected by respiratory system clearance of these particles via mucociliary escalator [56], additionally they can reach the GI tract through water, food or they can be injected as part of drugs or as drug delivery devices [44].

7.2. Risk assessment:

When the toxic hazard of nanoparticles is inspected Different methods have been proposed and investigated in the course of nanotoxicological studies' development, the most used in vitro method, is the study of the toxicity of nanomaterials in cell culture[9].

7.3. The toxicology of nanoparticles:

During the usage materials on general present a possibility of been toxic to the environment they are used in, the same possibility exists in the case of nanoparticles, yet nanoparticles and are dramatically different due to their specific features and ability to reach remotely inside the biological system then the bulk material can [10, 44]. These characteristics urge the scientific community motivated by environmental concerns to investigate thoroughly and carefully the toxicity of these new materials[10]. The investigation and assessment of the possible toxicological hazards of nanoparticles in the literature, is found to be generally done by grouping results into four categories based on the type of the material (Metals, Metal oxides, Carbon-based nanoparticles, Quantum dots)[57]. For demonstration, we shall only take two examples of these types.

8.3.1. Metals:

Because metallic nanoparticles present one of the most used classes of engineered nanomaterials, there an urging need to study and assess the presence of toxic risks and hazards when these particles interact with biological systems[6]. And although the mechanisms of this kind of interaction between nanoparticles and living organism are still poorly understood, yet the growth of such research trend is ever thriving, and every day more data are fed into the scientific corps concerning this subject [11].

As we find in literature the most studied nanomaterial in its class (metals) are **gold** nanoparticles, and although bulk gold has been considered always to be a safe material, yet due to the unexpected characteristics of these particles, many research groups undertook the task of investigating the cellular toxicity and uptake of these particles [9, 14, 58-61]. Gold nanoparticles have been found to be more taken up by cells when its diameter is in the range of 50 nm , also nanospheres have been found to be more up taken then nano-rodes [62], while even when particles are taken up by cells, nanogold particles with different surface modifications present no toxic hazard [63], It was also noticed that particles aggregate outside and enter the cell as an aggregate, yet no toxicity observed even for a long exposure (48h). The same result has been stated by [58, 61, 63].

Yet although a considerable number of research papers have stated the absence of gold nanoparticles toxicity, nevertheless we also find many articles which state the opposite, for example, these particles have been reported of been cytotoxic to the human carcinoma lung cell at specific particle concentrations [59]. Although we have found in a recent article a reference to the possible evidence of the extreme gold nanoparticles' toxicity for certain small particle sizes [60], nonetheless after examining literature on the subject we find that although there are certain condition where these particles can be hazardous to health especially at high concentrations yet the evidence of the general nontoxicity of AuNPs is much more compelling although there are special instances where this case does not hold .

Piccinno et al. reported that Silver is the most produced metallic nanomaterial by the year 2012, which urges to study their toxicity, moreover they demonstrated that a high-level exposure to these particles results in the medical condition known as argyria [64]. On the other hand a low exposure leads these nanoparticles to deposit on the skin and other parts of the body which might for some people lead to rashes, swelling and inflammation [65], also the high level concentration of silver nanoparticles can cause breathing problems and other problems related to the respiratory and the digestive system. Additionally, it has been reported that among a group of different metallic and other elements, solely nano-silver and nano-copper particles presented in all tests a toxic behaviour in aquatic organisms [57, 65-67]

8.3.2. Metal oxides:

Metal oxides are reported to be the most produced nanomaterials in the world [64]. They are used in a wide spectrum of applications, like the cosmetics industry, pharmaceutics and other aspects of human daily life. the widespread of these particles makes it necessary to investigate their toxicity, and assess the risks they present on the environment and especially on the human health [9].

The uptake and toxicity of metal oxide nanoparticles have been investigated by several groups whom have demonstrated that TiO_2 (2-5 nm) aggregate in the exposure room and then when they studied the lung response to the exposure of these aggregate, it was shown that they cause a minor inflammatory response in the necropsied with the possibility of recovery after exposure[9, 68]. TiO_2 have been showed to produce an increased oxidative stress at higher concentrations [69]. the cytotoxicity of TiO_2 has also been reported [70], with the creation of reactive oxygen species (ROS).

A comparative study of the toxicity of bulk ZnO , $ZnCl_2$ and ZnO nanoparticles have showed a comparable toxicity with a concentration value near 60 μg Zn/L [71], also the toxicity of ZnO nanoparticles to various bacterial systems and human T lymphocytes, have been reported [72]. Moreover CuO particles have been established to be the most cytotoxic, as well as they produce DNA damage and oxidative lesions when compared to different metal oxides (TiO_2, ZnO, $CuZnFe_2O_4$, Fe_3O_4, Fe_2O_3), and ZnO nanoparticles have been found to produce a cytotoxic behaviour and DNA damage while other type of materials have shown no or at best lower toxicity[9]. another study demonstrated that nano-ZnO particles are more toxic when compared to TiO2, CeO2 nanoparticles [73].

A study done on 24 different nanoparticulate materials have been undertaking under similar conditions, and conveyed that copper and zinc-based materials were the most toxic among the tested materials, while other materials showed lower and no toxic behaviour [74]. However, research into the toxicology of nanoparticles is in its early stages compared to the broad subject of toxicity, and so much more work is needed before any generalised declarations can be made regarding nanotoxicology [75].

8. Cohesion forces:

When we come to study particulate materials, we recognize that the main agent that defines the features of their behaviour is the interparticle forces that exist between the individual constituents. By studying these forces we distinguish two classes defined with respect to the distance range in which these forces take place [32], and they are as follows:

- **Contact forces** exist due to direct contact of particles with each other, and they manifest in the form of torque in most cases[76].
- **Non-contact forces** act at a distance and they are differentiated into three types. dispersion, electrostatic and capillary forces [77].

8.1. Dispersion forces:

These interactions otherwise known as van der Waals or Casimir forces are an important and an interesting aspect of the intermolecular interactions due to their unique quantum origins and their presence between any two neutral objects. The discussion of their origins and some of the aspects of their modelling processes are the subjects of the following three chapters.

8.2. The electrostatic forces:

The electrostatic interactions between individual particles come to existence when handling particulate materials mainly due to three processes which end up with charging those particles electrically[78, 79]:

- Friction between particles with what is called 'triboelectrification'.
- Contact charging.
- Columbic interactions.

The understanding of these interactions is interesting for many industrial applications like the pharmaceutical domain especially concerning the efficiency of dry powder inhalers [79], electro-photography [80] and others, yet these interaction forces can be disadvantageous, as they can be the origin of explosive behaviour of powders.

There are two different manifestations of this type of force; the first is the formation of double layers in the case of colloidal particles [81]. Yet when we consider the case of dry particulate materials, the electrostatic interactions are mainly studied using the image charge model approximation [82]. However, the simplest model of the interaction of two particles with charges q_1 and q_2 at a distance d, is given by the conventional coulomb equation for the electrostatic force [79, 83-85]:

$$F_e = \frac{q_1 . q_2}{4\pi\varepsilon . d^2}$$

(1.1)

Where ε is the permittivity of material in which particles are immersed.

8.3. The Capillary forces:

If the granular material contains a fair amount of a liquid phase this liquid inclines to accumulate in the spaces between the adjacent particles, where it would form what is known as liquid bridges [86]. This type of adhesion and cohesion force is very interesting since it can be controlled by regulating the amount of liquid present in the targeted granular material [76]. This force has two components [76]; the surface tension force F_s and the capillary pressure force F_p, which presents the product of the pressure difference and the liquid-vapor interface surface. the capillary force thus is given by the following relation [87] :

$$F_c = F_p + F_s = r_m^2 \Delta P \, \pi + 2 r_m \, \gamma \cos \alpha \qquad (1.2)$$

Where r is the radius of the meniscus, α is the deviation angle of the interface from the normal direction of this cross-section and ΔP is the reduction in pressure within the bridge with respect to the pressure outside and it is given approximately with Laplace equation as follows [76, 87]:

$$\Delta P = \gamma \left[\frac{1}{R_1} - \frac{1}{R_2} \right] \qquad (1.3)$$

Where r_1 is the out radius of the bridge curvature and r_2 is the inside radius as it is shown in **Fig.(1 .9)** .
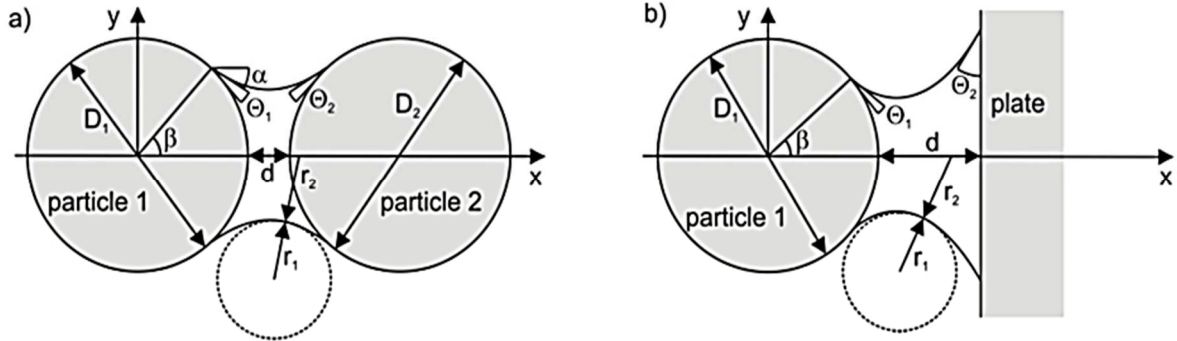
Figure 1.10: An idealized representation of liquid bridges between (a) two perfectly spherical particles, (b) a spherical particle and a flat surface [87].

Moreover, it is essential to notice that the manifestation of these different forces is very dissimilar, many studies have been conducted to compare the contribution of these forces to the total interaction [76, 82, 85, 88, 89], and it was noticed that for nanoparticles in dry environments (no capillary) the van der Waals forces are dominant. Since the focus of this study is the interactions of dry nanosized particulate materials, only dispersion forces are studied in this work.

10. Conclusions:

In this chapter we have discussed the different aspects of the study and technology of nanoparticles, we have also reviewed some of the toxicological aspects of these materials which put the subject of our work in perspective, and we emphasised the importance of understanding the dynamics of the interactions between those particles in order to predict and control the behaviour of these particles for better applications and better safety controls.

References:

1. de Mello Donegá, C., (2014), *Nanoparticles: workhorses of nanoscience. Springer, Berlin, Germany.*
2. Goddard III, W.A., et al.,(2007), *Handbook of nanoscience, engineering, and technology*: CRC press.
3. Khanna, P., et al., (2015), *Nanotoxicity: An Interplay of Oxidative Stress, Inflammation and Cell Death* .Nanomaterials. **5**(3): p. 1163-1180.
4. Groeneveld, E., (2012), *Synthesis and optical spectroscopy of (hetero)-nanocrystals.* Utrecht: Utrecht University.
5. Martin, C., et al., (2018), *Aluminum nanopowder: A substance to be handled with care.* Journal of Hazardous materials. **342**: p. 347-352.
6. Buzea, C., I.I. Pacheco, and K. Robbie, (2007), *Nanomaterials and nanoparticles: sources and toxicity.* Biointerphases. **2**(4): p. MR17-MR71.
7. Lungu, M., et al.,(2015), *Nanoparticles' Promises and Risks*: Springer International Publishing.
8. Rietmeijer, F.J. and I.D. Mackinnon, (1997), *Bismuth oxide nanoparticles in the stratosphere.* Journal of Geophysical Research: Planets (1991–2012). **102**(E3): p. 6621-6627.
9. Ray, P.C., H. Yu, and P.P. Fu, (2009), *Toxicity and environmental risks of nanomaterials: challenges and future needs.* J Environ Sci Health C Environ Carcinog Ecotoxicol Rev. **27**(1): p. 1-35.
10. Lewicka, Z.A. and V.L. Colvin, (2013), *Nanomaterial Toxicity, Hazards, and Safety.* p. 1117-1142.
11. Arora, S., J.M .Rajwade, and K.M. Paknikar, (2012), *Nanotoxicology and in vitro studies: the need of the hour.* Toxicol Appl Pharmacol. **258**(2): p. 151-65.
12. Roduner, E., (2006), *Size matters: why nanomaterials are different.* Chemical Society Reviews. **35**(7): p. 583-592.
13. Lüth, H., (2013), *Quantum Physics in the Nanoworld.* Quantum Physics in the Nanoworld: Schrödinger's Cat and the Dwarfs, Graduate Texts in Physics. ISBN 978-3-642-31237-3. Springer-Verlag Berlin Heidelberg, 2013.
14. Daniel, M.-C. and D. Astruc, (2004), *Gold nanoparticles: assembly, supramolecular chemistry, quantum-size-related properties, and applications toward biology, catalysis, and nanotechnology.* Chemical Reviews. **104**(1): p. 293-346.
15. Rotello, V.M.,(2004), *Nanoparticles: building blocks for nanotechnology*: Springer Science & Business Media, Berlin, Germany.
16. Nagarajan, R. and T.A. Hatton,(2008), *Nanoparticles: synthesis, stabilization, passivation, and functionalization.* Vol. 996. Amer Chemical Society.

17. Gorrasi, G. and A. Sorrentino, (2015), *Mechanical milling as a technology to produce structural and functional bio-nanocomposites.* Green Chemistry. **17**(5): p. 2610-2625.
18. Gao, G., (2004), *Nanostructures and nanomaterials: synthesis, properties and applications*: Imperial College Press, London, UK.
19. Kaul, A.B.,(2017), *Microelectronics to Nanoelectronics: Materials, Devices & Manufacturability*: CRC Press, Boca Raton, Florida, USA.
20. Fedlheim, D.L. and C.A. Foss,(2001), *Metal nanoparticles: synthesis, characterization, and applications*: CRC press, Boca Raton, Florida, USA.
21. Lim, T.-C.,(2010), *Nanosensors: theory and applications in industry, healthcare and defense*: CRC Press, Boca Raton, Florida, USA.
22. Khanna, V.K.,(2011), *Nanosensors: physical, chemical, and biological*: CRC Press, Boca Raton, Florida, USA.
23. Dharap, P., et al., (2004), *Nanotube film based on single-wall carbon nanotubes for strain sensing.* Nanotechnology. **15**(3): p. 379.
24. Kumar, D., et al., (2017), *Effect of single wall carbon nanotube networks on gas sensor response and detection limit.* Sensors and Actuators B: Chemical. **240**: p. 1134-1140.
25. Liang, Y., Y. Chen, and T. Wang ,(2004) ,*Low-resistance gas sensors fabricated from multiwalled carbon nanotubes coated with a thin tin oxide layer.* Applied Physics Letters. **85**(4): p. 666-668.
26. Abdulla, S., T.L. Mathew, and B. Pullithadathil, (2015), *Highly sensitive, room temperature gas sensor based on polyaniline-multiwalled carbon nanotubes (PANI/MWCNTs) nanocomposite for trace-level ammonia detection.* Sensors and Actuators B: Chemical. **221**: p. 1523-1534.
27. Gheibi, S., et al., (2015), *A new voltammetric sensor for electrocatalytic determination of vitamin C in fruit juices and fresh vegetable juice using modified multi-wall carbon nanotubes paste electrode.* Journal of Food Science and Technology. **52**(1): p. 276-284.
28. Nerlich, B., (2008), *Powered by imagination: nanobots at the Science Photo Library.* Science as Culture. **17**(3): p. 269-292.
29. Taton, T.A., (2002), *Nanostructures as tailored biological probes.* Trends in biotechnology. **20**(7): p. 277-279.
30. Salata, O.V., (2004), *Applications of nanoparticles in biology and medicine.* Journal of nanobiotechnology. **2**(1): p. 3.
31. Bose, A.,(2013), *Advances in particulate materials*: Elsevier, Amsterdam, Netherlands.
32. Zhu, H.P., et al., (2007), *Discrete particle simulation of particulate systems: Theoretical developments.* Chemical Engineering Science. **62** :(13)p. 3378-3396.
33. McCormick, P.G., et al., (2001), *Nanopowders synthesized by mechanochemical processing.* Advanced Materials. **13**(12-13): p. 1008-1010.
34. Kaye, B.H.,(2008), *Characterization of powders and aerosols*: John Wiley & Sons, New Jersey, United States.
35. Fröhlich, E,(2013) ,.*Nanoparticles in Biology and Medicine: Methods and Protocols. Edited by Mikhail Soloviev*, Wiley Online Library.
36. Mistry, A., S. Stolnik, and L. Illum, (2009), *Nanoparticles for direct nose-to-brain delivery of drugs.* Int J Pharm. **379**(1): p. 1.157-46
37. Sanchez-Dominguez, M. and C. Rodriguez-Abreu,(2016), *Nanocolloids: A meeting point for scientists and technologists*: Elsevier, Amsterdam, Netherlands.
38. André, P., et al., (2015), *Established and emerging nanocolloids: from synthesis and characterization to applications.* physica status solidi (c). **12**(1-2): p. 136-137.
39. Chen, Z., et al., (2016), *Preparation of nickel cobalt sulfide hollow nanocolloids with enhanced electrochemical property for supercapacitors application.* Scientific Reports. **6**: p. 25151.

40. Gatica, S.M., M.W. Cole, and D. Velegol, (2005), *Designing van der Waals forces between nanocolloids.* Nano Letters. **5**(1): p. 169-173.

41. Reineke, J.,(2012), *Nanotoxicity: Methods and Protocols*: Humana Press, New York, USA.

42. Pourmand, A. and M. Abdollahi, (2012), *Current opinion on nanotoxicology.* Daru. **20**(1): p. 95.

43. Ngô, C. and M.v.d. Voorde,(2013), *Nanotechnology in a Nutshell*: Springer, Berlin, Germany.

44. Oberdörster, G., E. Oberdörster, and J. Oberdörster, (2005), *Nanotoxicology: An Emerging Discipline Evolving from Studies of Ultrafine Particles.* Environmental Health Perspectives. **113**(7): p. 823-839.

45. Berry, J., et al., (1977), *A microanalytic study of particles transport across the alveoli: role of blood platelets.* Biomedicine/[publiée pour l'AAICIG]. **27**(9-10): p. 354-357.

46. Tu, J., K. Inthavong, and G. Ahmadi,(2012), *Computational fluid and particle dynamics in the human respiratory system*: Springer Science & Business Media.

47. Farkas, A. and I. Balashazy, (2008), *Quantification of particle deposition in asymmetrical tracheobronchial model geometry.* Comput Biol Med. **38**(4): p. 508-18.

48. Balásházy, I., W. Hofmann, and T. Heistracher, (2003), *Local particle deposition patterns may play a key role in the development of lung cancer.* Journal of Applied Physiology. **94**(5): p.1725-1719 .

49. Kim, C.S. and D.M. Fisher, (1999), *Deposition characteristics of aerosol particles in sequentially bifurcating airway models.* Aerosol Science & Technology. **31**(2-3): p. 198-220.

50. Comer, J., et al., (2000), *Aerosol transport and deposition in sequentially bifurcating airways.* Journal of biomechanical engineering. **122**(2): p. 152-158.

51. Oldham, M.J., (2000), *Computational fluid dynamic predictions and experimental results for particle deposition in an airway model.* Aerosol Science & Technology. **32**(1): p. 61-71.

52. Moskal, A. and L. Gradoń, (2002), *Temporary and spatial deposition of aerosol particles in the upper human airways during breathing cycle.* Journal of Aerosol Science. **33**(11): p. 1525-1539.

53. Maynard, A.D. and E.D. Kuempel ,(2005) ,*Airborne Nanostructured Particles and Occupational Health.* Journal of Nanoparticle Research. **7**(6): p. 587-614.

54. Tinkle, S.S., et al., (2003), *Skin as a route of exposure and sensitization in chronic beryllium disease.* Environmental Health Perspectives. **111**(9): p. 1202.

55. Delie, F., (1998), *Evaluation of nano- and microparticle uptake by the gastrointestinal tract.* Advanced Drug Delivery Reviews. **34**(2–3): p. 221-233.

56. Bailey, M.R. and M. Roy, (1994), *Annexe E. clearance of particles from the respiratory tract.* Annals of the ICRP. **24**(1–3): p. 301-413.

57. Sharifi, S., et al., (2012), *Toxicity of nanomaterials.* Chemical Society Reviews. **41**(6): p. 2323-2343.

58. Goodman, C.M., et al., (2004), *Toxicity of gold nanoparticles functionalized with cationic and anionic side chains.* Bioconjugate Chemistry. **15**(4): p. 897-900.

59. Patra, H.K., et al., (2007), *Cell selective response to gold nanoparticles.* Nanomedicine: Nanotechnology, Biology and Medicine. **3**(2): p. 111-119.

60. Senut, M.C., et al., (2006) ,*Size-dependent toxicity of gold nanoparticles on human embryonic stem cells and their neural derivatives.* Small. **12**(5): p. 631-646.

61. Wang, S., et al., (2008), *Challenge in understanding size and shape dependent toxicity of gold nanomaterials in human skin keratinocytes.* Chemical Physics Letters. **463**(1-3): p. 145-149.

62. Chithrani, B.D., A.A. Ghazani, and W.C. Chan, (2006), *Determining the size and shape dependence of gold nanoparticle uptake into mammalian cells.* Nano Letters. **6**(4): p. 662-668.

63. Connor, E.E., et al., (2005), *Gold nanoparticles are taken up by human cells but do not cause acute cytotoxicity.* Small. **1**(3): p. 325-327.

64. Piccinno, F., et al., (2012), *Industrial production quantities and uses of ten engineered nanomaterials in Europe and the world.* Journal of Nanoparticle Research. **14**.(9)

65. Carlson, C., et al., (2008), *Unique cellular interaction of silver nanoparticles: size-dependent generation of reactive oxygen species.* The journal of physical chemistry B. **112**(43): p. 13608.13619-

66. Bondarenko, O., et al., (2013), *Toxicity of Ag, CuO and ZnO nanoparticles to selected environmentally relevant test organisms and mammalian cells in vitro: a critical review.* Archives of Toxicology. **87**(7): p. 1181-1200.

67. Griffitt, R.J., et al., (2008), *Effects of particle composition and species on toxicity of metallic nanomaterials in aquatic organisms.* Environmental Toxicology and Chemistry. **27**(9): p. 1972-1978.

68. Grassian, V.H., et al., (2006), *Inhalation exposure study of titanium dioxide nanoparticles with a primary particle size of 2 to 5 nm.* Environmental Health Perspectives. **115**(3): p. 397-402.

69. Jin, C.-Y., et al., (2008), *Cytotoxicity of titanium dioxide nanoparticles in mouse fibroblast cells.* Chemical Research in Toxicology :(9)21 .p. 1871-1877.

70. Park, E.-J., et al., (2008), *Oxidative stress and apoptosis induced by titanium dioxide nanoparticles in cultured BEAS-2B cells.* Toxicology Letters. **180**(3): p. 222-229.

71. Franklin, N.M., et al., (2007), *Comparative toxicity of nanoparticulate ZnO, bulk ZnO, and ZnCl2 to a freshwater microalga (Pseudokirchneriella subcapitata): the importance of particle solubility.* Environmental Science & Technology. **41**(24): p. 8484-8490.

72. Reddy, K.M., et al., (2007), *Selective toxicity of zinc oxide nanoparticles to prokaryotic and eukaryotic systems.* Applied Physics Letters. **90**(21): p. 213902.

73. Xia, T., et al., (2008), *Comparison of the mechanism of toxicity of zinc oxide and cerium oxide nanoparticles based on dissolution and oxidative stress properties.* ACS nano. **2**(10): p. 2121-2134.

74. Lanone, S., et al., (2009), *Comparative toxicity of 24 manufactured nanoparticles in human alveolar epithelial and macrophage cell lines.* Part Fibre Toxicol. **6**: p. 14.

75. Oberdörster, G., V. Stone, and K. Donaldson, (2007), *Toxicology of nanoparticles: a historical perspective.* Nanotoxicology. **1**(1): p. 2-25.

76. Seville, J., C. Willett, and P. Knight, (2000), *Interparticle forces in fluidisation: a review.* Powder Technology. **113**(3): p. 261-268.

77. Masuda, H., K. Higashitani, and H. Yoshida,(2006), *Powder technology: fundamentals of particles, powder beds, and particle generation*: CRC Press, Boca Raton, Florida.

78. Bailey, A., (1984), *Electrostatic phenomena during powder handling.* Powder Technology. **37**(1): p. 71-85.

79. Xu, Z., H.M. Mansour, and A.J. Hickey, (2011), *Particle Interactions in Dry Powder Inhaler Unit Processes: A Review.* Journal of Adhesion Science and Technology. **25**(4-5): p. 451-482.

80. Mizes, H., et al., (2000), *Small particle adhesion: measurement and control.* Colloids and Surfaces A: Physicochemical and Engineering Aspects. **165**(1): p. 11-23.

81. Schmidt, R.,(1999), *Comportement des matériaux dans les milieux biologiques: Applications en médecine et biotechnologie.* Vol. 7. PPUR presses polytechniques.

82. Zhou, H., M. Götzinger, and W. Peukert, (2003), *The influence of particle charge and roughness on particle–substrate adhesion.* Powder Technology. **135-136**: p. 82-91.

83. Takeuchi, M., (2006), *Adhesion forces of charged particles.* Chemical Engineering Science. **61**(7): p. 2279-2289.
84. Suresh, L. and J.Y. Walz, (1996), *Effect of Surface Roughness on the Interaction Energy between a Colloidal Sphere and a Flat Plate.* J Colloid Interface Sci. **183**(1): p. 199-213.
85. Krupp, H.,(1967), *Particle adhesion, theory and experiment*: Advan. Colloid Interface Sci. 1 (1967), 111-239.
86. Johanson, K., et al., (2003), *Relationship between particle scale capillary forces and bulk unconfined yield strength.* Powder Technology. **138**(1): p. 13-17.
87. Dörmann, M. and H.-J .Schmid, (2015), *Simulation of Capillary Bridges between Particles.* Procedia Engineering. **102**(0): p. 14-23.
88. Feng, J.Q. and D.A. Hays, (2003), *Relative importance of electrostatic forces on powder particles.* Powder Technology. **135-136**: p. 65-75.
89. Li ,Q., et al., (2004), *Interparticle van der Waals force in powder flowability and compactibility.* Int J Pharm. **280**(1-2): p. 77-93.

CHAPTER 2:

Dispersion interactions between molecules

"Speak English!' said the Eaglet. 'I don't know the meaning of half those long words, and I don't believe you do either!"

Lewis Carroll, Alice in Wonderland.

1. Historical background

As it is accustomed in scientific writing, the study of any subject must be proceeded by a historical account of the timeline on which this subject had evolved. The origin and nature of intermolecular forces have been investigated since the atomic hypothesis was first introduced into the corpus of scientific inquiry. within this picture of the material world, it is stated that the nature of bulk matter can be explained returning to its microscopic constituents namely molecules and atoms. When such an approach is applied to explain experimental data collected on materials and more importantly on gases, the need for a better understanding of intermolecular forces was strongly recognized and emphasized. kinetic theory in its prime days was formulated by regarding molecules as hard objects without considering any long-range interaction between them. This model was fairly successful in explaining some simple properties of gases, Boyle's and Charles' laws, and even viscosity and thermal conductivity. Yet when this model was used to explain the detailed behaviour of real gases, especially when it came to the critical problem of why real gases did not obey the ideal gas law. Thus It was recognized that a need for a more realistic model was crucial and this it should involve the existence of a force field between the constituent molecules whose range is greater than their dimensions [2].

The Dutch physicist J. D. van der Waals (1837–1923) attempted to solve this problem by considering the effect of an attractive force between molecules when modelling the behaviour of real gases [1]. And In 1873 he arrived at his well-known equation of state for gases and liquids (**Eq.2.1**). in this model, b is subtracted from the total volume to account for the finite size of molecules, and correction term a/V^2 is added to the pressure P to account for the attractive intermolecular forces which now we recognise and name as the as van der Waals forces [2-4]:

$$\left(P + a/V^{\,2}\right)\left(V - b\right) = R_G T \tag{2.1}$$

At Columbia University, influenced by the suggestion of Debye, S.C. Wang [5] used the at that moment new wave mechanics, and thus proposing a simple model of a pair of hydrogen atoms as the two electrons of the atoms oscillate within the same plane [6]. he found using this approach that there is undeniably an attractive force at large distances compared to atomic size, with a potential energy that varies as the inverse-sixth power of distance, where r is the atomic separation. the model proposed thus is found to be written in the following general form [2]:

$$U = -C_6 \cdot r^{-6}$$
(2.2)

Although his predictions offered no real interpretation of the phenomenon, however the result which he obtained was crucially important since it has for the first time demonstrated, that according to the new quantum mechanics two neutral atoms (with no permanent dipoles) exert an attractive force on each other [2].

The simplest theoretical description of this force was proposed soon later by London [5]. It was based on a model of an atom or molecule that act as a Drude oscillator, the oscillation of electrons generate instantaneous dipoles along with higher multipoles, where the London dispersion energy is only the first term of this multipole expansion series of the attraction energy demonstrated as follows [2, 6]:

$$E = -\frac{C_6}{r^6} - \frac{C_8}{r^8} - \frac{C_{10}}{r^{10}} \cdots$$
(2.3)

Later these forces started to be approached for macroscopic bodies, aiming at calculating these forces at a macroscopic scale. The famous and most cited model was that which was proposed by H.C. Hamaker in 1937 [7]. In his model he integrated over all the inverse sixth-power potentials of each two-body interaction, this method is what is known now as the pairwise summation method [2, 3, 7]. After further inquiries, J.Th.G. Overbeek concluded intuitively that the dispersion force between macroscopic particles was much weaker than that calculated by Hamaker. He hypothesised that the dispersion force was not an instantaneous interaction and that it is transmitted at the speed of light, so as a result of this assumption this force is weakened at large distances. H.B.G. Casimir and D. Polder after corresponding with their Overbeek who passed to them his remarks on this retardation effect, they confirmed theoretically that his conjecture was correct [8], demonstrating in their calculations that for distance larger than the characteristic frequency start to fall as r^{-7} [2].

After a remark from Bohr regarding the relation between the early finding of Casimir with polder and the concept of zero-point energy. Casimir later studied the variation of zero-point energy in a system of two perfectly conducting parallel plates in vacuum (**Fig.2.1**), and he demonstrated that there is a pressure generated on the plates due to quantum vacuum fluctuations leading to an attractive force pushing these plates closer to each other[9]. This effect is now known as the Casimir effect [10-12].

Although Casimir was successful in encompassing the retardation in the theory of dispersion forces between macroscopic bodies along with demonstrating the physical effect of vacuum fluctuations, yet a more realistic model had to be developed in order to study real materials with dielectric properties. This was accomplished by E.M. Lifshitz in Moscow in 1954 [13], where

he considered electrical fluctuations in bulk continuum matter without referring to its molecular constituents [2]. This theory was a great success since it accounted for all many-body interactions, as well as retardation [14]. Later Lifshitz along with his colleagues Dzyaloshinskii and Pitaevskii (DLP) generalized his model by including the existence of a third material dielectric medium between the interacting objects [15, 16].
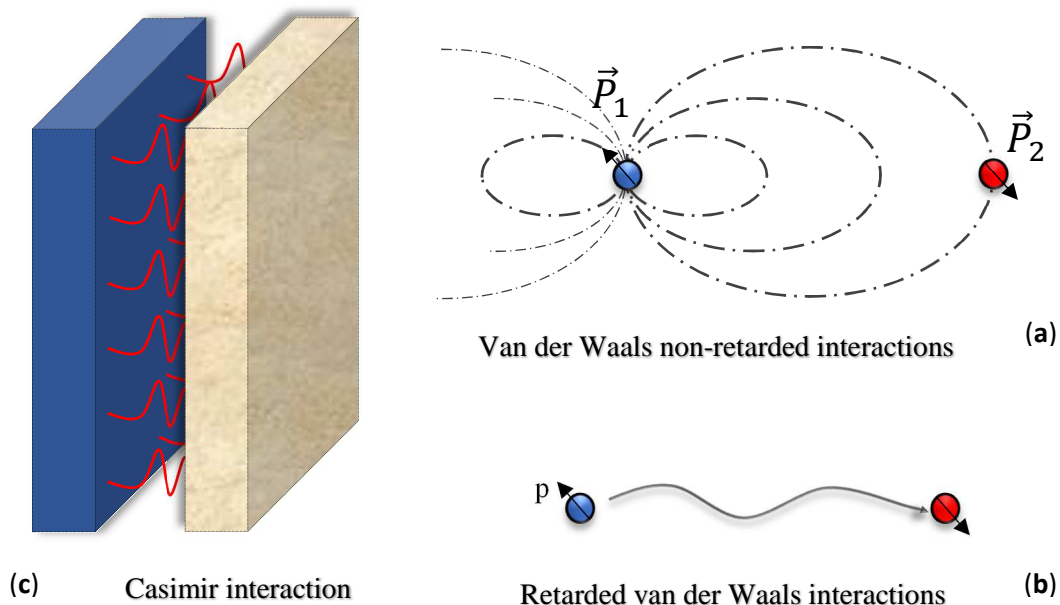
Figure 2.1: Key manifestations of dispersion forces; (a) London model of an instantaneous dipole $\vec{P}_1$ generating a field inducing a dipole $\vec{P}_2$ simultaneously leading to non retarded dispersion attraction, (b) The effect of retardation is considered by introducing the finite speed of light into the interaction, (c) When macroscopic objects are involved, dispersion forces rise in the form of a Casimir pressure.

Many surprising and critical findings were discovered within this theoretical approach (Dzyaloshinskii, Lifshitz and Pitaevskii theory), the most important of them is the existence of a repulsive along with the known attractive force between objects, that is depending on the nature of the medium [16].

2. Classification of intermolecular forces

When we study the interaction between molecules/atoms we distinguish two major types of attraction and repulsion forces; short-range and long-range interactions. short-range forces are primarily occurring as a result of the overlap the electronic charge clouds associated with each nucleus [6, 17, 18]. This is a repulsive force arising from electronic repulsions which can also be explained in the language of quantum theory by the tendency of the wavefunction to adapt the state as to maintain the Pauli antisymmetric requirement[1] [6].

---

[1] Or otherwise know in theoretical physics as Exclusion Principle, where it stated that in a quantum system, two or more fermions of the same kind cannot be in the same (pure) quantum state.

Table 2.1: different types of intermolecular forces classified into two categories.

long range	short range
electrostatic	Exchange-repulsion
induction	Exchange-induction
Dispersion	Exchange-Dispersion
Resonance	charge transfer
magnetic	
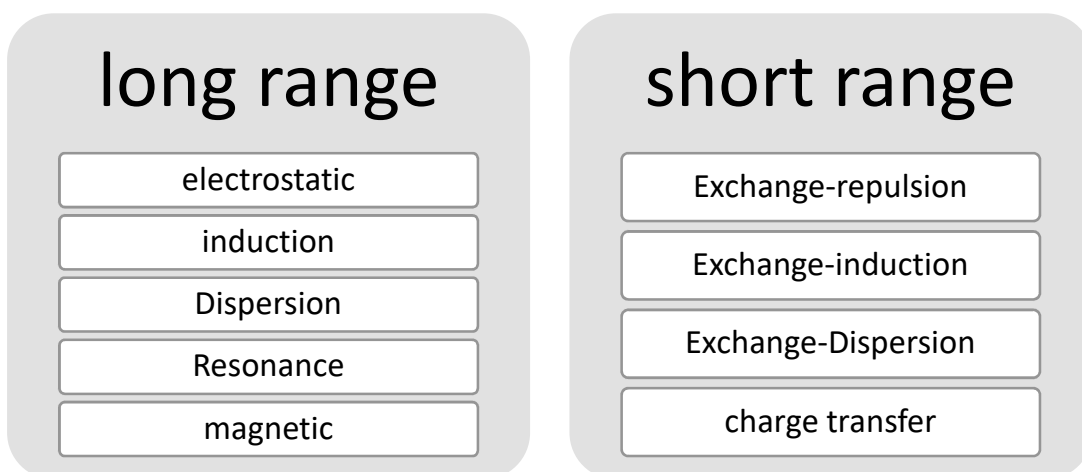
On other hand, as for the case of the long-range interactions, we distinguish three kinds: the first is the electrostatic forces, which arise from the classical static interactions between molecules' charge distributions which can be either repulsive or attractive, and these are strictly pairwise additive and can be attractive or repulsive [3, 17].

2.1. Van der Waals forces:

The long-range forces manifested in the induction and dispersion interactions fall in the category of known van der Waals forces **Fig.(2.2)**, and in this category, we recognise three know types of forces that have been identified and modelled and proved to have the same mathematical form as the one proposed for the intermolecular forces following the work of wang [2]. These forces are as follows:

- **Keesom interactions:** this force is purely electrostatic with it happening between excited molecules with permanent dipoles.
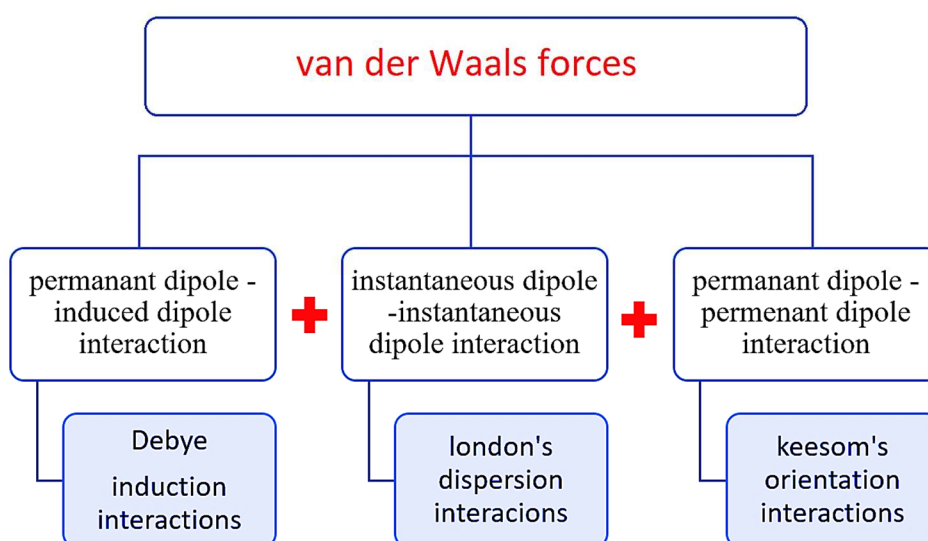
Figure 2.2: classification of van der Waals forces.

- **Debye interactions:** the induction force named after Peter J.W. Debye is the force that rises due to the existence of an excited permanent dipole which induces a neutral molecule at proximity producing another dipole.
- **London interactions**: or dispersion forces occurs from the interactions of instantaneous dipoles rising from the quantum fluctuations of electronic clouds in molecules/atoms which means that these forces are purely quantum mechanical and universal meaning that it happens between any two atoms at close sufficient distance to each other.

For most of the cases, the dispersion forces are the dominant contribution to the total van der Waals interactions, except in the case of highly polar materials in which other contributions become crucially important. Due to this fact, in most situations where the van der Waals forces are modelled, Keesom's and Debye's forces are neglected to focus thus only on dispersion London interactions. the table below shows some examples of the contribution of dispersion forces to the overall interaction [3].

Table 2.2: contribution of dispersion London forces to the intermolecular interaction, for different molecules with different polarity [3].

Interacting species	The contribution of London forces to the vdW forces in (%)
Ne-Ne	100
HBr-HBr	96
HCl-HCl	86
NH_3-NH_3	57
H_2O-H_2O	24

3. Quantum mechanical discerption:

In order to model the interaction between atoms or molecules, we introduce here in this chapter a quantum mechanical approach which hopefully would give the reader the sufficient and coherent knowledge about the nature of these forces and their origins.

3.1. The Born–Oppenheimer approximation:

As it is known from basic quantum theory, The behaviour of a system of non-relativistic particles in time independent potentials is governed by the time-independent Schrödinger equation [17, 19]:

$$H\left|\Psi\right\rangle = E\left|\Psi\right\rangle \tag{2.4}$$

Where H is the Hamiltonian operator and E is the energy the eigenvalue of the operator and Ψ is the wave function of the system under consideration. The Hamiltonian operator can be given as follows [17, 20, 21]:

$$H = -\frac{1}{2}\sum_{i=1}^{N}\frac{\hbar^2}{M_i}\vec{\nabla}_i^2 - \frac{1}{2}\sum_{j=1}^{n}\frac{\hbar}{m_e}\vec{\nabla}_j^2$$

$$+ \frac{e^2}{4\pi\varepsilon_0}\left(\sum_{\substack{i,i'=1\\i'>i}}^{N}\frac{Z_i Z_{i'}}{|R_{i'}-R_i|} - \sum_{i=1}^{N}\sum_{j=1}^{n}\frac{Z_i}{|r_j-R_i|} + \sum_{\substack{j,j'=1\\j'>j}}^{n}\frac{1}{|r_{j'}-r_j|}\right) \quad (2.5)$$

Where **Z** is the charge of the nucleus "i", e is the charge of the proton, and $\vec{\nabla}_j^2$ and $\vec{\nabla}_j^2$ are the Laplacians which operate on nuclear and electronic coordinates, respectively [20]. The physical interpretation of the terms of this Hamiltonian is well defined, and by that, it can be rewritten in a simplistic form as follows [20]:

$$H = \hat{T}_e + \hat{T}_n + \hat{V}_{ee} + \hat{V}_{nn} + \hat{V}_{en} \quad (2.6)$$

Where the first two terms $\hat{T}_e$ and $\hat{T}_n$ are the kinetic energies of the nucleus and electrons respectively, $\hat{V}_{nn}$ is the potential energy of the repulsions between the nuclei and $\hat{V}_{ee}$ is that between the electrons, and the last term $\hat{V}_{en}$ is the coulomb potential of the attractive force between electrons and nuclei.

The Schrödinger equation generally cannot be solved analytically, thus several approximations are needed to find a satisfactory solution. One of such methods is stated so that the heavy nuclei which have smaller velocities compared to that of the electrons, is then considered to be perceived by electrons as fixed in space. in such a picture the Schrödinger equation can be separated into two distinctive parts, where each one describes the electronic and nuclear wave functions respectively. By using this method which is known as the Born–Oppenheimer approximation, the problem is reduced to solving the electronic Schrödinger equation [17, 20]:

$$\left(H_{el} + V_{nuc}\right)\psi_{el} = E\psi_{el} \quad (2.7)$$

With the Hamiltonian assigned to describe the motion of the electrons is given as :

$$H_{el} = -\frac{\hbar^2}{2m_e}\sum_{j=1}^{n}\vec{\nabla}_j^2 - \frac{e^2}{4\pi\varepsilon_0}\sum_{j=1}^{N}\sum_{i=1}^{n}\frac{Z_i}{r_{ji}} + \frac{e^2}{4\pi\varepsilon_0}\sum_{\substack{j,j'=1\\j'>j}}^{n}\frac{1}{r_{jj'}} \quad (2.8)$$

The electronic energy includes the contribution from internuclear repulsion, meaning that even though the nuclear-nuclear repulsion potential does not affect the solution of the Schrodinger equation but rather shift its eigenvalues [17, 22]:

$$E = E_{el} + V_{nuc} \quad (2.9)$$

V can be neglected in **Eq.(2.7)** which leaves us with the electronic Schrödinger equation:

$$H_{el}\psi_{el} = E_{el}\psi_{el} \tag{2.10}$$

The eigenfunction of the is problem is the electronic wavefunction which describes the motion of electrons. Although this wavefunction is independent of the momenta of the nuclei, it has a parametric dependence on their positions.

$$\psi_{el} = \psi_{el}\left(\vec{r}_j, \{\vec{R}_i\}\right) \tag{2.11}$$

The Schrödinger equation is then solved for different nuclear configurations where each of them corresponds to a different molecular electronic state. The same assumptions can be set for the case of nuclear motion, where we consider that as the nuclei move, the electronic energy changes smoothly as a function of R_i. Hence, have the nuclear Schrödinger Equation:

$$H_{nuc}\psi_{nuc} = E_{mol}\psi_{nuc} \tag{2.12}$$

Where the is the potential energy for nuclear motion in the average field of the electrons, and the nuclear Hamiltonian is written as follows:

$$H_{nuc} = -\frac{1}{2}\sum_{i=1}^{N}\frac{\hbar^2}{M_i}\vec{\nabla}_i^2 + E\left[\{\vec{R}_i\}\right] \tag{2.13}$$

The general approximation of the molecular wavefunction appearing in **Eq.(2.1)** can be written thus to be as follows [17] :

$$\Psi\left(\vec{r}_j, \{\vec{R}_i\}\right) = \psi_{el}\left(\vec{r}_j, \{\vec{R}_i\}\right)\psi_{nuc}\left(\{\vec{R}_i\}\right) \tag{2.14}$$

Since the electronic energy E_{el} is a function of nuclear coordinates, it may be used to define the concept of an intermolecular potential or an interaction energy which is the case we are interested about in this work. Solving this wave equation is not evident and difficult to solve, and this difficulty is mainly due to The Coulombic repulsion term in the Hamiltonian of this problem since it makes it impossible separated the Hamiltonian into distinct components for each electron [17, 22].

3.2. Perturbation theory approximation:

When we have a time-independent Schrodinger equation the solution can be approximated using time-independent perturbation theory which alters SE to be written as follows [19, 22]:

$$\left(H_0 + \lambda H_{int}\right)|\psi\rangle = E_i|\psi\rangle \tag{2.15}$$

Where the parameter λ is a number that changes from 0 to 1. At the end of calculations, this parameter is eliminated by setting it equal to 1, which corresponds to the case where the perturbation is acting fully. When $\lambda=0$, **Eq.(2.15)** is reduced to the unperturbed problem stated in following eigenvalue equation [17, 22]:

$$H_0 \left| \psi^{(0)} \right\rangle = E_i^{(0)} \left| \psi^{(0)} \right\rangle \tag{2.16}$$

Where H_0 is the unperturbed Hamiltonian, E_0 is the energy of the unperturbed system. Thus, the state of this quantum system in this approach is approximated by a series that is written in power of λ as follows:

$$\left| \psi \right\rangle = \left| \psi^{(0)} \right\rangle + \lambda \left| \psi^{(1)} \right\rangle + \lambda^2 \left| \psi^{(2)} \right\rangle + \cdots \tag{2.17}$$

And similarly, the energy of the system is written as:

$$E_i = E_i^{(0)} + E_i^{(1)} + E_i^{(2)} + \cdots \tag{2.18}$$

Where $\left| \psi^{(1)} \right\rangle$, $\left| \psi^{(2)} \right\rangle$, ... and $E^{(1)}$, $E^{(2)}$, ...are perturbative corrections to the unperturbed wavefunction $\left| \psi^{(0)} \right\rangle$ and energy $E^{(0)}$, respectively. We have the formulas for these series in terms of the unperturbed state **(Eq.2.19)** and energy **(Eq.2.20)**, and they are given as follows[17]:

$$\left| \psi \right\rangle = \left| \psi_i^{(0)} \right\rangle + \sum_{j^{(0)} \neq i^{(0)}} \frac{\left\langle \psi_j^{(0)} \left| H \right| \psi_i^{(0)} \right\rangle}{E_i^{(0)} - E_j^{(0)}} \left| \psi_j^{(0)} \right\rangle + \cdots \tag{2.19}$$

And

$$E_i = E_i^{(0)} + \left\langle \psi_i^{(0)} \left| H_{\text{int}} \right| \psi_i^{(0)} \right\rangle + \sum_{j^{(0)} \neq i^{(0)}} \frac{\left\langle \psi_i^{(0)} \left| H_{\text{int}} \right| \psi_j^{(0)} \right\rangle \left\langle \psi_j^{(0)} \left| H_{\text{int}} \right| \psi_i^{(0)} \right\rangle}{E_i^{(0)} - E_j^{(0)}} + \cdots \tag{2.20}$$

The solution then is reduced to the problem of finding the ground unperturbed state and then derive the corrections through the formulas proposed within the perturbative framework.

3.3. The interaction of two molecules:

For a system of two interacting atoms we can present the unperturbed Hamiltonian of this system as the sum of molecular Hamiltonians of the two species [17]:

$$H_0 = H_0^A + H_0^B \tag{2.21}$$

The eigenstates of this Hamiltonian are product wavefunctions $\psi_m^A \psi_n^B$, and its eigenenergy is given as the sum:

$$\begin{aligned}
H_0 \left| \psi_m^A, \psi_n^B \right\rangle &= \left(H_0^A + H_0^B \right) \left| \psi_m^A, \psi_n^B \right\rangle \\
&= \left(E_m^A + E_n^B \right) \left| \psi_m^A, \psi_n^B \right\rangle \\
&= E_0 \left| \psi_m^A, \psi_n^B \right\rangle
\end{aligned} \tag{2.22}$$
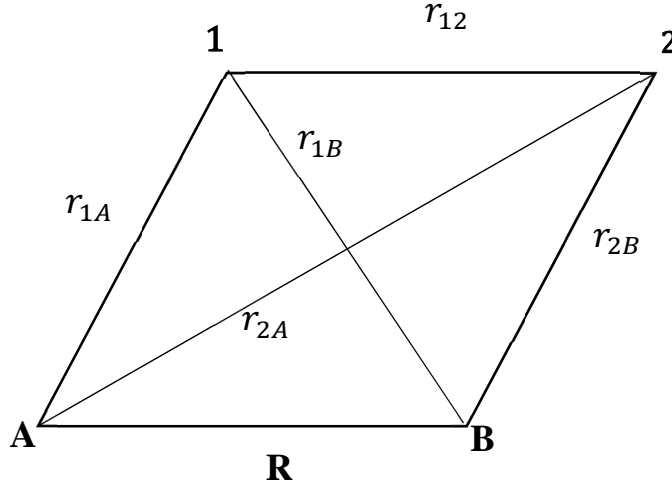
Figure 2.3: model case used to calculate dispersion interactions between two hydrogen atoms A and B with electrons 1 and 2 respectively

For this system of two isolated molecules and from perturbation theory presented above the energy can be written with respect to the interaction potential $V(A, B)$ as follows:

$$E = E_s^B + E_r^A + \left\langle \psi_S^B, \psi_r^A \left| V\left(A, B\right) \right| \psi_r^A, \psi_S^B \right\rangle$$

$$- \sum_m \sum_n \frac{\left| \left\langle \psi_0^B, \psi_0^A \left| V\left(A, B\right) \right| \psi_0^A, \psi_0^B \right\rangle \right|^2}{\left(E_m^A + E_n^B\right) - \left(E_0^A + E_0^B\right)} + \cdots \qquad (2.23)$$

Where the energy and the wavefunctions of the isolated molecules are E_r^A, E_s^B and E_r^A, E_s^B, respectively.

The perturbation is defined as the interaction potential V (A, B) which defines the electrostatic interaction between the particles α (electrons and nuclei) constituting molecule A and those from B. This potential is defined as the sum of all those interactions, and it is written as follows [6, 17]:

$$V\left(A, B\right) = \frac{1}{4\pi\varepsilon_0} \sum_{\alpha \in A} \sum_{\beta \in B} \frac{e_\alpha^A e_\beta^B}{r_{\alpha\beta}} \qquad (2.24)$$

Where e_α^A and e_β^B are the charges of the interacting constituent particles of molecules A and B respectively, and $r_{\alpha\beta}$ is the distance between these particles. this potential can be rewritten with respect to charge distribution by introducing a mathematical formula including delta function. A more detailed of this transformation is thoroughly found in stone (2013) [6].

The charge distribution of particles can be expanded as a Taylor series and so be expressed it in terms of electric multipole moments, this expansion produces the perturbation operator which is written as follows [6, 17, 23]:

$$V(A,B) = \frac{1}{4\pi\varepsilon_0} \begin{cases} \sum\limits_{\alpha} \dfrac{e_{\alpha}^A e_{\beta}^B}{r} + \left(\sum\limits_{\alpha} e_{\alpha}^A \mu_i(B)T_i - \sum\limits_{\beta} e_{\beta}^B \mu_i(A)T_i \right) \\[2mm] -\mu_i(A)\mu_j(B)T_{ij} + \left(\sum\limits_{\alpha} e_{\alpha}^A Q_{ij}(B)T_{ij} - \sum\limits_{\beta} e_{\beta}^B Q_{ij}(A)T_{ij} \right) \\[2mm] -\left(\mu_i(A)Q_{jk}(B)T_{ijk} - \mu_i(B)Q_{jk}(A)T_{ijk} \right) + Q_{ij}(B)Q_{kl}(B)T_{ijkl} \\[2mm] +\left(\sum\limits_{\alpha} e_{\alpha}^A Q_{ijk}(B) - \sum\limits_{\beta} e_{\beta}^B Q_{ijk}(A) \right) T_{ijk} + \cdots \end{cases} \tag{2.25}$$

The terms of this series express the monopole-monopole, charge-dipole, dipole-dipole interactions [17]. Following stone (2013)[6], we present a tensorial representation of the gradient operators developed from the multipole expansion which is presented in the general formula as follows:

$$T_{ij\cdots\zeta} = \vec{\nabla}_i \vec{\nabla}_j \cdots \vec{\nabla}_\zeta \frac{1}{r} \tag{2.26}$$

For neutral atoms /molecules the terms with charge contribution vanishes, which leads to the series to be written as follows [17] :

$$V(A,B) = \frac{1}{4\pi\varepsilon_0} \begin{cases} -\mu_i(A)\mu_j(B)T_{ij} - \left(\mu_i(A)Q_{jk}(B)T_{ijk} \\[2mm] -\mu_i(B)Q_{jk}(A)T_{ijk} \right) + Q_{ij}(B)Q_{kl}(B)T_{ijkl} + \cdots \end{cases} \tag{2.27}$$

From the definition of the gradients, the tensor elements are expressed as follows:

$$T = -\frac{\widehat{u}_i}{r^2} \tag{2.28}$$

$$T_{ij} = -\frac{1}{r^3}\left(I_{ij} - 3\widehat{u}_i\widehat{u}_j \right) \tag{2.29}$$

$$T_{ijk} = \frac{3}{r^4}\left(I_{ij}\widehat{u}_k + I_{ik}\widehat{u}_j + I_{jk}\widehat{u}_i - 5\widehat{u}_i\widehat{u}_j\widehat{u}_k \right) \tag{2.30}$$

These tensorial gradient elements are very important since they play a key role in the calculations of the atomistic approach which is studied and formulated in chapter 4 in this dissertation.

3.4. Deriving long-range forces:

When the perturbation operator is introduced to the perturbed energy written in the series in **Eq.(2.25)** we end up with this operator acting on each order of perturbation separately, through calculation we recognise that each order presents a type of interaction, with the first order perturbation, is the origin of electrostatic interactions and the second order contains both induction and dispersion forces. Thus, the total interaction energy results from subtracting the energies of the molecules from the total perturbed energy which leaves us with the energy

associated from long range interactions to be written as the sum of the different types of these forces as follows [17, 24]:

$$E_{long\ range} = E_{elelctrostatic} + E_{induction} + E_{dispersion} \tag{2.31}$$

Since we are interested in this work only about the interaction between electrically neutral bodies the first term vanishes, leaving us with only the second order perturbation term. The second-order describes both induction and dispersion energies. To demonstrate this, we consider separately the terms in the sum for only one molecule is excited and the other is in its ground state which presents the induction interactions, and the terms where both of them are excited [6]. The second-order correction can thus be written as the sum of the contributions to the intermolecular interaction energy arising from those three terms [17].

$$E^{(2)} = E_{ind}^{A} + E_{ind}^{B} + E_{disp} \tag{2.32}$$

Giving each contribution is calculated in the perturbative approach as follows [6, 17]:

$$E_{ind}^{A} = -\sum_{m \neq 0} \frac{\langle E_0^B, E_0^A | V(A,B) | E_m^A, E_0^B \rangle \langle E_0^B, E_m^A | V(A,B) | E_0^A, E_0^B \rangle}{E_m^A - E_0^A} \tag{2.33}$$

$$E_{ind}^{B} = -\sum_{n \neq 0} \frac{\langle E_0^B, E_0^A | V(A,B) | E_0^A, E_n^B \rangle \langle E_n^B, E_0^A | V(A,B) | E_0^A, E_0^B \rangle}{E_n^B - E_0^B} \tag{2.34}$$

$$E_{disp} = -\sum_{m \neq 0}\sum_{n \neq 0} \frac{\langle E_0^B, E_0^A | V(A,B) | E_m^A, E_n^B \rangle \langle E_n^B, E_m^A | V(A,B) | E_0^A, E_0^B \rangle}{\left(E_m^A + E_n^B\right) - \left(E_0^A + E_0^B\right)} \tag{2.35}$$

The induction energy E_{ind} can be simplistically understood as a classical electrostatic interaction between a permanent multipole moments of one monomer with the induced multipole moments of the second [3, 25]. To further simplify the situation we consider that the interaction does not involve any polar species (i.e. no permanent dipoles), therefore the only contribution that survives and exists for all cases is that of dispersion interactions [3].

4. Dispersion forces:

These forces are relatively weak, which makes perturbation theory as the most suitable method to calculate them [6], the first assumption to be introduced to simplify the calculations of dispersion energy is to ignore the overlap of the wave functions by considering the distance is much bigger than molecules dimensions[17]. Although in practice this overlap is never null, yet this approximation hold since we consider that the error decreases rapidly with increasing distances, and even in fairly short distances the error is marginal and this overlap can be excluded from the theory [6].

There are two main approaches that we can take to study and calculate the interaction between molecules/ atoms, the first one is the quantum mechanical perturbative approach which we have set its theoretical basics above, and it is the one first used by London to evaluate the

full theory that describes dispersion forces between molecules [5, 6]. This can be accomplished by substituting the perturbation potential operator within the formula derived for dispersion energy from the second order correction terms. A simple form would be by considering only the first term of the operator which describes the dipole-dipole interaction and disregard higher multipole interactions [17, 26]. Using the tensorial representation presented above we find that the dipole-dipole energy is written as follows, Where the states $|0\rangle$, $|m\rangle$, $|0'\rangle$ and $|n\rangle$ symbolize $|\psi_0^A\rangle$, $|\psi_m^A\rangle$, $|\psi_0^B\rangle$ and $|\psi_n^B\rangle$[5, 6]:

$$E_{disp} = \frac{1}{(4\pi\varepsilon_0)^2} T_{ij} T_{i'j'} \sum_{n \neq 0} \sum_{m \neq 0} \frac{\langle 0|\mu_i^A|m\rangle\langle m|\mu_j^A|0\rangle\langle 0'|\mu_k^B|n\rangle\langle n|\mu_l^B|0'\rangle}{\left(E_m^A + E_n^B\right) - \left(E_0^A + E_0^B\right)} \qquad (2.36)$$

The first term of tensor product produces energy dependence on the distance by a factor r^{-6}, the last term can be developed using Unsöld or average-energy approximation, following London (1937) [5, 6, 27]. Nevertheless even though with this approximation it is still impossible to evaluate the exact value of the energy a more detailed discussion of these calculations would be found to be sufficient in [6]. Going on with further simplifications of this model lead us to the famous formula proposed by London [5, 28, 29]:

$$E_{disp}(r) = -\left\{ \frac{3}{2} \hbar \frac{\omega_1 \omega_2}{\omega_1 + \omega_2} \alpha_1(0) \alpha_2(0) \right\} \frac{1}{r^6} \qquad (2.37)$$

Where $\hbar$ is the reduced Planck constant, ω_1 and ω_2 are the characteristic frequencies of the two species, and α_1 and α_2 are the static polarizabilities of those species and r is the distance between the centre points of the interacting atoms/molecules [3, 26, 30]. The first term inside the bracket is the constant C_6 which is related to the nature of the interacting species, which leads us to the formula stated before for the dispersion energy between molecules (**Eq.2.3**).

The other method is the Drude model which was also used by London in his paper [5], and in this approach constituents of matter (atoms/molecules) are replaced by harmonic dipole oscillators [4] in which the electron cloud is attached to the nucleus by a harmonic potential. The atomic dipole is proportional x the displacement of electrons from the centre of the nucleus, and the interaction energy of two adjacent dipoles is proportional to the product their moments. Accordingly, the Hamiltonian for the system is written in the form [6]:

$$H = \frac{1}{2m}\left(p_A^2 + p_B^2\right) + \frac{1}{2}k\left(x_A^2 +_B^2 + 2cx_A x_B\right) \qquad (2.38)$$

where c is a coupling constant, m is the mass of the electronic cloud and k is the force constant. This equation can be separated into two uncoupled oscillators [6]:

$$H = \frac{1}{4m}\left(p_A + p_B\right)^2 + \frac{1}{4}k\left(1+c\right)\left(x_A + x_B\right)^2$$
$$+ \frac{1}{4m}\left(p_A - p_B\right)^2 + \frac{1}{4}k\left(1-c\right)\left(x_A - x_B\right)^2 \qquad (2.39)$$

Therefore, the normal mode frequencies $\omega_\pm$ can be written as $\omega_0\sqrt{1 \pm c}$, where ω_0 is the frequency of an isolated oscillator which is related to the zero-point energy[2] that is known to be equal to $\hbar/2\omega_0$ [5, 11]. The lowest energy of this coupled system is given as follows [6]:

$$E_0 = \frac{1}{2}\hbar\left(\omega_+ + \omega_-\right) \tag{2.40}$$

By substituting the normal mode frequencies with their relation stated above and expand the square root; the energy is found to be given as [6]:

$$E_0 = -\frac{1}{2}\hbar\omega_0\left(2 + \frac{1}{4}c^2 + \frac{5}{64}c^4 + \cdots\right) \tag{2.41}$$

The first term of this series presents simply the self-energy of the coupled system when this energy is subtracted from the total energy we are left with the other terms presenting the dispersion energy with the first surviving term is equivalent to the result found from perturbation theory for a system of identical particles [5] :

$$E_{disp} = -\left(\frac{3\hbar\omega_0\alpha^2}{4}\right)\frac{1}{r^6} \tag{2.42}$$

Table 2.3: Strength of Dispersion Interaction between Quasi-Spherical Nonpolar Molecules of Increasing Size [3].

Molecules	Molecular Diameter (nm)	Polarizability $\alpha_0/4\pi\varepsilon_0$ (10^{-30} m^3)	London Constant "C_6" (10^{-79} Jm^6)	
			Theoretical	Measurement
Ne-Ne	0.308	0.39	3.9	3.8
Ar-Ar	0.376	1.63	50	45
CH$_4$-CH$_4$	0.400	2.60	102[c]	101[c]
Xe-Xe	0.432	4.01	233	225
CCl$_4$-CCl$_4$	0.550	10.5	1520	2960

5. The Axilrod-Teller-Muto (ATM) potential

For a system of more than three neutral molecules interacting between them, if the perturbation calculation is pursued to the third order, interactions between triplets of atoms appear [31]. In these calculations, induction forces are neglected and many-body repulsion and

---

[2] Zero-point energy is the lowest level of energy a quantum system has, this force is also known to be related to quantum fluctuations of vacuum which are used to calculate the interaction between macroscopic bodies as Casimir did in the case of conducting plates. They can be explained as the energy related to creation and annihilation of virtual particles in the quantum vacuum state.

dispersion terms are included (ElrodandSaykally1994). The formula for this interaction from the perturbative approach is written as follows [6, 17, 31, 32] :

$$E^{(3)} = \sum_m \sum_n \sum_l \frac{\langle 000|V_{int}^{AB}|mn0\rangle\langle mn0|V_{int}^{BC}|m0\ell\rangle\langle m0\ell|V_{int}^{CA}|000\rangle}{\left(\Delta E_{m0}^A + \Delta E_{n0}^B\right)\left(\Delta E_{m0}^A + \Delta E_{\ell0}^C\right)} \qquad (2.43)$$

where V is the interaction Hamiltonian between any two molecules. The bra/kets that express the state of the system is the product of the states of the three interacting molecules A, B and C in order, where 0 indicates the ground state of that wavefunction and m, n, and l are the excited states of these molecules respectively [6]. The result is the Axilrod–Teller–Muto triple-dipole dispersion interaction, which was first given independently by Axilrod and Teller (1943) and by Muto (1943):

$$E^{(3)} = C_9 \frac{\left(1 + 3\cos\theta_A \cos\theta_B \cos\theta_C\right)}{r_{AB}^3 r_{BC}^3 r_{AC}^3} \qquad (2.44)$$

For a linear triplet of interacting dipoles, which means the angles are $\theta_B = \theta_C = 0°$ and $\theta_A = 180$, the formula of the interaction energy becomes as follows [31] :

$$E^{(3)} = -C_9 \frac{2}{r_{AB}^3 r_{BC}^3 r_{AC}^3} \qquad (2.45)$$

Where the constant C_9 is written in terms of complex dynamic polarizabilities of the three interacting molecules as follows [6]:

$$C_9 = \frac{3\hbar}{\pi} \int_0^\infty \alpha^A(i\omega)\alpha^B(i\omega)\alpha^C(i\omega)d\omega \qquad (2.46)$$
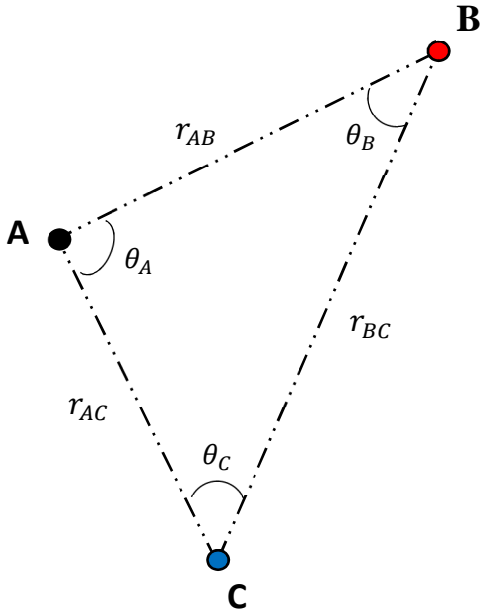
Figure 2.4 : The case model proposed first by Axilrod and Teller (1943) for a system of three neutral non-polar atoms (A, B and C) interacting with dispersion forces. Where the arbitrary geometrical configuration depends on r_{AB}, r_{BC} and r_{CA} the distances between these atoms and the angles θ_C, θ_C and θ_C, which they produce with respect to each other.

If we consider the interacting molecules are identical, A simpler formula is given in terms of the static polarizabilities as follows [33]:

$$C_9 = \frac{9}{16} \hbar \omega_0 \alpha^3 \tag{2.47}$$

The geometrical factor which depends on the angles makes this potential different from ordinary dipole-dipole dispersion interaction derived by London because as a result of this trigonometric dependence on the geometrical configuration of the triplet under consideration, the force can thus be repulsive for certain geometries, whereas the London interaction is always attractive [6]

6. Retardation effect:

6.1. Theoretical developments:

In the previous sections we introduced the calculation of dispersion forces by means of perturbative quantum theory, yet these calculations assume the instantaneity of the interaction, and do not hold any information about the delay in the interaction that results from the limited speed of electromagnetic waves transmitted from and to the involved molecules [4, 6]. The picture depicted within this approach is presented graphically in **Fig.(2.5)** using the rules of Feynman diagrams where we notice that the interaction potential does not evolve in time meaning the interaction is instantaneous.

When the Schrodinger formalism stated earlier in this chapter is adopted, the problem becomes more difficult to solve including retardation. this is due to the fact that this approach is non-relativistic and does not include the propagation of fields assuming thus static interaction potentials between electrons [17].
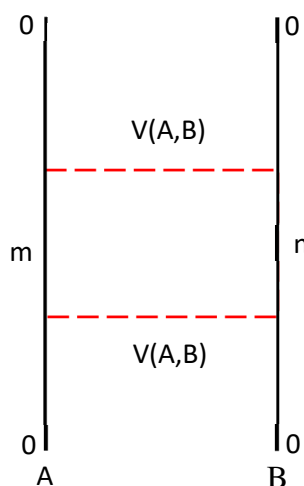
Figure 2.5:

The Feynman diagram representing the Contribution of static dipole-dipole interaction to dispersion potential at second-order of perturbation theory. The solid vertical lines represent the state of the interacting species , time flows upward, and the dashed horizontal lines depicts the instantaneous interaction [1].

A realistic relativistic picture would involve this retardation, where the virtual photons which are transmitted from molecule A take at the time r_{AB}/c to reach and polarize the other molecule B, then this latter molecule reacts and responds by another photon which also takes the same amount of time leading to an overall delay of about r_{AB}/c. at large separations, This effect leads to a weaker correlation and ultimately to the decrease of the intensity of the dispersion interaction between molecules [4, 17, 28].
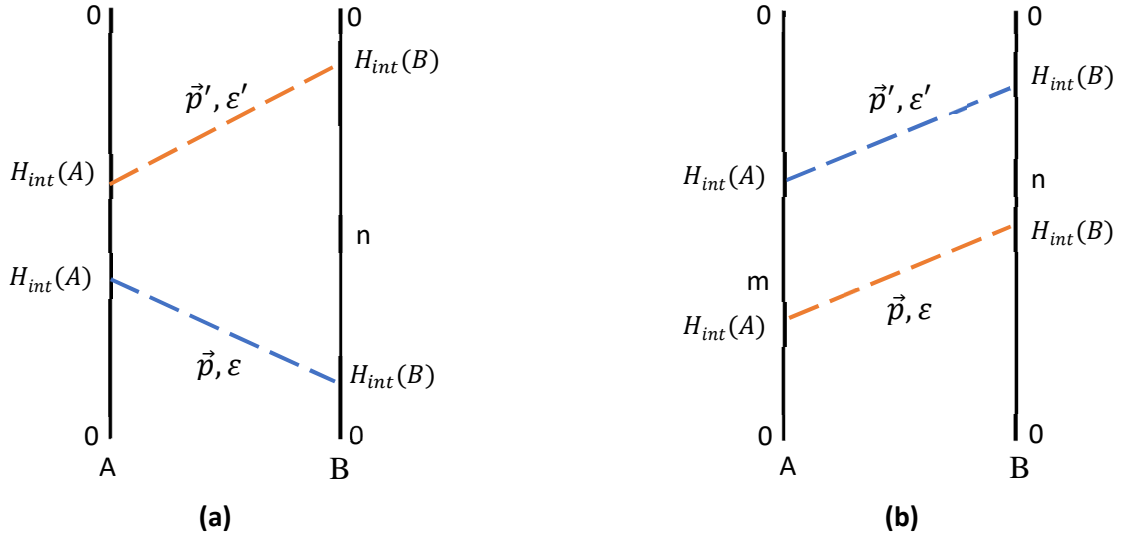
Figure 2.6: Two examples of the twelve time-ordered Feynman diagrams used for calculating the retarded dispersion potential where the two molecules exchange two photons with the modes $\vec{p}', \varepsilon'$ and $\vec{p}, \varepsilon$ [17, 34].

The inclusion of this effect to the Schrodinger formalism is possible using the same concept used in the retarded oscillator model [4]. Consequently, it is essential to introduce time-dependent interaction potentials and this can be achieved by using diagrammatic time-dependent perturbation theory to introduce time into the calculations and thus introduce retardation to the state of the system [35]. As it was inferred earlier in this section, dispersion interactions are understood as a result of the exchange of virtual photons between the coupled molecules. Therefore, for two nonpolar neutral molecules A and B, where both are in their electronic ground states, the total Hamiltonian for the system is given by [17].

$$H = H_0 + H_{int} \tag{2.48}$$

Where the ground state Hamiltonian H_0 includes the molecular Hamiltonians H_A and H_B of the both interacting species A and B respectively, and the contribution H_{rad} from the radiation field Hamiltonian. Additionally, the interaction Hamiltonian can be also written as the sum of the interaction Hamiltonians of individual molecules[17, 34]:

$$H_{int} = H_{int}(A) + H_{int}(B) \tag{2.49}$$

Going through the tedious calculation of the different approaches proposed to solve the problem we find the same result demonstrated by Casimir and polder [8] which states that the interaction between two neutral atoms at short distances is proportional to r^{-6}, a similar result to that of London's non-retarded model. However, when the distance between the interacting species becomes very large, the retardation becomes significant leading the forces to decay faster proportional to r^{-7} [8]. And the formula for the ratardid dispersion interaction energy is given as follows:

$$E\left(r \gg \lambda\right) = -\hbar c \, \frac{23}{4\pi} \cdot \frac{\alpha_1 \alpha_2}{r^7} \tag{2.50}$$

Where c is the speed of light, $\hbar$ is the reduced Planck constant, α_1 and α_2 are the static polarizabilities of the tow species and r is the distance between their centre points.

6.2. Correction function approximation:

When attempting to produce a single model that expresses both regimes retarded and non-retarded, dispersion interaction energy between two molecules $E(r)$, is approximated by introducing a correction factor $f(p)$ to the London non-retarded dispersion energy [36, 37]:

$$E\left(r\right) = -\frac{C_6}{r^6} f\left(p\right) \tag{2.51}$$

Where $f(p)$ depends on p (the dimensionless reduced distance) which is given by $p = 2\pi r/\lambda$, With λ is the Characteristic wavelength which is generally set with the value 100 nm [36, 37].

These correction factors are derived numerically using interpolation and data fitting techniques to produce simple function from the exact data calculated by the means of quantum electrodynamical techniques used by Casimir. The earliest Overbeek approximation was proposed by Overbeek and Kruyt [38], their model was expressed by an empirical function of two parts, where each part is valid within a certain range of the distance or in this case the reduced distance:

$$f\left(p\right) = \begin{cases} 1.10 - 0.14p & \text{for } p \in \left]0;3\right[\\ 2.45/p - 2.04/p^2 & \text{for } p \in \left]3;\infty\right[\end{cases} \tag{2.52}$$

A second-hand approximation of Overbeek's expressions was later introduced by Schenkel and Kitchener [39]. their model was written in a single relation written as follows :

$$f\left(p\right) = 2.45/p - 2.17/p^2 + 0.59/p^3 \tag{2.53}$$

The approximation was under the condition that the reduced energy is bigger than 0.5. nevertheless, when This equation is compared to Overbeek's model gave a discrepancy less than 15% for large distances [37, 39]. A better expression of the correction function $f(p)$ which was derived from numerically from Casimir's calculations was proposed by Nandarajah and Chen [40]. Their formula was fairly accurate when compared to the data from Casimir's model, giving thus an error less than 10%, which makes it the most precise approximation found in the terature to date.

$$f\left(p\right) = \frac{b}{p+b} \tag{2.54}$$

Where b=3.1

These models are compared graphically in **Fig.(2.7)**, where we show that for distance larger than the characteristic wavelength (i.e. larger than 100 nm) these models coincide giving close

results with the discrepancy decreasing with larger distances. However, we notice that for small distances the model proposed by Schenkel and Kitchener produces extremely erroneous results with an error reaching 10^3 % for close proximities nevertheless the other functions still give close results which reasonably describe the effect of retardation.
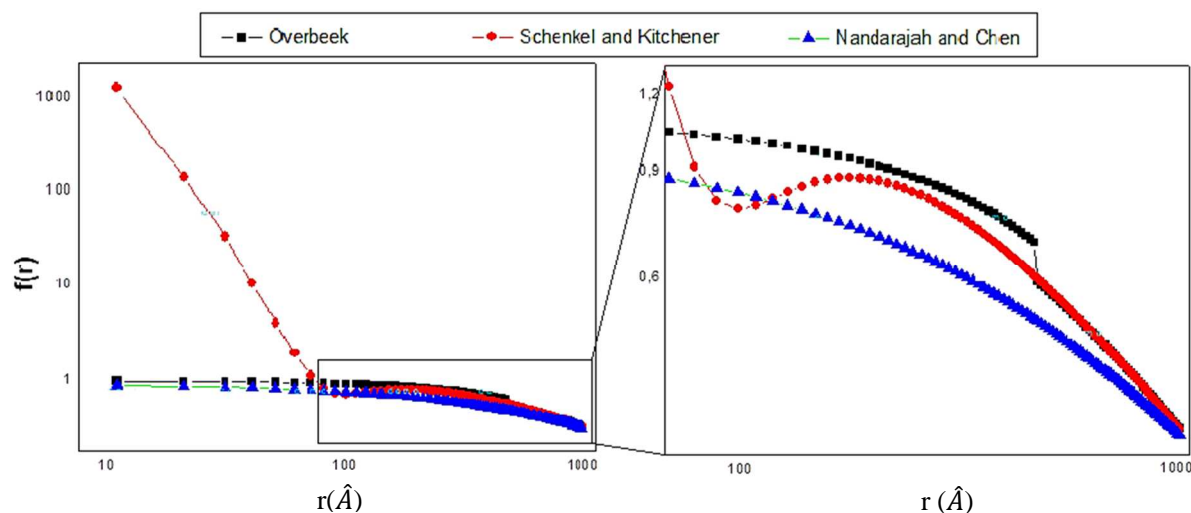
Figure 2.7: comparison between the three correction functions for increasing distances.

Although these approximations are crude, yet they have been very useful for developing models of the interaction between macroscopic bodies which include the effect of retardation Their application and resulting models are demonstrated in the next chapter.

7. conclusions:

We have surveyed and built the basic theoretical formulation of dispersion interactions between molecules and atoms, where we used for this approach the quantum theory concentrating on the application of perturbation theory to describe the origins and behaviour of these interactions between nonpolar particles. the effect of retardation is also explained and the basic physical interpretation of this phenomena is demonstrated in a simple way. In the end, a semiclassical method which was used also in literature is demonstrated, where the retardation is approximated by a correction function added to the formula of non-retarded dispersion forces which was demonstrated earlier by London. This chapter is a keystone for any initiation into the subject of dispersion interactions. And a building block for the subsequent chapters.

References

1. Van der Waals, J. D. (1873). *Over de Continuiteit van den Gas-en Vloeistoftoestand* (Vol. 1). Sijthoff.
2. Rowlinson, J.S.,(2005), *Cohesion: a scientific history of intermolecular forces*: Cambridge University Press, Cambridge, UK.
3. Israelachvili, J.N.,(2011), *Intermolecular and surface forces*: Academic press.
4. Langbein, D., (1974), *Theory of van der Waals Attraction*, in *Springer tracts in modern physics*Springer. p. 1-139.
5. London, F., (1937), *The general theory of molecular forces.* Transactions of the Faraday Society. **33**: p. 8b-26.

6. Stone, A.,(2013), *The theory of intermolecular forces*: Oxford University Press, Oxford, UK.

7. Hamaker, H., (1937), *The London—van der Waals attraction between spherical particles.* Physica. **4**(10): p. 1058-1072.

8. Casimir, H. and D. Polder, (1948), *The influence of retardation on the London-van der Waals forces.* Physical Review. **73**(4): p. 360.

9. Casimir, H.B. *On the attraction between two perfectly conducting plates*. in *Proc. Kon. Ned. Akad. Wet.* 1948.

10. Rodriguez, A.W., F. Capasso, and S.G. Johnson, (2011), *The Casimir effect in microstructured geometries.* Nature photonics. **5**(4): p. 211.

11. Milonni, P.W.,(2013), *The quantum vacuum: an introduction to quantum electrodynamics*: Academic press, Cambridge, Massachusetts

12. Simpson, W.M. and U. Leonhardt,(2015), *Forces of the quantum vacuum: An Introduction to Casimir Physics*: World Scientific Publishing Company.

13. E. Lifshitz,(2012) , *The theory of molecular attractive forces between solids*, in : J.Sykes, and D. Ter Haar, Perspectives in Theoretical Physics : The Collected Papers of E.M.Lifshitz, pp. 329-349, Pergamon Press .

14. Israelachvili, J.N.,(2011), *Intermolecular and surface forces: revised third edition*: Academic press, Cambridge, Massachusetts.

15. Israelachvili, J. and B. Ninham, (1977), *Intermolecular forces—the long and short of it.* J Colloid Interface Sci. **58**(1): p. 14-25.

16. Dzyaloshinskii, I.E.e., E. Lifshitz, and L.P. Pitaevskii, (1961), *General theory of van der waals' forces.* Physics-Uspekhi. **4**(2): p. 153-176.

17. Salam, A.,(2010), *Molecular quantum electrodynamics: long-range intermolecular interactions*: John Wiley & Sons, New Jersey, United States.

18. Salasnich, L.,(2014), *Quantum Physics of Light and Matter: A Modern Introduction to Photons, Atoms and Many-Body Systems*: Springer, Berlin, Germany.

19. Shankar, R.,(2012), *Principles of quantum mechanics*: Springer Science & Business Media, Berlin, Germany.

20. Hatz, R., (2016), Computational Studies of Dispersion Interactions in Coinage and Volatile Metal Clusters.

21. Anapolitanos, I. and I.M. Sigal, (2017), *Long-Range Behavior of the van der Waals Force.* Communications on Pure and Applied Mathematics. **70**(9): p. 1633-1671.

22. Arrighini, P.,(2012), *Intermolecular forces and their evaluation by perturbation theory*. Vol. 25. Springer Science & Business Media, Berlin, Germany.

23. Margenau, H., N.R. Kestner, and D. Ter Haar,(1971), *Theory of intermolecular forces*: Elsevier Science, Amsterdam, Netherlands.

24. Heßelmann, A. and G. Jansen, (2002), *Intermolecular induction and exchange-induction energies from coupled-perturbed Kohn–Sham density functional theory.* Chemical Physics Letters. **362**(3): p. 319-325.

25. Moszyński, R., S.a.M. Cybulski, and G. Chal/asiński, (1994), *Many-body theory of intermolecular induction interactions.* The Journal of Chemical Physics. **100**(7): p. 4998-5010.

26. Verdult, M., (2010),*A microscopic approach to van-der-Waals interactions between nanoclusters: The coupled dipole method*, MS thesis, Utrecht University, 2010. Google Scholar.

27. Buckingham, A.D., (1967), *Permanent and induced molecular moments and long-range intermolecular forces.* Advances in chemical physics: intermolecular forces. p. 107-142.

28. Mahanty, J. and B.W. Ninham,(1976), *Dispersion forces*. Vol. 5. Academic Press, London, UK.

29. Buhmann, S.Y.,(2013), *Dispersion forces I: Macroscopic quantum electrodynamics and ground-state Casimir, Casimir–Polder and van der Waals Forces*. Vol. 247. Springer, Berlin, Germany.

30. Parsegian, V.A.,(2005), *Van der Waals forces: a handbook for biologists, chemists, engineers, and physicists*: Cambridge University Press, Cambridge, United Kingdom.

31. Axilrod, B. and E. Teller, (1943), *Interaction of the van der Waals type between three atoms.* The Journal of Chemical Physics. **11**(6): p. 299-300.

32. Axilrod, B., (1951), *Triple-Dipole Interaction. I. Theory.* The Journal of Chemical Physics. **19**(6): p. 719-724.

33. Kim, H.-Y., (2015), *An Efficient Coupled Dipole Method for the Accurate Calculation of van der Waals Interactions at the Nanoscale*, in *Applied Spectroscopy and the Science of Nanomaterials:* Springer, Berlin, Germany. p. 85-119.

34. Salam, A.,(2016), *Non-relativistic QED theory of the Van der Waals dispersion interaction*: Springer, Berlin, Germany.

35. Craig, D.P. and T. Thirunamachandran,(1998), *Molecular quantum electrodynamics: an introduction to radiation-molecule interactions*: Courier Corporation.

36. Clayfield, E., E. Lumb, and P. Mackey, (1971), *Retarded dispersion forces in colloidal particles—exact integration of the Casimir and Polder equation.* J Colloid Interface Sci. **37**(2): p. 382-389.

37. Gregory, J., (1981), *Approximate expressions for retarded van der waals interaction.* J Colloid Interface Sci. **83**(1): p. 138-145.

38. Overbeek, J.T.G., (1952), *The interaction between colloidal particles.* Colloid science. **1**: p. 245-277.

39. Schenkel, J. and J. Kitchener, (1960), *A test of the Derjaguin-Verwey-Overbeek theory with a colloidal suspension.* Transactions of the Faraday Society. **56**: p. 161-173.

40. Anandarajah, A. and J. Chen, (1995), *Single correction function for computing retarded van der Waals attraction.* Journal of Colloid and Interface Science. **176**(2): p. 293-300.

CHAPTER 3

Dispersion forces between macroscopic objects

"After years in utter darkness, I force my eyes into the light. For I must retain my sight, that I might view the wholeness of the void, objectively."

Justin K. McFarlane Beau

1. Defining terminology:

Dispersion forces defined in the first chapter as simply the force acting between neutral bodies, they have a macroscopic manifestation making in them a macroscopic quantum phenomenon. The study of these forces at a microscopic level was as early as the first formulation of the quantum wave mechanics in the 30's, yet still until now there are remarkable problems with calculating them for certain cases of minute sizes or arbitrary geometries. Before we embark on our discussion of the different techniques used to model macroscopic dispersion interactions, we introduce a convention of the terms (**Fig.3.1**) which is more or less used in a great portion of published papers in the domain, although this convention can be discussed critically, we will consider it for being the most appealing and less problematic.

| Casimir | Casimir-polder | Van der Waals |
| effect/interaction | interaction | interactions |
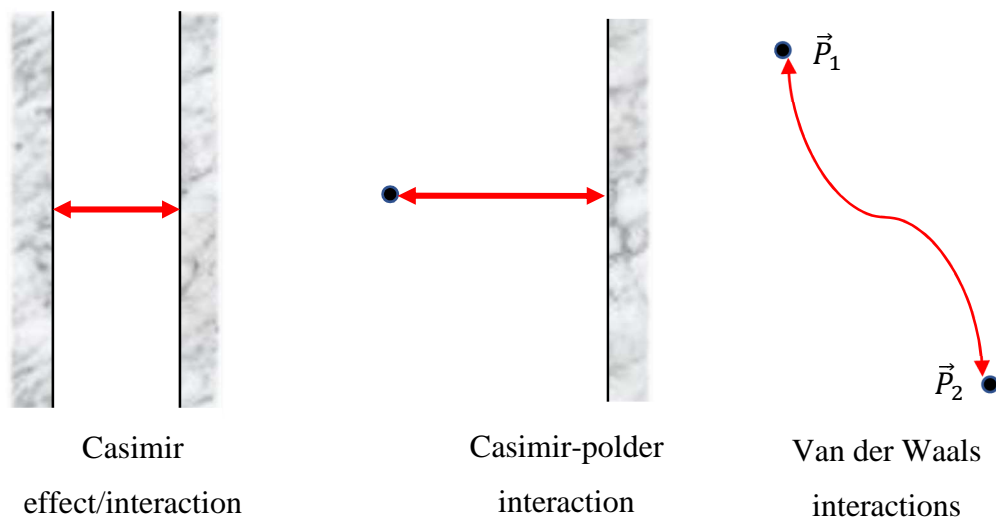
Figure 3.1: The three basic aspects of dispersion forces.

The term van der Waals forces although is the sum of induction orientation and dispersion forces, as it has been established in the previous chapter, it is reserved to indicate solely the dispersion forces between individual atoms or molecules, this term is also used when the models under question are atomistic models where the force is derived from the interactions between constituting molecular/atomic individuals [1-3]. The interaction between single atoms and macroscopic bodies we use the term Casimir polder interaction after the first retarded calculation of this type of interaction by Casimir and polder [4]. The term Casimir interaction is reserved for the force acting between macroscopic bodies. And These types of forces acting at different levels are termed as dispersion forces in general [2].

2. Modelling techniques

2.1. The pairwise summation approach (Hamaker)

Starting from the acting dispersion forces which exist between two symmetrical and electrically neutral atoms. As it was stated and demonstrated briefly in chapter 2, the potential interaction energy is given by the following formula [1]:

$$E_A = -\frac{C_6}{r^6} \tag{3.1}$$

Where C_6 is a constant that depends on the characteristics of the molecule and r is the distance between centre points of the two molecules.

To calculate dispersion interaction forces between two macroscopic objects, Hamaker assumed that these forces are additive and thus the total interaction energy can be calculated by summing all the interactions of individual pairs of molecules or atoms [2, 5]:

$$E = \int_{v_1} \rho_1 dr^3 \int_{v_2} \rho_2 dr^3 \frac{C_6}{r^6} \tag{3.2}$$

where ρ_1, ρ_2 are the number of molecules per unit volume in the two bodies, v_1 and v_2 are their volumes. When considering a system of two interacting infinite half spaces as shown in the **Fig.(3.2)**, Hamaker demonstrated using the integral in **Eq.(3.2)** that the free dispersion energy $E_\parallel(D)$ for a surface unit is given by [5]:

$$E_\parallel(d) = -\frac{A_H}{12\pi} \cdot \frac{1}{d^2} \tag{3.3}$$

Where the Hamaker constant is defined primarily in the pairwise summation approach as $A_H = \pi^2 \rho^2 \lambda$, and d is the distance between these surfaces. Similarly, Hamaker obtained the interaction energy for dissimilar spherical particles [5]:

$$E_{s-s}(r) = -\frac{A_H}{6}\left[\frac{2R_1R_2}{r^2-(R_1+R_2)^2}+\frac{2R_1R_2}{r^2-(R_1-R_2)^2}+\ln\left[\frac{r^2-(R_1+R_2)^2}{r^2-(R_1-R_2)^2}\right]\right] \tag{3.4}$$

Where R_1 and R_2 the radii of the two interacting particles and r is the distance between their centers.
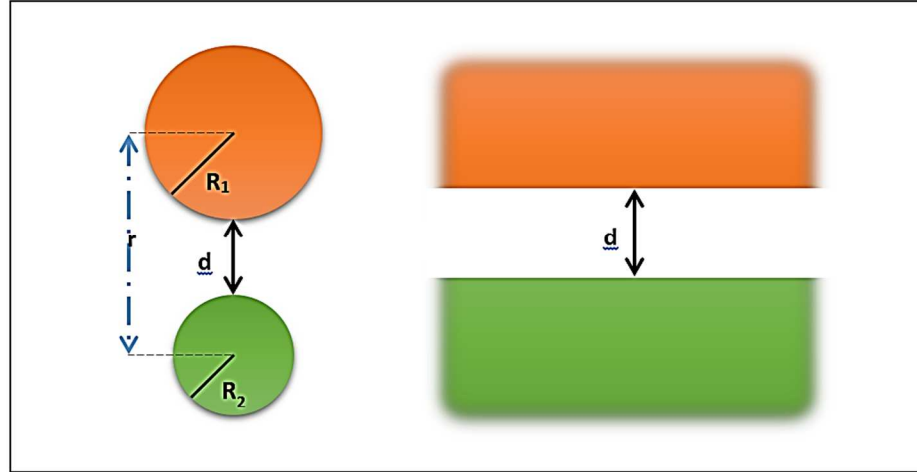
Figure 3.2: The Van der Waals interactions between two spheres, and between two parallel half-spaces.

when the particles are at close proximity ($[r/(R_1 + R_2)] \rightarrow 1$), **Eq.(3.4)** is simplified mathematically to the well-known formula of the dispersion interaction energy [5, 6] :

$$E_{s-s}(d \ll R) = -\frac{A_H}{6} \frac{R_1 R_2}{(R_1 + R_2)} \frac{1}{d}$$ (3.5)

This model has been and still is used to calculate dispersion forces between particulate materials, especially in Powder sciences and technologies [7-12].

Additionally, it should be noticed that the Hamaker constant is given approximately for an interaction between two different materials in the air as [8, 13, 14] :

$$A_{12} = \sqrt{A_{11}A_{22}}$$ (3.6)

Where A_{11} and A_{22} are Hamaker constants for the two material constituting the particles [13]. Moreover, if we considered the presence of a third material between the two bodies; this constant is given by introducing the contribution of the medium to the formula as follows [14]:

$$A_{123} = \left(\sqrt{A_{11}} - \sqrt{A_{33}}\right)\left(\sqrt{A_{22}} - \sqrt{A_{33}}\right)$$ (3.7)

Since its first proposal by Hamaker, the pairwise summation approach was popular for decades due to its utility, yet only basic geometries have been studied due to the rigid mathematics faced when attempting to calculate these forces for non-symmetrical arbitrary shapes. The different models for the basic shapes studied can be found to be reviewed sufficiently in the literature [1, 15-17]. There are though some papers that attempted at calculating these forces between non-traditional geometrical configurations [17], the most interesting one is the model developed for the interaction between two torus-shaped particles [18], this study is of such significance due to its possible applications in hemodynamics, as it can be used to calculate the contribution of dispersion forces to the cohesion of blood cells [18].

The table below shows the interaction energy for basic geometries at close proximity, where all these models are derived by going through the Hamaker integration process.

Table 1.1: the VdW interaction force models proposed for different geometries [15, 19].

Geometry	Interaction energy
Parallel half-spaces	$E = \dfrac{A}{12\pi d^2}$
Sphere with radius R and half space	$E = \dfrac{AR}{6d}$
Two identical spheres of radius R	$E = \dfrac{AR}{12d}$
Cylinder with radius R and half space	$E = \dfrac{A\sqrt{R}}{12\sqrt{2}d^{3/2}}$
Two identical parallel cylinders	$E = \dfrac{A\sqrt{R}}{24d^{3/2}}$
Two perpendicular cylinders	$E = \dfrac{AR}{6d}$

Using the pairwise summation approach with a different technique by introducing a weight function to the calculations [16], derived a simple elegant model where the interaction energy between similar and highly symmetrical basic geometries (i.e. spherical, cylindrical and cubic) is given in a single formula [16, 20]:

$$E_m(d) = -A_H \left[2\pi \cdot R_{eff}\right]^{1-m/2} \Gamma\left(1+m/2\right) L^m d^{-(1+m/2)} \qquad (3.8)$$

Where m = 0, 1, 2 for spheres, cylinders and cubes respectively, Γ is The gamma function, L the length of the particle, and the effective radius R_{eff} is given for perfectly spherical objects and cylinders as follows:

$$R_{eff} = \begin{cases} R_1 R_2/(R_1 + R_2) & ; m = 0 \\ \sqrt{R_1 R_2/(R_1 + R_2)} & ; m = 1 \end{cases} \qquad (3.9)$$

2.2. The Proximity-Force approximation:

Proximity-Force Approximation (PFA) theorem (also known as The Derjaguin approximation) is a mathematical technique used to derive the interaction force between curved objects at very close proximities from the interaction energy between paralleled surfaces [1, 21]. The general form of this method is widely used in calculating different adhesion and cohesion surface related forces [22-25]. This method is also used in other theoretical domains such as nuclear physics.

The dispersion interaction energy E_{PFA} between two objects at vicinity is given by the general formula of the PFA theorem which states [22, 24, 26] :

$$E_{PFA}(d) = 2\pi \int_{d}^{\infty} R_{eff} E_{\parallel}(r) \cdot dr \qquad (3.10)$$

With $E_{\parallel}$ is the free interaction energy between two semi-infinite plates, and the effective radius R_{eff} is chosen with respect to the geometry of the interacting objects. For spherical particles, the result of this method agrees with Hamaker's simple equation which also share the condition of a small distance compared to particle's dimensions, thus proving how powerful is this method. nevertheless, it should be emphasized that although the condition on which this approximation is established, limits its applicability, yet this method is fairly accurate in studying cohesion and adhesion for large systems.
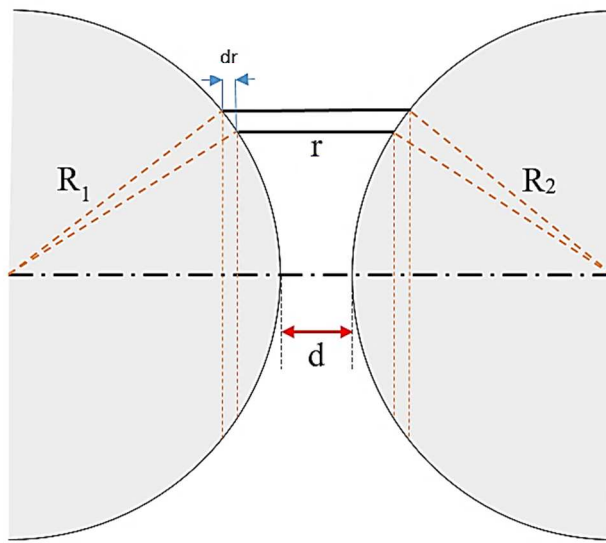
Figure 3.3 : Scheme of the Derjaguin approximation for spherical particles with radii R_1 and R_2 at close proximity (distance d << R_1 ,R_2), where the interaction force between the two spheres is calculated by summing (integrating) the forces between small circular sections of the particles [1].

There have been some attempts to generalize the PFA method with the attention of overcoming the geometrical restrictions of this approach. The surface element integration [27] and the Surface Integration Approximation [28], thus have been proposed. These modelling techniques have been introduced for calculating van der Waals forces between colloidal particles. moreover, even though these two approaches are constructed upon different assumptions, still, they produce the same result [29].

In the Surface element integration method (**SEI**), the interaction energy between two objects of arbitrary geometries is calculated by taking the interaction energy per unit area between two infinite flat plates $E(r)$, and then double-integrate it over the planes on which the surface of these objects are projected [27, 30] , the general formula for this technique is given as follows [31]:

$$E(r) = \int_{S} n_2 \cdot k_2 \frac{n_1 \cdot k_1}{|n_1 \cdot k_1|} E_{\parallel}(r) dS \qquad (3.11)$$

With n_1 and n_2 are the unit normal vectors pointing outward the surface of objects under consideration, k_1 and k_2 present the unit vectors pointing in the direction of the z axes which is considered in both objects' coordinate system to face each other.

The **SEI** method has been used primarily to calculate the interaction between an infinite half-space with a particle of arbitrary shape [27], and with a particle of a randomly generated rough surface [30]. Another recent work used the same method to calculate the adhesion force between colloidal cylindrical and spherical particles [31].

2.3. Retardation in Macroscopic Bodies:

A simple approach to calculating the retarded dispersion forces between macroscopic bodies would be by introducing in the integrand in **Eq.(3.2)** the correction functions previously stated in Chapter 2. Henceforth, within the framework of Hamaker's pairwise summation method, several models have been proposed in the literature for calculating the retarded dispersion energy between macroscopic bodies. Accordingly, and by using the two expressions for the retarded interaction energy between two atoms **(Eq.2.52)**, Overbeek [32] developed a two-part model which was a modification of Hamaker's formula for the interaction energy between flat surfaces.

Moreover, through a full Hamaker integration and based on the two-part Overbeek's correction function, Clayfield et al.[33] calculated a complete expression for the retarded dispersion interaction energy between dissimilar spherical particles with different radii, as well as between a spherical particle and a flat surface. Yet from a practical prospect, the implementation of this model in a program presents a tedious procedure. Thereby, Gregory [23] proposed a single expression which agreed fairly well with Overbeek's calculations [34].

$$E\left(d\right)=-\frac{A_H}{12\pi d^2}\left[\frac{1}{1+bd\,/\,\lambda}\right]$$
(3.12)

Where the value of b is chosen to be 5.32. furthermore , Gregory proposed an expression to calculate the retarded interaction energy [34]. However, this model is still restricted by the geometrical condition $(d \ll R)$ inherited from his usage of the Derjaguin approximation to obtain his formula:

$$E_{Gre}^{Rt}=-\frac{A_H}{12d}R\left[1-\frac{bd}{\lambda}\ln\left(1+\frac{\lambda}{bd}\right)\right]$$
(3.13)

Ho and Higuchi [35] proposed a model to calculate the retarded interaction energy for spherical particles of different radii. However, this model is only valid for distances larger than 8 nm and for particle radius greater than 2 μm :

$$E_{Ho}^{Rt}=-\frac{A_H}{12d}R\left[\frac{1}{1+11.12d\,/\,\lambda}\right]$$
(3.14)

Using their correction function, and through a full Hamaker integration scheme, Chen and Anandarajah [36] also calculated the interaction energy and force between dissimilar spherical particles, and between a sphere and a plane surface. It should be noticed that the terms in brackets in **Eq.(3.12-14)**, is the correction to the nonretarded energy, where this correction term will be used in this chapter to study the effect of retardation from each model in the section dedicated to results and discussions.

2.4. The Casimir effect:

After the investigation of the effect of retardation on the van der Waals forces that Casimir and polar [4] have conducted leading to the result stated above (**Eq.2.50**), Casimir has discovered a relation between these forces and the zero point energy variation , a relation with which he pursued in studying the effect of these forces at a macroscopic scale [37] , and fortunately, this pursue proved to be fruitful at the highest level. Casimir calculated that in the case of two perfectly neutral conducting infinite plates at proximity, an attractive force (pressure) is exercised on the plates, and the intensity of this force was found to be written as follows [38, 39]:

$$P(d) = -\frac{\pi^2}{240}\frac{\hbar c}{d^4} \tag{3.15}$$

This form shows no dependency on anything except the topological boundaries originated from the presence of plates [40], a result which is inherited from the fact that the objects are considered to be perfect conductors. Moreover, the constant c (speed of light) is incorporated in the model as a result of the relativistic contribution to the interaction energy between these objects.
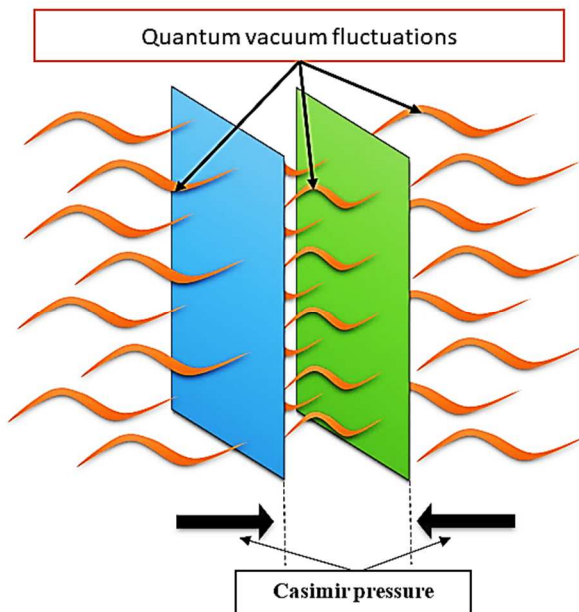
Figure 3.4: the Casimir pressure between two parallel perfectly conducting plates due to quantum vacuum fluctuations [38].

This force is pure quantum mechanical Since the force acting between two conducting plates in a vacuum is zero when considering the classical electromagnetic theory [40]. The significance of demonstrating the existence of such effect lies in the physical implications derived from the theory of Casimir interaction of perfect mirrors/conducting plates. The theory states that as the vacuum is effected by the presence of an object which enforces boundary conditions on the quantum fluctuations existing in the vacuum state, the zero-point energy is altered [40]. in the case of two parallel plates, the quantum fluctuations are limited between these objects, a pressure rises due to the energy difference (**Eq.3.16**) between the total allowed

modes inside the boundary (between the plates) and the modes outside the boundary [20, 39, 41-43]:

$$E(z) = \frac{\hbar}{2} \sum_i \left[\omega_i(z) - \omega_i(z \to \infty) \right]$$

(3.16)

Where $\omega_i(z)$ are the allowed mode satisfying the applied Boundary condition for two planes separated by a distance (z), and $\omega_i(z \to \infty)$ are those of the unbounded vacuum space [39, 41]. To calculate the Casimir effect between curved surfaces a simple way to do it would be by using the Derjaguin (PFA) approximation stated above with the interaction Casimir energy for parallel planes is given as:

$$E_{cas}(d) = -\frac{\pi^2}{720} \frac{\hbar c}{d^3}$$

(3.17)

2.4.1. Worldline calculations of the Casimir effect:

The worldline approach is a novel method inspired by new developments in string theory combined with Monte Carol algorithms [44, 45]. The main usage of this technique is studied numerically fluctuating scalar fields under Dirichlet boundary conditions, that is without going through the tedious complex theoretical calculations [44, 46, 47]. therefore, this method presents a promising technique for calculating the Casimir force between macroscopic bodies without going through the cumbersome mathematical developments of the classically used Quantum electrodynamical methods [48].

This formalism of the Casimir effect problem has surfaced 15 years as H.Gies et al. [44] proposed this technique to overcome some of the theoretical problems encountered in calculating the Casimir interaction between nonplanar objects [44]. And since then, this method has been applied to many geometries which are relevant to the experimental measurements of this effect, such as the case of sphere-plane or cylinder-plane configurations [44].

The results calculated through this method were compared with that which were derived using the proximity force approximation, consequently, the scheme of the worldline calculations has been proven to coincide perfectly with the results of the PFA method for distances at which the latter is fully functional and fairly accurate [22, 49]. Moreover, this technique has the feature of been applicable to arbitrary distances making this approach to go beyond the geometrical restrictions of the PFA theorem [22].

The effect of edge on the Casimir interactions is noticed to be studied for the first in literature – to the best of our knowledge - using this method, where the cases studied were the interaction between a half-plane and an infinite plane for a perpendicular arrangement [46], and a parallel one [48]. This method is still new and poorly used in literature, yet it gives some prospect insight for been applicable to study numerically the effect of geometrical conditions of the interacting objects such as curvature and roughness, thus we emphasise the importance and the interest of exploring the worldline research direction to study these effects.

2.4.2. The macroscopic theory of Van der Waals forces (DLP method):

Although the result of Casimir is elegant in its form, yet a more realistic model had to be developed for real materials which exhibit dielectric properties. Therefore, Lifshitz generalized the findings of Casimir to real materials by developing a macroscopic phenomenological theory that unifies all earlier theories in one model which encompasses all contributing physical effects. He proposed that regard dispersion interactions to be occurring through the fluctuating electromagnetic field, which is always existing inside the adsorbing medium and extending outside partly as radiated travelling waves from the object in the form of standing waves that disappear exponentially as we move away from the surface of that object [50], the keystone of this approach is to start from the optical properties of objects and calculate the van der Waals forces from the full optical spectrum [13, 50].
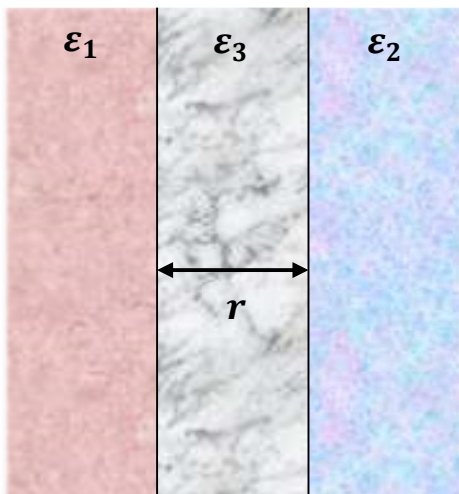
Figure 3.5 : The model-case proposed by Dzyaloshinskii, Lifshitz and Pitaeskii to calculate the Van der Waals interactions for parallel half-filled spaces separated by a third medium [1].

Lifshitz idea was generalized later by him and collaborators from Mosco by considering the existence of third dielectric medium filling the space between the interacting objects [51], this was the general **DLP** (after Dzyaloshinskii, Lifshitz and Pitaeskii) theory of the Casimir effect .to explore the result of this model , let us consider a system of two half-spaces separated by a material medium as it is shown in **Fig.(3.5)**, where all the three parts of space has different dielectric constants which are stated as follows [43]:

$$\varepsilon_i\left(z\right)=\begin{cases}\varepsilon_1 \ ; z<0 \\ \varepsilon_2 \ ; 0<z<r \\ \varepsilon_3 \ ; r>z\end{cases} \tag{3.18}$$

The non-retarded interaction energy between two half-spaces separated by a distance (d) is given at finite temperature to be [51, 52]:

$$E\left(d\right)=\frac{k_BT}{2\pi}\sum_{n=0}^{\infty}\int_0^{\infty}\ln\left[1-\Delta_{13}\Delta_{23}e^{-2kd}\right]kdk \tag{3.19}$$

With k is the transverse wavenumber of the fluctuating electromagnetic field. $\Delta_{13} \ and \ \Delta_{23}$ and are given with the general formula [52-54]:

$$\Delta_{jk} = \frac{\varepsilon_j\left(i\,\omega_n\right)-\varepsilon_k\left(i\,\omega_n\right)}{\varepsilon_j\left(i\,\omega_n\right)+\varepsilon_k\left(i\,\omega_n\right)} \tag{3.20}$$

Additionally, The dielectric permittivity of the materials along the imaginary frequency axis can be calculated using the Kronig-Kramers relations [13, 54] :

$$\varepsilon(i\,\omega_n) = 1 + \frac{2}{\pi}\int_0^\infty \frac{\omega\varepsilon''(\omega)}{\omega^2+\omega_n^{\,2}} \tag{3.21}$$

Where ε'' is the imaginary part of the dielectric frequency dependent function $\varepsilon(\omega) = \varepsilon'(\omega) + \varepsilon''(\omega)$. This relation poses a problem since for the result to be obtained the integration must be over the entire optical spectrum which is not always available. Therefore, a more simplified formula for the dielectric permittivity is proposed by Ninham and Persegian (1970) [54, 55]:

$$\varepsilon(i\,\omega_n) = 1 + \frac{\varepsilon_\infty-\varepsilon_0}{1+\omega_n/\omega_M} + \frac{\varepsilon_\infty-n_0^2}{1+\left(\omega_n/\omega_I\right)^2} + \frac{n_0^2-1}{1+\left(\omega_n/\omega_U\right)^2} \tag{3.22}$$

Where ω_M, ω_I, ω_U are respectively the characteristic microwave, infrared, and ultraviolet absorption frequencies and n_0 is the refractive index in the visible range. Furthermore, and with simple mathematical developments, the DLP model for the Casimir interaction energy (per unit area) between real dielectric materials is found to be written as follows [13]:

$$E_{123}(d) = -\frac{A_{123}}{12\pi}\frac{1}{d^{\,2}} \tag{3.23}$$

It is clearly noticed that this formula is of the same form as the one calculated by Hamaker from the pairwise summation approach (**Eq.3.2**), with one difference, the formula of Hamaker constant is changed to a one that incorporates wholly the optical spectrum of the interacting materials, and it should also be emphasized that for the retarded regime the effect of retardation is incorporated within this constant in contrast to the pairwise retarded approximation's stated earlier in this chapter. Moreover, this constant is now given within the framework of DLP theory as follows [52]:

$$A_{123} = \frac{3}{2}kT\sum_{n=0}^\infty\sum_{s=1}^\infty \frac{\left(\Delta_{13}\Delta_{23}\right)^s}{s^3} \tag{3.24}$$

For planar geometries, it is satisfactory to use this formula to evaluate the value of the Hamaker constant. Nevertheless, it has been demonstrated that there are some geometrical configurations for which the form of Δ_{ij} is changed [56]. Which proves that the geometry of particles can be a significant factor that determines and differentiates Hamaker constant. Another more simple and practical equation for the Hamaker constant is proposed [6]:

$$A_{123} \approx \frac{3}{4}k_BT\left(\frac{\varepsilon_1-\varepsilon_3}{\varepsilon_1+\varepsilon_3}\right)\left(\frac{\varepsilon_2-\varepsilon_3}{\varepsilon_2+\varepsilon_3}\right) + \frac{3h\omega_e}{16\sqrt{2}}\frac{\left(n_1^2-n_3^2\right)\left(n_2^2-n_3^2\right)}{\left[\left(n_1^2+n_3^2\right)\left(n_2^2+n_3^2\right)\right]^{3/4}} \tag{3.25}$$

With n_i are the refraction indices for medium 1,2 and 3.

Furthermore, The Casimir effect for perfectly conducting plates can be obtained from the DLP model by taking the limiting case for $\varepsilon_1, \varepsilon_2 \rightarrow \infty$ and for the intermedium to be a vacuum state with $\varepsilon_3 = 1$ [57]. The interaction energy as given by the previous models suffer from a divergence and infinite outcome as the separation distance goes to zero ($d \rightarrow 0$), this problem is overcome by considering a minimum distance beyond which the objects cannot approach due to the finite size of atoms constituting their surfaces. therefore, by introducing this cut-off distance d_0 to the model, the interaction Casimir energy is given as[52, 54]:

$$E_{12}(d = 0) = \frac{A_H^{(12)}}{12\pi} \frac{1}{d_0^2}$$

(3.26)

In this equation the third medium separating the interacting planes is considered to be vacuum; thus replacing ε_3 in Hamaker constant with 1.

Although the DLP approach incorporates in its calculations all major effects characterising dispersion interactions between the macroscopic object (**Fig.3.6**), still its complexity hinders its applications to random arbitrary geometries. A problem which is faced in all approaches proposed in literature, and although there are some propositions to overcome this set back such as that proposed in by Roman Velazquez and Bo (2008) [42] or the latter paper by which uses the scattering T-matrix technique [58], yet there are still more inherited problems in these approaches to overcome. It should be also emphasised that the approach based on the scattering T-matrix is a very promising one that ought to be investigated and developed[59]. So due as a consequence of the challenging mathematical calculations faced within this modelling framework, most of the papers have considered only simple geometries, focusing on those related to experimental settings used to measure these forces, namely the following configurations; sphere-infinite half-space [60-63], cylinder-plate [64] and sphere-sphere [65-67] which had no experimental verifications till lately [68]. A simpler approach for calculating the interaction between curved surfaces would be, as proposed earlier, the application of the proximity force theorem using the result stated previously for half spaces.
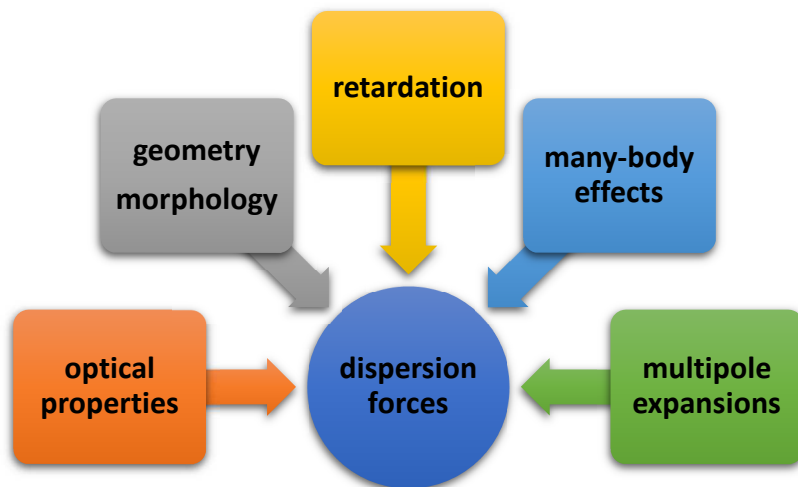
Figure 3.6: Physical effects that must be incorporated in a complete theory of dispersion forces.

3. Results and discussions:

3.1. The effect of particles' geometry

In this section, we shall investigate the effect of particles' geometry on the van der Waals interactions between macroscopic particles for different sizes. This is done with the aim to study the effect of geometry at a basic level for nanoparticles compared to the larger one. Moreover, we shall consider in our study three basic geometries; cubic, spherical and parallel cylindrical particles (**Fig.3.7**). the model used in our calculations is that which is introduced earlier in **Eq.(3.8).**
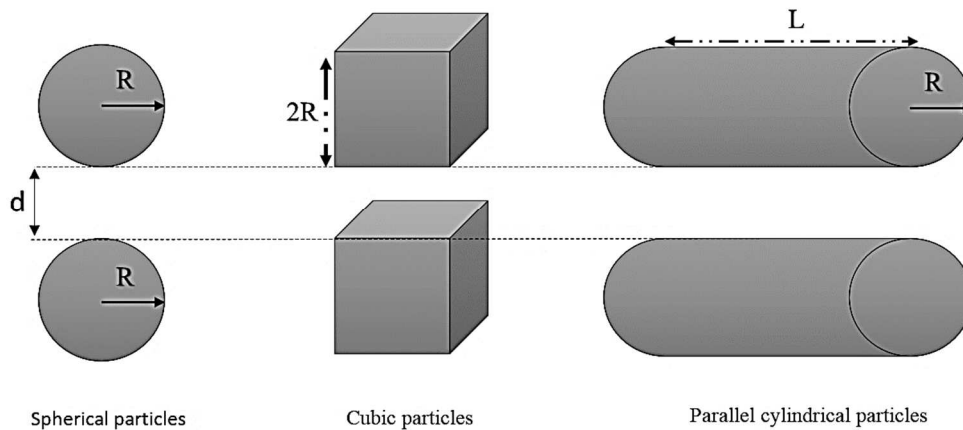
Figure 3.7: Layout of the three studied geometries.

We consider the particles to be of the same material which excludes the effect of its properties incorporated within Hamaker constant, and this is done by introducing the energy in the dimensionless form (E_{vdW}/A_H). additionally, to exclude the effect of weight in the calculations the mass of particles is considered to be constant which is translated mathematically into a constant volume, thus particles are considered to have the same volume V as a model sphere of a radius R^*.

Thus, the interaction energy which modelled by **Eq.(3.8)** is reformulated to new expressions dependent only on particles' volume. This can be attained by substituting R_{eff} and L with their counterparts' expressions related to R shown in **Tab. (3.2)**, and R is replaced by expressions related to the volume V as shown in the third column of **Tab. (3.2)**. this leads to the attended formulas of the interaction energy which variates only with respect to particles' volume, which help us to investigate the effect of geometry separately from all other effects.

Tab. (3.2) illustrates the geometrical parameters used for cylindrical particles depending on the value of n. For a constant volume, when n increases the cylindrical particle becomes more like a long thin wire. Alternatively, when n decreases less than 1, the cylinder becomes more similar to a thin disc, in this work, the condition L>R is assumed, thus, n will be chosen to have three values greater than 1 {n = 2,10,100}.

Table 3.2: Parameters used to calculate the interaction energy and force.

Geometrical parameters		L	R_{eff}	R
Particles' geometry	**Cubic**	$2 \cdot R$	------	$(V)^{1/3}/2$
	Spherical	------	$R/2$	$(3V/4\pi)^{1/3}$
	Cylindrical	$n \cdot R$	$\sqrt{R/2}$	$(V/n\pi)^{1/3}$

Fig. (3.8) show the effect of geometry on the van der Waals interactions energy groups of particles: **Nanoparticles**; where we choose a model particle size with R* =10 nm (**Fig.3.8.a**). And with R*= 100 nm (**Fig.3.8.b**). And **Sub-micronic** particles which are used for comparison (**Fig.3.8.c**), where we choose the radius of the model particle to be 500nm. We emphasize the fact that even for micronic particles when we introduce the size of the model particle into the cylindrical particle calculations for the higher value of n, the resulting shape is still considered in the nanosized limit because the volume would be mainly distributed along the length of particle producing the shape of a nanowire.

For nanoparticles, by the comparison between the three shapes, we notice that the effect of geometry is more recognizable for small distances less than 5 % of particle's size. When the distance increases the interaction energy of the geometries converges, which means that the effect of geometry is becoming less influential. It should be stated that the interaction energy for cylinders increases with *n* because there is a relation between *n* and the area of proximal surface of particles, since the van der Waals energy is mainly related to the surface [6]. The increase in the area of the surface at proximity between particles leads to an increase of interacting surface atoms, which in its turn increases the interaction energy.

For distances of the same order as the size, the curvature of the particle's surface becomes less influential. This means that the interacting atoms on the surface at these distances look at the same distance for each other, even for curved surfaces. These results and interpretations are valid only for cubic particles and spherical particles due to the similarity in their geometry. Moreover, for small distances, cubic particles give a high value of energy then spheres because the curvature of particles surface plays a significant role and interacting surface atoms at proximity interact with a strong correlation to the bending of the surface. Therefore, a high bending of the surface leads to a lower total interaction and a flat surface as in the case of cubic particles gives the highest value of the interaction energy.

By extrapolation from the inter-crossings of the graphs, parametric expressions are proposed to determine the relation between the geometries. These relations demonstrate the cases where the geometries give nearly the same value of the energy.

Table 3.3: derived parametric relations for the intersection points of different energy graphs.

Geometries	Cube-cylinder	Sphere-cylinder
Parametric relations	$\dfrac{R^*}{d \cdot n} \approx \dfrac{2}{100}$	$\dfrac{n \cdot R^*}{d} \approx 6$
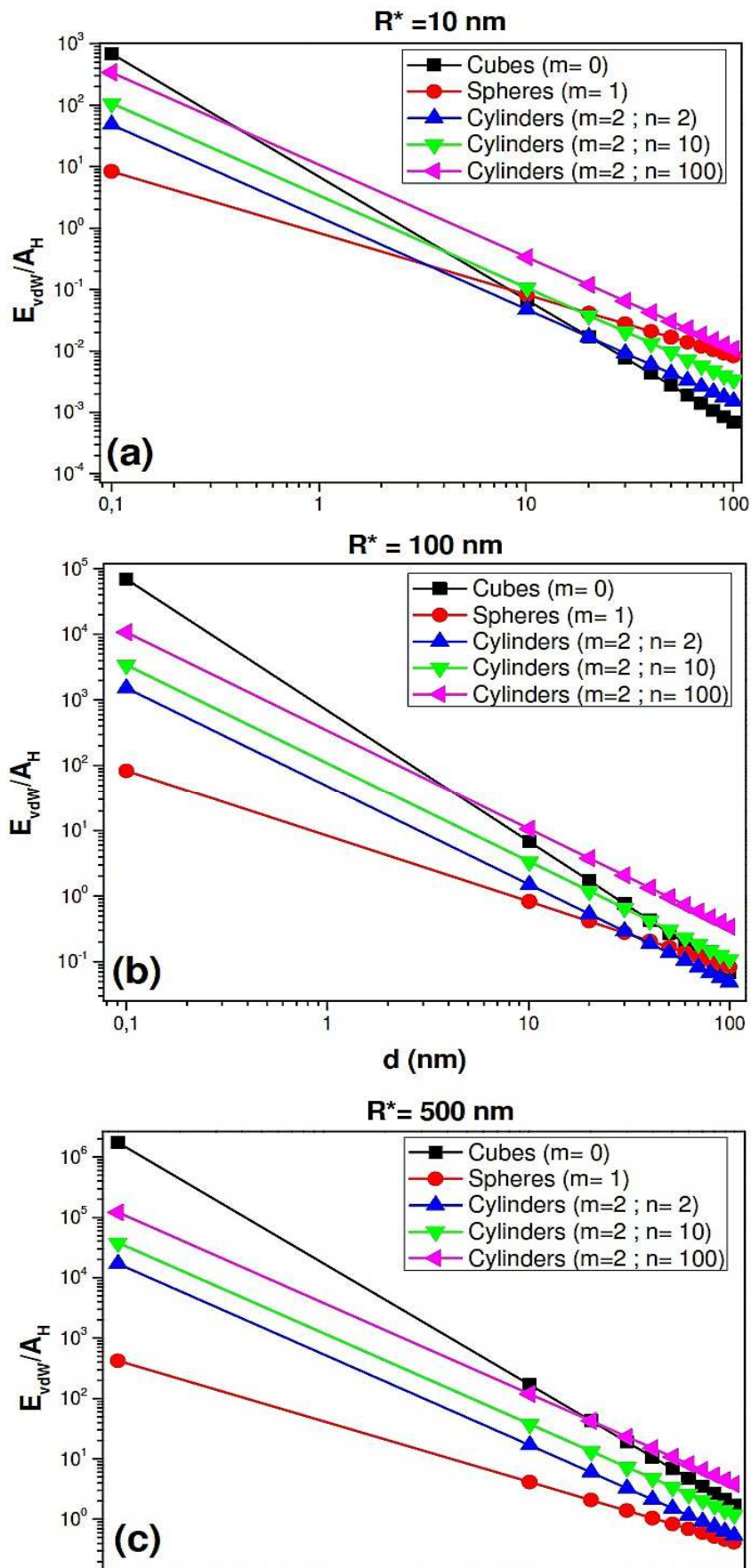
Figure 3.8: effect of geometry of particles on the van der Waals interaction energy.

3.2. The effect of retardation

To investigate the effect of retardation on the vdW interaction energy. This effect is calculated using the expressions of Ho and Higuchi **(Eq.3.14)**, and of Gregory **(Eq.3.13)**. These models are compared with the simple expression proposed by Hamaker **(Eq.3.4)** for the non-retarded energy between spherical particles. More importantly, the full exact results of Clayfield et al. [33] are also included in the comparison.

The dispersion interaction energies calculated from these models are illustrated in **Fig. (3.9)** with respect to particle radius for an intermediate distance of 10 nm. These models are analysed to investigate the influence of different parameters (size, distance and shape) on the dispersion interactions of macroscopic bodies. Since the result of Clayfield include the effect of temperature and to exclude this effect we consider that Hamaker constant takes the same value chosen by Clayfield ($A_H = 25kT$), where k is the Boltzmann constant and T is the temperature.
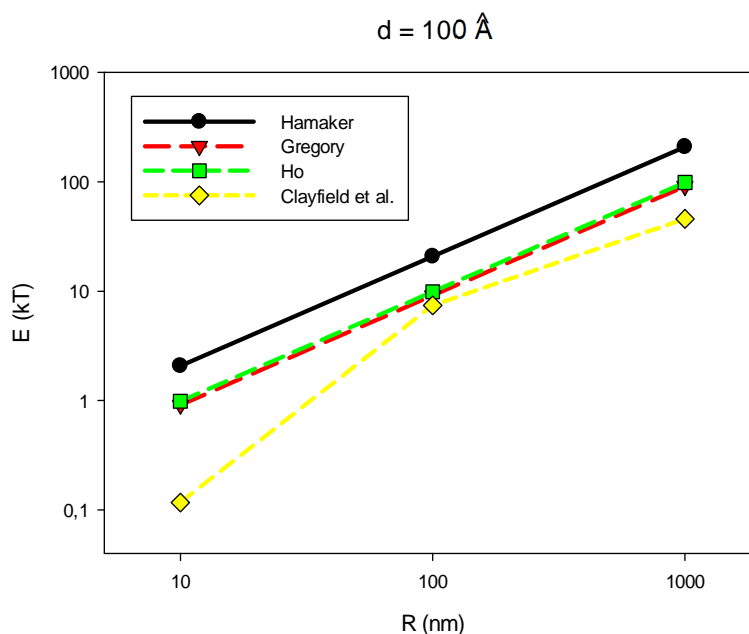
Figure 3.9: The retarded dispersion interaction energy compared for different models plotted against the particle's radius for a distances d=10nm.

We notice from **Fig.(3.9)** that the retardation is found constant when calculated with the model of Ho and Higuchi and that of Gregory, thus showing no dependence on particle's size, yet the result of Clayfield shows a dramatically different behaviour since they show that this effect is higher for nanoparticle, and only give similar results (With a slight discrepancy) as those of the other models when particle's size is larger than 100 nm.

Fig.(3.10) shows the same comparison for different distance with particle's size fixed at 100 nm. We notice that the three models give similar results up to a distance of 10nm, and for the larger distance, we notice the effect of retardation calculated with Clayfield's model is bigger. Since the effect of dispersion forces is not strongly effective at extremely large distances compared to the size of particles, the discrepancy between the full exact result of Clayfield and those of other models can be excluded although it is somewhat noticeable.
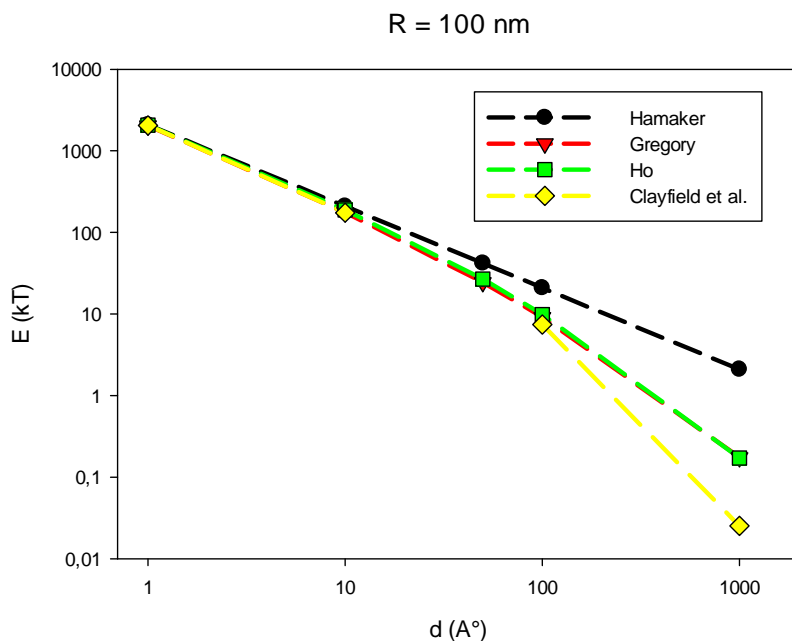
R = 100 nm

Figure 3.10: The van der Waals interaction energy with particle radius (R=100 nm).

Furthermore, we use results obtained from the model proposed by Clayfield in his cumbersome two-page long formula. the three particle sizes are chosen so as to include the limits of nanosized particles where R is 20 nm for extremely small nanoparticles and R= 100 for the limit which presents the changing point to the nano-regime as indicated in chapter 1. For comparison, we also include micronic particles R=1μm. Thus the effect of retardation T_{clay} (in percentage %) calculated from Clayfield's results is presented in **Fig.(3.11).**
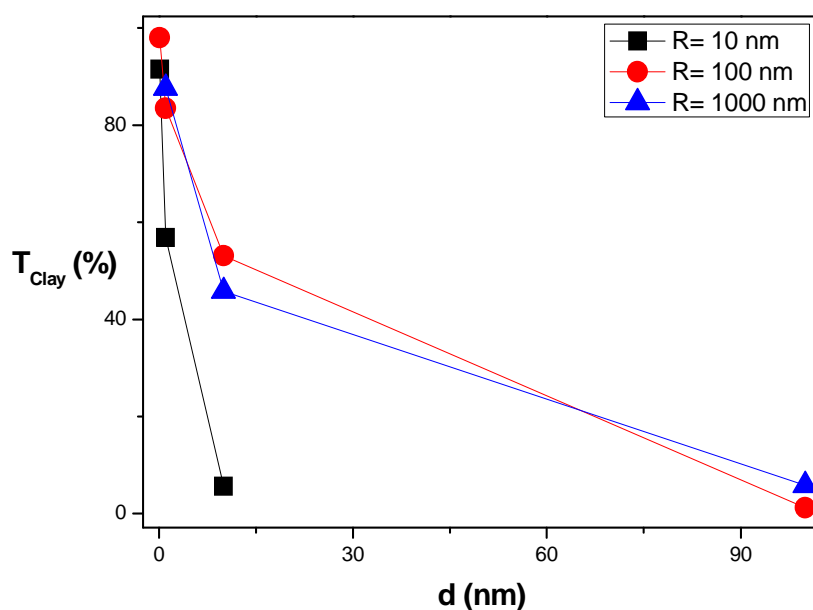
Figure 3.11: The effect of retardation calculated from Clayfield's model **[69]**.

Fig.(3.11) display a very interesting result, where we notice that for particle's radius larger than 100 nm the effect of retardation behaves the same, showing thus no dependence on particle's size. However, for extremally small nanoparticles the effect is shown to be more dramatic and consequently leading to a rapid decay of the interaction energy. Thus, we conclude from these remarks that there is a strong dependence of retardation on particles size at the nanoscale, meaning that nanoparticles behave differently as expected when it comes to the effect of retardation on dispersion interactions.

Since the model of Clayfield is hard to manipulate and cumbersome when it comes to the programming process, we propose that the model of Ho and Higuchi be modified by introducing different values of the constant B in the following generalised relation of Ho and Higuchi's formula:

$$E_{Ho}^{Rt} = -\frac{A_H}{12d} R \left[\frac{1}{1 + \mathrm{B}d/\lambda} \right]$$

(3.27)

The chosen of the value of B which Ho and Higuchi[35] have used is taken assumed for the instance of particles' size near 100 nm. Nonetheless, for other cases of different sizes and interparticle distances, this value must be changed in order for the model to coincide perfectly with the result obtained from Clayfields. we propose in the table below we propose different values of the constant B that can be used for different particle's size and distance, where we notice that for large particles (R ≥ 100 nm) almost all calculated values are close relatively, however, the case of small nanoparticles is quite different with this constant having bigger values than those calculated for larger particles.

Table 3.4: calculated values of the constant B.

Distance in A°	Particle radius (A°)		
	100	1000	10000
1	93,14	20,09	/////
10	76	19,72	14,14
100	168,25	8,83	11,82
1000	////	82,34	16,24

Furthermore, to examine the influence of particle's size and geometry on the retardation effect, the retarded van der Waals interaction for two interacting atoms is compared with that of macroscopic bodies, where spheres and flat surfaces are chosen in our case. The retardation of the energy between atoms is calculated using the (**Eq.2.54**) proposed by Nandarajah and Chen (1995)[70]. For microscopic bodies, the retardation of the energy between flat surfaces is calculated using the correction function proposed by Gregory (**Eq.3.12**), and for spherical

particles, we use the models of Ho and Higuchi, and of Clayfield. Thus **Fig.(3.11)** shows the comparison between the retardation effect for all these different cases.
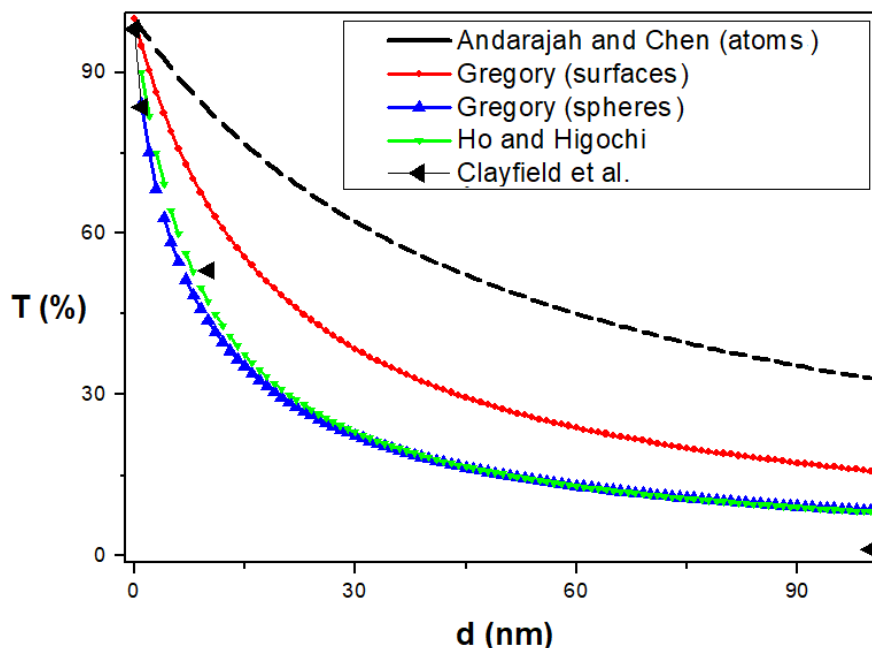
Figure 3.12: The retardation effect on the van der Waals interaction energy for different objects.

   Fig.(3.12) demonstrates the previous results when the interparticle distance d exceeds 10 nm, the interaction energy is shown to decrease to less than 50% of its non-retarded value. Additionally, when this effect is calculated using the model of Gregory or Ho et Higuchi, particle's size is verified easily to not be involved to the retardation term in the models proposed for the van der Waals interaction energy. Since these models were developed approximately without any consideration to the effect of particle's size, as shown in the previous section of this chapter.

   Moreover, this energy is shown to decay faster for spherical particles than for surfaces, where the discrepancy between the two is up to 30 %. Therefore, it can be stated that retardation is related to particle's shape. The effect of retardation is also demonstrated to be more significant for macroscopic particles than for single coupled atoms. Thus, from all previous results, we can conclude that this effect is not only dependent on the distance between particles but also on particles' size and geometry, especially in the case of nanoparticles.

3.3. The retardation effect (an atomistic pairwise approach):

  The van der Waals interaction energy between atomic nano-clusters can be calculated in the simplest form using the pairwise summation approach proposed by Hamaker [5]. The total van der Waals interaction energy $W_T(E)$ is given as the sum of all the interactions between individual atoms as shown in **Eq.(3.2)**:

$$E_T = -\sum_{i=1}\sum_{j=1}\frac{C_6}{r_{ij}^6}$$

(3.28)

Where r_{ij} respectively is the distance between the i-th dipole and the j-th dipole in clusters 1 and 2. The retarded van der Waals interaction energy is also given in the following formula:

$$E_T^{Rt} = -\sum_{i}\sum_{j}\frac{C_6}{r_{ij}^6}f\left(r_{ij}\right)$$

(3.29)

To study the correction factor of the interaction energy between large groups of atoms we consider the ratio illustrated in **Eq.(3.30)** between the global retarded and non-retarded dispersion energies:

$$T\left(r\right) = \frac{E_T^{Rt}}{E_T}$$

(3.30)

The geometrical configuration chosen for this study is a 2-D rectangular cluster of atoms. The distance between atoms is taken to be $1\hat{A}$ for most of our calculations. **Fig.(3.12)** demonstrates the chosen orientations of these clusters with respect to each other. A comparison between the two configurations aligned (**Fig.3.13.a**) and parallel (**Fig.3.13.b**) would demonstrate the effect of atomic distribution in space (cluster geometry) on the global retardation of the van der Waals interaction energy between two symmetrical nano-clusters. The dimensions are expressed by the number of atoms per dimension, and Since the clusters are chosen to be rectangular, a single number 'n' is considered, this number ranges from 1 to 10^4. The calculations also would be calculated using a code in **FORTRAN**, and the flow chart of the algorithm used here is given in "**appendix I**", where this flow chart can be used for arbitrary geometries.
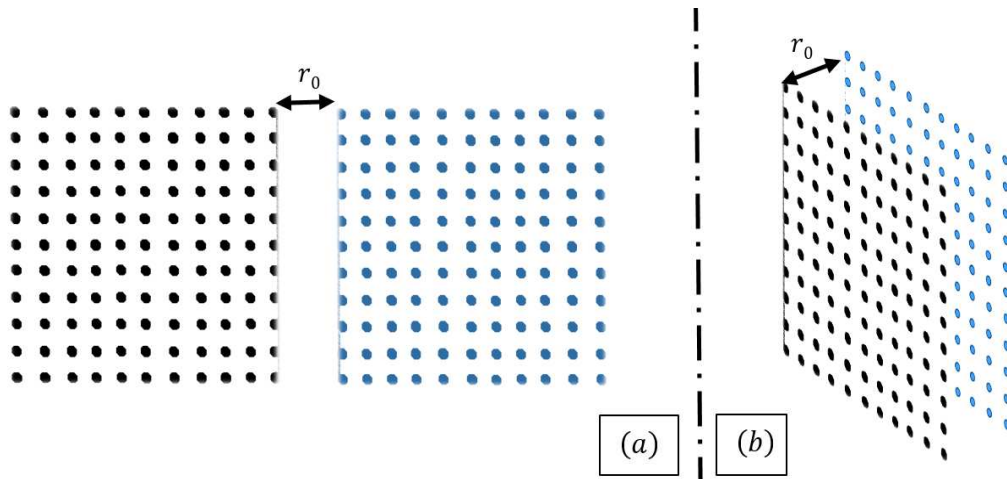
Figure 3.13: The configurations of the atomic clusters studied.

The reduced retarded interaction energy between clusters is compared with the non-retarded one as illustrated in **Fig.(3.13)**. For the comparison to be significant, the number 'n' is chosen as the highest value fixed in this work, which corresponds to (n=10^4). The retarded interaction energy is shown to give smaller value than that of the non-retarded case. The difference between

the two cases is shown to increase with increasing distances, which means that the effect of retardation rises with respect to the distance.
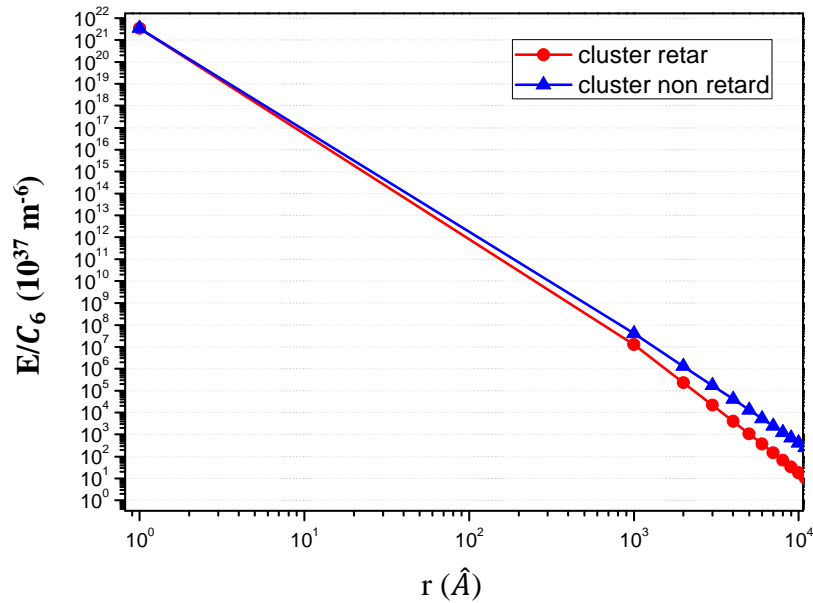
Figure 3.14: The reduced energy compared for the retarded and non-retarded cases.

Eq.(3.31) shows the discrepancy S(%) between the retardation effect for clusters $T(r)$ and for single atom $f(r)$. This value is calculated to illustrate the effect of the number n on the retardation of the interaction energy between clusters.

$$S(\%) = 100 \times \frac{f(r) - T(r)}{f(r)} \tag{3.31}$$
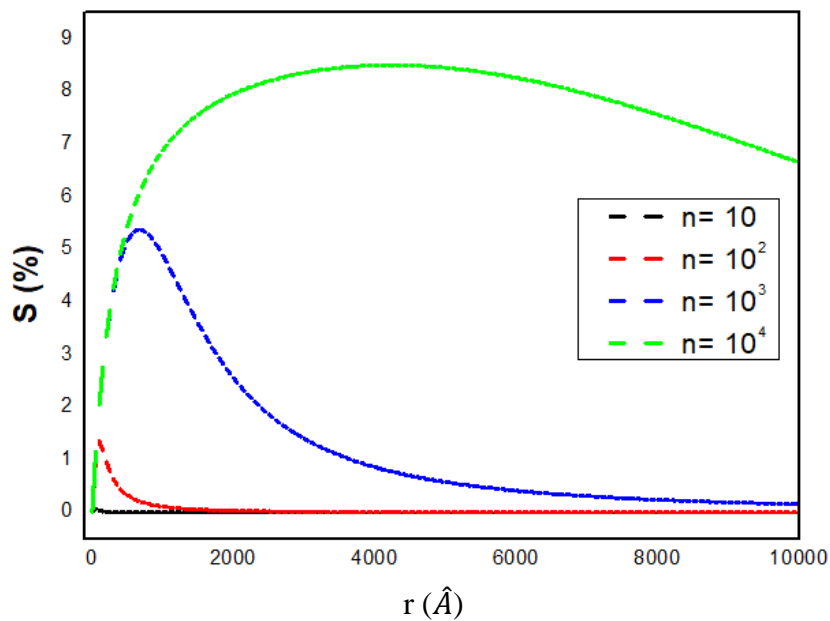
Figure 3.15: The discrepancy behaviour with respect to the distance for different value of 'n'.
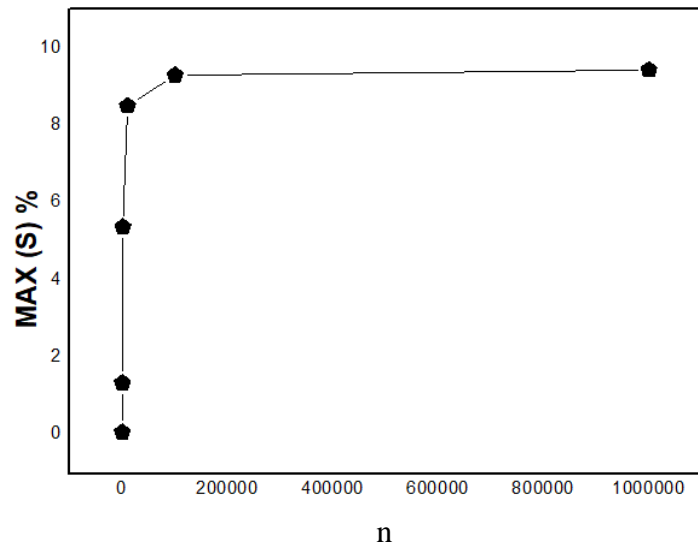
Figure 3.16: The evolution of the maximum value of S.

Fig.(3.16) shows that the discrepancy S increases with the number n. S is also shown to have an upper limit ($\cong 10$ %). These results demonstrate that there is a minor impact of the number of atoms on the retardation effect on the interaction of clusters, and this effect does not exceed 10 % discrepancy from the retardation for a single atom. A positive value of S shows that the effect of retardation is always greater for clusters than for single atoms. The behaviour of the value of S can be easily verified to be the same for both configurations. However, when S is compared for short distances as illustrated in **Fig.(3.17)**, parallel 2-D clusters give smaller results. This means that in this case, the effect of retardation is smaller at short distances. The result demonstrates that the distribution of atoms in space effects retardation on small distances. In other words, the retardation effect is strongly related to cluster geometry at short distances.
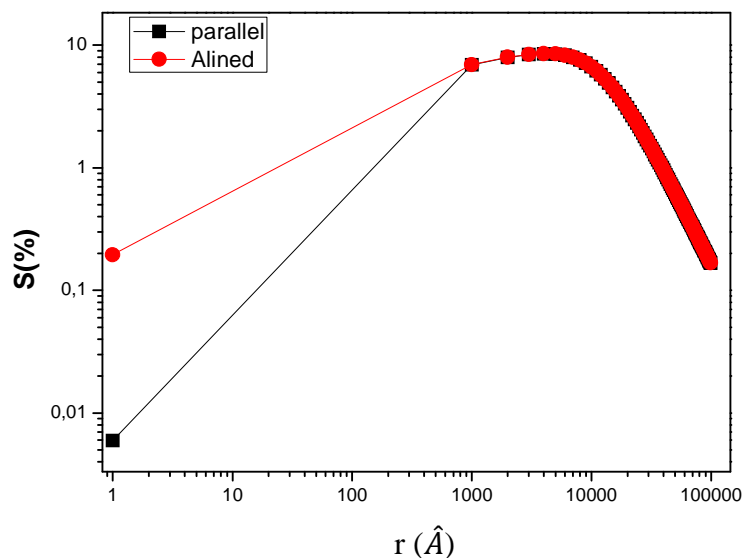
Figure 3.17: The discrepancy S compared for aligned and parallel clusters for $n=10^4$.

To study the effect of geometry on the retardation of the interaction energy, S is investigated by the same method as the correction functions f and T. The value ΔS is calculated in percentage using **Eq.(3.32)**, with the indices 'para' and 'align' indicating respectively parallel clusters and aligned clusters:

$$\Delta S\% = 100 \times \frac{S_{para} - S_{align}}{S_{align}} \tag{3.32}$$
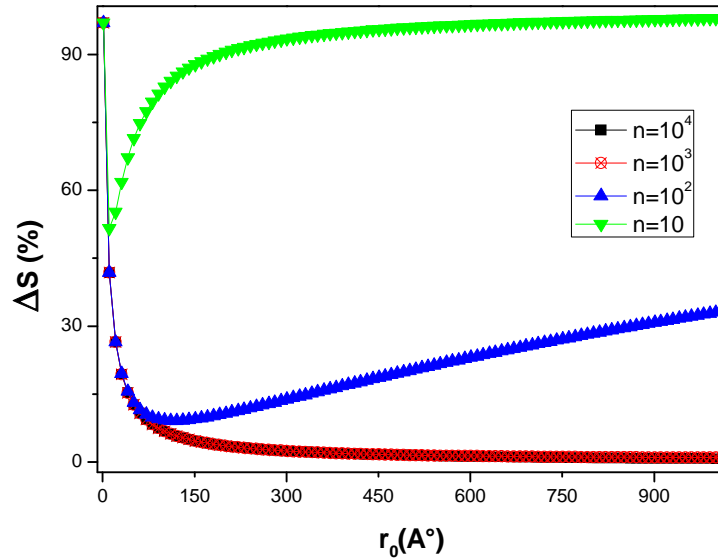
Figure 3.18: ΔS plotted with respect to the distance for different value of n.

The difference ΔS is shown to be higher for distances smaller than the number (r << n), which supports and generally) these the previous results. As the distance increases ΔS decreases, indicating that the geometry becomes less significant for larger distances of the same order of clusters' dimensions. For extremely large distances (r_0 >> n), ΔS increases again. These results show that the effect of these forces is only noticeable at short distances though no value was integrated practically, however it is valuable for a global understanding of these forces behaviour.

Additionally, it should be remarked that for small clusters (n<100), the effect of geometry is significant even for all distances $\{\forall r_0; \Delta S \geq 50\%\}$. This result is very important since it implies a necessity to consider the effect of geometry when modelling the retarded dispersion interactions between nano-clusters. The same result stated earlier using the other models which were developed from Hamaker's integration. This problem was solved empirically by introducing a modified version of Schenkel's model in **Eq.(3.27)** with new values of the parameter B given for nanoparticles in **Tab. (3.4)**. and Although this modified model is not based on a more fundamental calculations such as Quantum electrodynamic methods, yet it is excepted to be sufficiently more accurate the widely used Hamaker's model.

Since this modified model is a better approximation to dispersion forces, it can thus be incorporated within the study of the dynamics of nanoparticulate materials. In the case of

nanocolloids, we can use this model to better predict the stability of the colloid suspension, which is crucial for certain delicate applications of such materials specially in pharmaceutics and biomedicine. Additionally, when simulating nano-aerosols deposition in the environment and within the human respiratory system, using this model to account for the interactions between these particles would lead for a more realistic and accurate simulations of these processes which would lead for a better understanding of the risk involved with handling and exposure of this type of materials, and ultimately for better security measurements.

4. Conclusions:

We have reviewed in this chapter the basic models of dispersion interactions between macroscopic objects, where the theoretical limitations of those models were briefly stated. We then use some of the proposed models to study the effect of the geometry of particles by comparing three basic shapes: cubic, cylindrical and spherical. The results show that the effect of geometry is significant for interparticle distances less than 20% of particles' radius, with parametric relations proposed to relate between the interaction energy for different geometries. The retarded vdW interactions are also investigated, where it was demonstrated that the effect of retardation is highly dependent on particle size and shape as well as the distance. And hence a need for a new model for the retarded van der Waals interactions between nanoparticles was emphasized. the influence of cluster dimensions and geometry on the retardation effect of dispersion energy is also investigated. Two basic configurations of 2D symmetrical (rectangular) clusters are investigated (parallel and aligned). The impact of the number of atoms on the retardation effect on the interaction of clusters is shown to be less than 10 % of discrepancy when compared to the retardation for two interacting atoms. The distribution of atoms in space (geometry) is also shown to have a strong significance at small distances. This result implies a dependency of retardation on the geometry of clusters.

References:

1. Israelachvili, J.N.,(2011), *Intermolecular and surface forces*: Academic press, Cambridge, Massachusetts.
2. Buhmann, S.Y.,(2013), *Dispersion forces I: Macroscopic quantum electrodynamics and ground-state Casimir, Casimir–Polder and van der Waals Forces*. Vol. 247. Springer, Berlin/Heidelberg, Germany.
3. Israelachvili, J. and B. Ninham, (1977), *Intermolecular forces—the long and short of it.* Journal of Colloid and Interface Science. **58**(1): p. 14-25.
4. Casimir, H. and D. Polder, (1948), *The influence of retardation on the London-van der Waals forces.* Physical Review. **73**(4): p. 360.
5. Hamaker, H., (1937), *The London—van der Waals attraction between spherical particles.* Physica. **4**(10): p. 1058-1072.
6. Israelachvili, J.N.,(2011), *Intermolecular and surface forces: revised third edition*: Academic press, Cambridge, Massachusetts.
7. Hartley, P.A., G.D. Parfitt, and L.B. Pollack, (1985), *The role of the van der Waals force in the agglomeration of powders containing submicron particles.* Powder Technology. **42**(1): p. 35-46.

8.   Masuda, H., K. Higashitani, and H. Yoshida,(2006), *Powder technology: fundamentals of particles, powder beds, and particle generation*: CRC Press, Boca Raton, Florida.

9.   Fatah, N., D. Turki, and M. Chaib, (2005), *Numerical simulation of fluidised cohesive powders.* IChemE. **7**: p. 11.

10. Seville, J., C. Willett, and P. Knight, (2000), *Interparticle forces in fluidisation: a review.* Powder Technology. **113**(3): p. 261-268.

11. Liu, H., Y. Guo, and W. Lin, (2015), *Simulation of shock-powder interaction using kinetic theory of granular flow.* Powder Technology. **273**: p. 133-144.

12. Xu, Z., H.M. Mansour, and A.J. Hickey, (2011), *Particle Interactions in Dry Powder Inhaler Unit Processes: A Review.* Journal of Adhesion Science and Technology. **25**(4-5): p. 451.

13. Krupp, H.,(1967), *Particle adhesion, theory and experiment*: Advan. Colloid Interface Sci. 1 (1967), 111-239.

14. Visser, J., (1972), *On Hamaker constants: A comparison between Hamaker constants and Lifshitz-van der Waals constants.* Advances in Colloid and Interface Science. **3**(4): p. 331.

15. Parsegian, V.A.,(2005), *Van der Waals forces: a handbook for biologists, chemists, engineers, and physicists*: Cambridge University Press, Cambridge, UK.

16. Mahanty, J. and B.W. Ninham,(1976), *Dispersion forces*. Vol. 5. Academic Press London.

17. Montgomery, S.W., M.A. Franchek, and V.W. Goldschmidt, (2000), *Analytical Dispersion Force Calculations for Nontraditional Geometries.* Journal of Colloid and Interface Science. **227**(2): p. 567-584.

18. Ohshima, H. and A. Hyono, (2009), *The van der Waals interaction between two torus-shaped colloidal particles.* Journal of Colloid and Interface Science. **332**(1): p. 251-253.

19. Bhushan, B.,(2010), *Handbook of micro/nano tribology*: CRC press, Boca Raton, Florida.

20. Román-Velázquez, C.E. and B.E. Sernelius, (2008), *Numerical study of the effect of structure and geometry on van der Waals forces.* Journal of Physics A: Mathematical and Theoretical. **41**(16): p. 164008.

21. Graf, K. and M. Kappl,(2006), *Physics and chemistry of interfaces*: John Wiley & Sons.

22. Gies, H. and K. Klingmüller, (2006), *Casimir effect for curved geometries: Proximity-Force-Approximation validity limits.* Physical Review Letters. **96**(22): p. 220401.

23. Gregory, J., (1981), *Approximate expressions for retarded van der Waals interaction.* Journal of Colloid and Interface Science. **83**(1): p. 138-145.

24. Russel, W.B., D.A. Saville, and W.R. Schowalter,(1989), *Colloidal dispersions*: Cambridge university press, Cambridge, UK.

25. Svetovoy, V. and G. Palasantzas, (2015), *Influence of surface roughness on dispersion forces.* Advances in Colloid and Interface Science. **216**: p. 1-19.

26. Sernelius, B.E. and C.E. Román-Velázquez, (2009), *Test of the proximity force approximation*. in *Journal of Physics: Conference Series*. IOP Publishing, Bristol, United Kingdom.

27. Bhattacharjee, S. and M. Elimelech, (1997), *Surface element integration: a novel technique for evaluation of DLVO interaction between a particle and a flat plate.* Journal of Colloid and Interface Science. **193**(2): p. 273-285.

28. Dantchev, D. and G. Valchev, (2012), *Surface integration approach: A new technique for evaluating geometry dependent forces between objects of various geometry and a plate.* Journal of Colloid and Interface Science. **372**(1): p. 148-163.

29. Fosco, C.D., F.C. Lombardo, and F.D. Mazzitelli, (2014), *Derivative-expansion approach to the interaction between close surfaces.* Physical Review A. **89**(6): p. 062120.

30. Bhattacharjee, S., C.-H. Ko, and M. Elimelech, (1998), *DLVO interaction between rough surfaces.* Langmuir. **14**(12): p. 3365-3375.

31. Li, K. and Y. Chen, (2012), *Evaluation of DLVO interaction between a sphere and a cylinder.* Colloids and Surfaces A: Physicochemical and Engineering Aspects. **415**: p. 218.

32. Overbeek, J.T.G., (1952), *The interaction between colloidal particles.* Colloid science. **1**: p. 245-277.

33. Clayfield, E., E. Lumb, and P. Mackey, (1971), *Retarded dispersion forces in colloidal particles—exact integration of the Casimir and Polder equation.* Journal of Colloid and Interface Science. **37**(2): p. 382-389.

34. Gregory, J., (1981), *Approximate expressions for retarded van der waals interaction.* J Colloid Interface Sci. **83**(1): p. 138-145.

35. Ho, N.F. and W. Higuchi, (1968), *Preferential aggregation and coalescence in heterodispersed systems.* Journal of Pharmaceutical Sciences. **57**(3): p. 436-442.

36. Chen, J. and A. Anandarajah, (1996), *Van der Waals attraction between spherical particles.* Journal of Colloid and Interface Science. **180**(2): p. 519-523.

37. Casimir, H.B. *On the attraction between two perfectly conducting plates*. in *Proc. Kon. Ned. Akad. Wet.* 1948.

38. Lambrecht, A., (2002), *The Casimir effect: a force from nothing.* Physics World. **15**(9): p. 29.

39. Milton, K.A.,(2001), *The Casimir effect: physical manifestations of zero-point energy*: World Scientific, Singapore.

40. Bordag, M., et al.,(2009), *Advances in the Casimir effect*. Vol. 145. Oxford University Press, UK.

41. Noguez, C. and C. Román-Velázquez, (2004), *Dispersive force between dissimilar materials: Geometrical effects.* Physical Review B. **70**(19): p. 195412.

42. Román-Velázquez, C.E. and E.S. Bo, (2008), *Numerical study of the effect of structure and geometry on van der Waals forces.* Journal of Physics A: Mathematical and Theoretical. **41**(16): p. 164008.

43. Bordag, M.,(1999), *The Casimir Effect 50 Years Later: Proceedings of the Fourth Workshop on Quantum Field Theory Under the Influence of External Conditions, 14-18 September 1998, Leipzig, Germany*: World Scientific, Singapore.

44. Gies, H., K. Langfeld, and L. Moyaerts, (2003), *Casimir effect on the worldline.* Journal of High Energy Physics. **2003**(06): p. 018.

45. Schubert, C., (2001), *Perturbative quantum field theory in the string-inspired formalism.* Physics Reports. **355**(2-3): p. 73-234.

46. Gies, H. and K. Klingmüller, (2006), *Worldline algorithms for Casimir configurations.* Physical Review D. **74**(4): p. 045002.

47. Edwards, J.P., (2015), *Unified theory in the worldline approach.* Physics Letters B. **750**: p. 312-318.

48. Gies, H. and K. Klingmüller, (2006), *Casimir edge effects.* Physical Review Letters. **97**(22): p. 220405.

49. Aehlig, K., et al., (2011), *Casimir forces via worldline numerics: Method improvements and potential engineering applications.* arXiv preprint arXiv:1110.5936.

50. E. Lifshitz, (1956), *The theory of molecular attractive forces between solids*, in : J.Sykes, and D. Ter Haar, , (2012), *Perspectives in Theoretical Physics : The Collected Papers of E.M.Lifshitz, pp. 329-349,* Pergamon Press.

51. Dzyaloshinskii, I.E.e., E. Lifshitz, and L.P. Pitaevskii, (1961), *General theory of van der waals' forces.* Physics-Uspekhi. **4**(2): p. 153-176.
52. White, L.R., (2010), *van der Waals interaction energy and disjoining pressure at small separation.* Journal of Colloid and Interface Science. **343**(1): p. 338-343.
53. Klimchitskaya, G.L. and V.M. Mostepanenko, (2015), *Casimir and van der Waals forces: Advances and problems.* arXiv preprint arXiv:1507.02393.
54. Van Oss, C.J., M.K. Chaudhury, and R.J. Good, (1988), *Interfacial Lifshitz-van der Waals and polar interactions in macroscopic systems.* Chemical Reviews. **88**(6): p. 927-941.
55. Ninham, B. and V. Parsegian, (1970), *Van der Waals forces: special characteristics in lipid-water systems and a general method of calculation based on the Lifshitz theory.* Biophysical Journal. **10**(7): p. 646-663.
56. Hopkins, J.C., et al., (2015), *Disentangling the effects of shape and dielectric response in van der Waals interactions between anisotropic bodies.* The Journal of Physical Chemistry C. **119**(33): p. 19083-19094.
57. Brevik, I., S.A. Ellingsen, and K.A. Milton, (2006), *Thermal corrections to the Casimir effect.* New Journal of Physics. **8**(10): p. 236.
58. Venkataram, P.S., et al., (2017), *Unifying Microscopic and Continuum Treatments of van der Waals and Casimir Interactions.* Physical Review Letters. **118**(26): p. 266802.
59. Ingold, G.-L. and A. Lambrecht, (2015), *Casimir effect from a scattering approach.* American Journal of Physics. **83**(2): p. 156-162.
60. Canaguier-Durand, A., et al., (2010), *Thermal Casimir effect in the plane-sphere geometry.* Physical Review Letters. **104**(4): p. 040403.
61. Bordag, M., et al., (2000), *Casimir force at both nonzero temperature and finite conductivity.* Physical Review Letters. **85**(3): p. 503.
62. Klimchitskaya, G. and V. Mostepanenko, (2001), *Investigation of the temperature dependence of the Casimir force between real metals.* Physical Review A. **63**(6): p. 062108.
63. Canaguier-Durand, A., et al., (2011), *Casimir interaction between a dielectric nanosphere and a metallic plane.* Physical Review A. **83**(3): p. 032508.
64. Bordag, M., et al., (2006), *Lifshitz-type formulas for graphene and single-wall carbon nanotubes: van der Waals and Casimir interactions.* Physical Review B. **74**(20): p. 205431.
65. Emig, T., et al., (2007), *Casimir forces between arbitrary compact objects.* Physical Review Letters. **99**(17): p. 170403.
66. Langbein, D., (1970), *Retarded dispersion energy between macroscopic bodies.* Physical Review B. **2**(8): p. 3371.
67. Mitchell, D. and B. Ninham, (1972), *Van der Waals forces between two spheres.* The Journal of Chemical Physics. **56**(3): p. 1117-1126.
68. Garrett, J.L., D.A. Somers, and J.N. Munday, (2018), *Measurement of the Casimir Force between Two Spheres.* Physical Review Letters. **120**(4): p. 040401.
69. Clayfield, E., E. Lumb, and P. Mackey, (1971), *Retarded dispersion forces in colloidal particles—exact integration of the Casimir and Polder equation.* J Colloid Interface Sci. **37**(2): p. 382-389.
70. Anandarajah, A. and J. Chen, (1995), *Single correction function for computing retarded van der Waals attraction.* Journal of Colloid and Interface Science. **176**(2): p. 293-300.

CHAPTER 4

Dispersion Many body interactions a Coupled dipole method

"Physics is really nothing more than a search for ultimate simplicity, but so far all we have is a kind of elegant messiness."

Bill Bryson, A Short History of Nearly Everything

1. Many-body affects and dispersion interactions:

In a complex system of many particles the interaction is not simple or pairwise summable, since the existence of other particles screens the interaction between the pairs and thereby effecting the total energy [1]. Therefore, in the discrete microscopic point of view of dispersion forces and for a complete theory, these many body screening effects have to be included within the corpus of the developed models. Accordingly, The total van der Waals interaction energy between a collection of molecules is given as the sum of all m-body contributions $E^{(m)}$ [2, 3]:

$$E = \sum_{i_1 < i_2}^{N} E^{(2)}(r_{i_1}, r_{i_2}) + \sum_{i_1 < i_2 < i_3}^{N} E^{(3)}(r_{i_1}, r_{i_2}, r_{i_3}) + \cdots$$
$$\cdots + \sum_{i_1 < i_2 \cdots < i_N}^{N} E^{(N)}(r_{i_1}, r_{i_2}, ..., r_{i_N}) \qquad (4.1)$$

If the total energy is assumed to be convergent and the higher m-body contribution terms are excluded, only the 2-body interactions survives and the interaction between macroscopic bodies is considered to be a result of the sum of two body interactions. This reduces the many body problem to the discrete pairwise summation formula proposed by Hamaker and studied in the previous chapter [2]:

$$E = \sum_{i=1}^{N} \sum_{j=1}^{N'} E^{(2)}(r_i, r_j) = \sum_{i=1}^{N} \sum_{j=1}^{N'} \frac{\lambda}{r_{ij}^6} \qquad (4.2)$$

However, this approach is clearly not complete or exact due to the serious limitations upon which it was built [4]. And although Lifshitz has solved this problem in his theory yet assuming the material to be continuum has proven also to be problematic if complex geometries are involved or extremely small nanoparticles or nanoclusters are studied, where the discrete morphology of matter is evident and influential.

A simple example is chosen from literature demonstrating the important contribution of many body effects to the total dispersion interaction energy between nanoparticles; the Axilrod-Teller-Muto potential has been used to incorporate 3-body interactions when calculating the vdW forces between silica spherical noncolloidal particles with the number of constituent atoms is 619 atoms[5]. And they found that this contributions accounts for 20% of the total interaction energy demonstrating thus the importance of many body interactions and their critical contribution to dispersion forces between nanoparticles [5]. Similar results are demonstrated throughout literature[6-11], thus urging researchers to develop a microscopic theory that includes all effects, mostly many body interactions and retardation. Accordingly, the Coupled dipole method was proposed and is developed.

2. The Coupled Dipole Method:

The first appearance of the coupled dipole method (CDM) was in a successive three articles by Bij Renne and Nijboer [12-14]. Lately this approach had resurfaced and reintroduced with applications to the interaction between spherical nanoparticles and the calculation of static polarizabilities of nanoclusters [11, 15, 16]. The CDM is an atomistic approach which has the unique property of accounting for all many body interactions contributing to the dispersion energy between two objects [11, 16]. This model has been used to demonstrate the limitation of the pairwise summation approach as well as the DLP theory especially for extremely small nanoparticles [11].

Till now, The CDM has been applied for certain limited cases such as the interaction of two identical nano-spheres [16], other applications are also demonstrated in literature for the case of graphitic nanostructures such as nanotubes, nanoribbon [9] and nanowiggles [17]. The CDM has been developed only for the non-retarded regime, yet a further enhancement of this method would make it the most suitable and accurate method for nanostructures and nanoclusters, especially those with complex geometrical arrangements [18].

There also some other applications demonstrated in literature of the same approach with slight differences[19-22],yet we shall not go through them since they were intended to study the interactions between molecules or incorporate dispersion forces within the process of modeling the structure and properties of materials[4, 23, 24].

2.1. Quantum theoretical basics of the theory:

Within the CDM framework each atom is replaced by a three-dimensional harmonic Quantum Drude Oscillator with the nucleus is placed at the center [19, 25], which means that at a basic level we have replaced Fermi statistics with Boltzmann statistics since the QDOs are distinguishable. In this model particles interact through long range Coulombic forces, and each of those particles is characterized by its mass, frequency, and charge(m, ω, e)[19]. The particle possesses an instantaneous dipole moment proportional to the oscillator displacement from equilibrium u_i. The Coupled Dipole Method Hamiltonian for an N-particle system is written as follows [8, 12, 19, 25]:

$$H = \sum_{i=1}^{2N} \frac{P_i^2}{2m} + \frac{m\omega_0^2}{2} \sum_{i=1}^{2N} u_i^2 - \frac{e^2}{2\varepsilon_0} \sum_{i>j}^{2N} u_i \cdot T_{ij} \cdot u_j \tag{4.3}$$

The first terms of the Hamiltonian present the kinetic and potential energy of the Harmonic oscillators, and the last terms defines the coupling between these oscillators by the dipole-dipole interaction tensor T_{ij}, where P_i represents the linear momentum of the ith particle [19, 25]. Therefore the vdW interaction energy for the full system of interacting clusters is calculated as the difference between the zero-point energies of the coupled and uncoupled oscillators [19]:

$$E_{vdW} = \frac{1}{2} \sum_{i=1}^{3N} \sqrt{\lambda_i} - \frac{3}{2} \sum_{i=1}^{N} \omega_i \tag{4.4}$$

Where λ_i are the matrix eigenvalues of the interaction Hamiltonian.

2.2. Formulation of the model:

To demonstrate the formulism of this approach let us consider two interacting clusters (1) and (2) with the number of atoms in each one is N and N' respectively. The interaction energy between these two clusters can be calculated by taking the total energy of the system of combined interacting particles and subtract the self-energies of each individual system when considered at large distance where the interaction vanishes [3, 18]:

$$V_{vdW} = V_{N+N'} - \left(V_N + V_{N'} \right) \tag{4.5}$$

The related energies of the interacting systems are calculated from the eigenvalue problems developed using the CDM framework. Initially, Each atom is considered as an instantaneous dipole P_i induced by a local electrical field $\vec{E}_{loc}(\vec{x}_i)$, with its dipole moment p_i is given as follows [16, 18, 26]:

$$\vec{p}_i = \alpha_i \cdot \vec{E}_{loc}\left(\vec{x}_i \right) \tag{4.6}$$

The local electric field $\vec{E}_{loc}(\vec{x}_i)$ is given as the sum of all instantaneous electric fields generated from instantaneously induced dipole moments of other atoms in the system [27]:

$$\vec{E}\left(\vec{x}_i \right) = \sum_{\substack{j=1 \\ j \neq i}}^{N} T_{ij} \cdot \vec{p}_j \tag{4.7}$$

The static dipole field tensor is given as it was demonstrated in chapter 2 within the multipolar expansion of the electrostatic potential of the interaction between molecules [15, 27, 28]:

$$T_{ij} = \begin{cases} \left(\dfrac{3\hat{n}_{ij}\hat{n}_{ij} - I}{r_{ij}^3} \right) & \text{for } i \neq j \\ 0 & \text{for } i = j \end{cases} \tag{4.8}$$

Where I is the identity matrix, n_{ij} is the unit vector and r_{ij} is the distance between the centers of atoms i and j. The oscillator model is employed for non-retarded vdW interaction energy the dynamic atomic polarizability of a Drude harmonic oscillator is[25]:

$$\alpha(\omega) = \left(\frac{e^2}{m}\right) \sum_k \frac{1}{\left(\omega_{0k}^2 - \omega^2\right)} = \sum_k \frac{\alpha_{0k}}{\left(1 - \frac{\omega^2}{\omega_{0k}^2}\right)} \tag{4.9}$$

To use this formula, we need the value of α_0 and ω_0 which can be calculated from the continuum theory using the clausius-mossotti relation [18] :

$$\frac{\varepsilon(i\omega) - 1}{\varepsilon(i\omega) + 2} = \frac{4\pi}{3} \rho\alpha(i\omega) \tag{4.10}$$

By substituting **Eq.(4.7)** in **Eq.(4.6)** we find a system of equations where each one is designated for a single atom in the system:

$$\vec{p}_i - \sum_{\substack{j=1 \\ j \neq i}}^{N} \vec{\alpha}_i \cdot \vec{T}_{ij} \cdot \vec{p}_j = 0 \tag{4.11}$$

Furthermore, by introducing the isotropic atomic polarizability of the Drude model [9, 11, 27], we then get an eigenvalue problem which is stated as follows:

$$\vec{p}_i - \frac{\alpha_{0i}}{\left(1 - \frac{\omega^2}{\omega_{0i}^2}\right)} \sum_{\substack{j=1 \\ j \neq i}}^{N} \vec{T}_{ij} \cdot \vec{p}_j = 0 \tag{4.12}$$

This can then be written as:

$$\vec{p}_i - \alpha_{0i} \sum_{\substack{j=1 \\ j \neq i}}^{N} T_{ij} \cdot \vec{p}_j = \left(\frac{\omega}{\omega_{0i}}\right)^2 \vec{p}_i \tag{4.13}$$

For a system of identical atoms ($\omega_{0i} = \omega_0$; $\alpha_{0i} = \alpha_0$), the problem can be rewritten as [18]:

$$(I + Q) \cdot \vec{P} = \left(\frac{\omega}{\omega_0}\right)^2 \cdot \vec{P} \tag{4.14}$$

Where $\vec{P}$ is a 3N column vector, I is 3N×3N identity matrix, and $Q = -\alpha \cdot T$ is also a 3N×3N matrix. and since frequency contributes a ground state energy of $\hbar\omega_k/2$. the total energy of a system of N-Drude oscillators is then given to be [25]:

$$V_N = \frac{\hbar}{2} \sum_{k=1}^{3N} \omega_k \tag{4.15}$$

The eigenvalue problem will be written so that the eigenvalues are ω_k/ω_0 and not (ω_k^2/ω_0^2), which makes it possible to solve the problem straightforwardly using standard diagonalization algorithms[18]:

$$(I+Q)^{1/2} \cdot \vec{P} = \left(\frac{\omega}{\omega_0}\right) \cdot \vec{P} \qquad (4.16)$$

The total van der Waals energy of the system is given thus as:

$$Tr\left[(I+Q)^{1/2}\right] = \sum_{k=1}^{3N}\left(\frac{\omega_k}{\omega_0}\right) = \frac{V_N}{\hbar\omega_0/2} \qquad (4.17)$$

If the case of two interacting nonpolar atoms is taken, the problem can be solved with few lines of calculations to give a solution of six eigenvalues which are written as follows:

$$\omega_z^{\pm} = \omega_0\left(1 \pm 2\gamma\right)^{1/2} \quad ; \quad \omega_x^{\pm} = \omega_y^{\pm} = \omega_0\left(1 \pm \gamma\right)^{1/2} \qquad (4.18)$$

Where for a system of identical particles such as the one is considered here in this work, we have $\gamma = \alpha_0/r^3$ with r is distance between the center points of the atoms, and the x and y eigenmodes are degenerate due to symmetry, the eigenmodes and their corresponding eigenvalues are demonstrated in the **Tab.(4.1)** below .

Table 4.1: eigenmodes and corresponding Eigenvalues in a system of two interacting non-polar atoms

Eigenmodes	**eigenvalues**
	$\omega_z^+ = \omega_0\left(1 + 2\gamma\right)^{1/2}$
	$\omega_x^+ = \omega_0\left(1 + \gamma\right)^{1/2}$
	$\omega_y^+ = \omega_0\left(1 + \gamma\right)^{1/2}$
	$\omega_z^- = \omega_0\left(1 - 2\gamma\right)^{1/2}$
	$\omega_x^- = \omega_0\left(1 - \gamma\right)^{1/2}$
	$\omega_y^- = \omega_0\left(1 - \gamma\right)^{1/2}$

For the total system of (N+N') particles, the eigenvalue problem is found to be as follows [18]:

$$\Omega \cdot \vec{P} = \lambda^2 \cdot \vec{P} \tag{4.19}$$

With Ω is the $(3N + 3N') \times (3N + 3N')$ interaction matrix, and its eigenvalues are the squared eigen-frequencies $\lambda^2 = (\omega/\omega_0)^2$. Ω is given in the following form [11]:

$$\Omega = \begin{pmatrix} I+Q & M \\ M' & I+Q' \end{pmatrix} \tag{4.20}$$

It should be recognized that Q and Q' are the interaction matrices for particles of the same object (inter-interactions), also M and M' are matrices presenting the interactions between atoms of different systems (intra-interactions)[18]. With Q is a 3N×3N traceless matrix, made of dimensionless dipole tensors connecting each two atoms within cluster (1), Q' is the 3N×3N matrix related to interactions between atoms of cluster (2). M is a 3N×3N' matrix representing the dipole interaction tensors (M_{ij}) connecting one atom in cluster (1) to another in (2), and M' is the transpose matrix of M representing the dipole tensor connecting an atom from cluster (2) to another in cluster (1). These matrices are defined in the following table with each element is an interaction tensor between two atoms. For the following calculations we take as a convention the labels (i,j) in T to present indices of atoms of the same system (cluster), on contrast the labels (k,m) in the M_{km} elements are indices of atoms of different system.

Table 4.1 : The interaction matrices defined with each element is a 3×3 matrix defining the interaction between atoms from the same cluster for Q and Q', and atoms of different clusters for M and M'.

$$Q = \begin{pmatrix} 0 & \Gamma_{12} & \Gamma_{13} & \cdots & \Gamma_{1N} \\ \Gamma'_{12} & 0 & \Gamma_{23} & \cdots & \Gamma_{2N} \\ \Gamma'_{13} & \Gamma'_{23} & 0 & \cdots & \Gamma_{3N} \\ \vdots & \vdots & \vdots & \ddots & \vdots \\ \Gamma'_{1N} & \Gamma'_{2N} & \Gamma'_{3N} & \cdots & 0 \end{pmatrix}$$

$$Q = \begin{pmatrix} 0 & \Gamma_{12} & \Gamma_{13} & \cdots & \Gamma_{1N'} \\ \Gamma'_{12} & 0 & \Gamma_{23} & \cdots & \Gamma_{2N'} \\ \Gamma'_{13} & \Gamma'_{23} & 0 & \cdots & \Gamma_{3N'} \\ \vdots & \vdots & \vdots & \ddots & \vdots \\ \Gamma'_{1N'} & \Gamma'_{2N'} & \Gamma'_{3N'} & \cdots & 0 \end{pmatrix}$$

$$M = \begin{pmatrix} M_{11} & M_{12} & M_{13} & \cdots & M_{1N} \\ M_{21} & M_{22} & M_{23} & \cdots & M_{2N} \\ M_{31} & M_{32} & M_{33} & \cdots & M_{3N} \\ \vdots & \vdots & \vdots & \ddots & \vdots \\ M_{N'1} & M_{N'2} & M_{N'3} & \cdots & M_{N'N} \end{pmatrix}$$

$$M' = \begin{pmatrix} M_{11} & M_{21} & M_{31} & \cdots & M_{N'1} \\ M_{12} & M_{22} & M_{32} & \cdots & M_{N'2} \\ M_{13} & M_{23} & M_{33} & \cdots & M_{N'3} \\ \vdots & \vdots & \vdots & \ddots & \vdots \\ M_{1N} & M_{2N} & M_{3N} & \cdots & M_{N'N} \end{pmatrix}$$

From the eigenvalue problems for both single system (**Eq.4.16**) and the total combined system (**Eq.4.19**), we can demonstrate using TCDM that the total exact dimensionless non-retarded dispersion energy W_{vdw} is given in the following form:

$$W_{vdw} = \frac{V_{vdW}}{\hbar\omega_0/2} = \left\{ Tr\left[\Omega^{1/2}\right] - Tr\left[\left(I+Q\right)^{1/2}\right] - Tr\left[\left(I+Q'\right)^{1/2}\right] \right\} \tag{4.21}$$

Where the term $\hbar\omega_0/2$ comes from the fact that each normal mode frequency contributes with an energy equals to the value of this term [18]. It should be noted as well that the assumption of isotropic atomic polarizability made here is purely for computational reasons and the general form of anisotropic atomic polarizability can be implemented within the CDM approach.

The various methods which are used for computing van der Waals forces and the exact CDM method developed in this chapter were compared [29]. The comparison was made for two identical spheres with the number of particles in each one is N=2340 atoms. And the spheres diameters is taken to equal 5.88 nm in order to be introduced into the continuum methods. Due to the discrete placement of the atoms within the cluster, analytical methods (e.g. DLP, Hamaker) far over-estimate the result for small gaps. The two-body sum approaches the exact CDM value at far distances, since multi-body effects mostly disappear. At much larger separations than shown on **Fig.(4.1)** the CDM and Lifshitz theory converge to the same result, as expected. Results from the Derjaguin approximation are remotely off even at large distances [29].
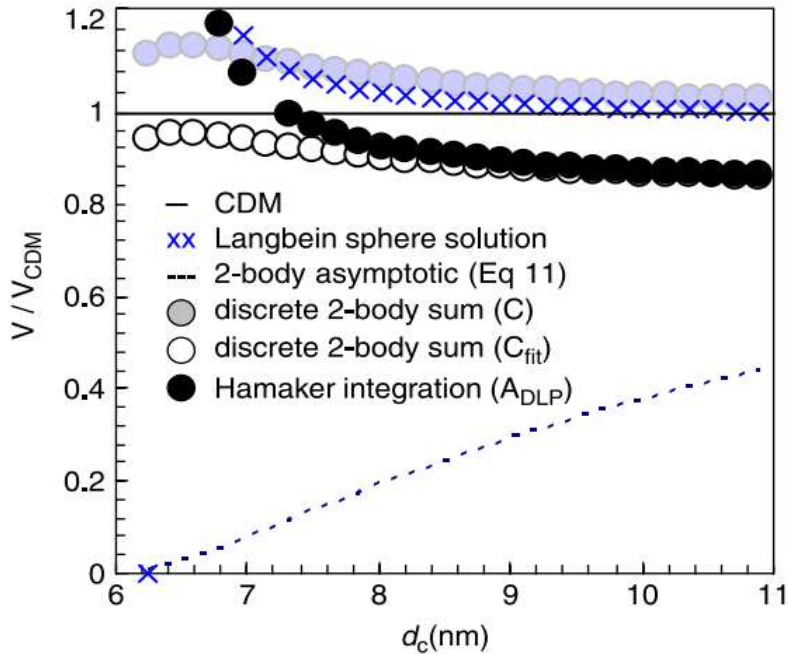
Figure 4.1: a comparison between the CDM approach and other methods for identical spherical nanoparticles with radius 5.88 nm (reprinted from ref.[29])

2.3. The Trace Coupled Dipole Method (TCDM):

Since the calculation of the trace of the square root of a matrix is a hard problem which involves computationally expensive calculations, the terms of this equation can be each developed using a binomial expansion to series of powered matrices. We start by writing the first term as follows [18]:

$$Tr\left[\Omega^{1/2}\right] = Tr\left[\left\{\begin{pmatrix} I & 0 \\ 0 & I \end{pmatrix} + \begin{pmatrix} Q & M \\ M' & Q' \end{pmatrix}\right\}^{1/2}\right]$$

(4.22)

We have the mathematical formula of the binomial expansion which states that:

$$\left(1+A\right)^{1/2} = \sum_{n=0}^{\infty} c_n A^n$$

(4.23)

Where the coefficients c_n are given as follows:

$$\begin{cases} c_0 = 1 \\ c_n = c_{n-1}\left(\dfrac{3}{2n}-1\right) & for \ n \neq 0 \end{cases}$$

(4.24)

By introducing the of all terms, the total interaction energy than can be written as [18]:

$$W_{vdW} = \left\{\sum_{n=0}^{\infty} c_n Tr\left[\begin{pmatrix} Q & M \\ M' & Q' \end{pmatrix}^n\right] - \sum_{n=0}^{\infty} c_n Tr\left[Q^n\right] - \sum_{n=0}^{\infty} c_n Tr\left[\left(Q'\right)^n\right]\right\}$$

(4.25)

The vdW interaction energy thus can be written as a sum of a series of (n) contributions:

$$W_{vdW} = \sum_{n=0}^{\infty} W^n$$

(4.26)

With the n-th order contribution to the interaction energy is given as [18]:

$$W^n = c_n\left\{Tr\left[\begin{pmatrix} Q & M \\ M' & Q' \end{pmatrix}^n\right] - Tr\left[Q^n\right] - Tr\left[\left(Q'\right)^n\right]\right\}$$

(4.27)

These contributions should not be mistaken for n-body interactions, a general demonstration of this statement will be thoroughly presented in this paper. This approach was verified to give about 99% the same result as the exact CDM approach for n=10, and with calculation time far less than that needed to solve the eigenvalue problem demonstrated in **Eq.(4.27).** this method is very efficient in the case where the eigenvalues of the single atoms are not needed which is the case of systems of identical particles as adopted in this work henceforth.

3. New algebraic model derived from the TCDM

Although the application of the trace coupled dipole method to calculate the interaction energy is somewhat straightforward computationally, yet we shall further continue with the aim to present a model that does not only calculates the final interaction energy with less computational burden but also presents a general understanding of the interaction process. Therefore, we write the first term of **Eq.(4.27)** as the sum of two matrices:

$$\begin{pmatrix} Q & M \\ M' & Q' \end{pmatrix}^n = \left[\begin{pmatrix} Q & 0 \\ 0 & Q' \end{pmatrix} + \begin{pmatrix} 0 & M \\ M' & 0 \end{pmatrix} \right]^n \tag{4.28}$$

Now the matrix can be expanded as series using the binomial expansion given as follows:

$$(A+B)^n = \sum_{k=0}^{n} c_{n,k} A^n B^{n-k} \quad with \ c_{n,k} = \frac{n!}{k!(n-k)!} \tag{4.29}$$

Denoting the matrices, A and B such that:

$$A = \begin{pmatrix} Q & 0 \\ 0 & Q' \end{pmatrix} \quad ; \quad B = \begin{pmatrix} 0 & M \\ M' & 0 \end{pmatrix} \tag{4.30}$$

Although the product of matrices A and B is not commutative$(AB \neq BA)$ for the general case, we assume the trace of their product to be constant for any permutation. This assumption holds completely for identical clusters due to the consequent inherited commutatively of A and B, a further inspection of the validity of this assumption for different atomic configurations and different cluster sizes can be investigated separately. Since the main aim is to study the interaction between identical clusters, we thus further continue our calculations upon this assumption. Therefore, the trace of this matrix can then be written as the sum of traces of the single terms of the series:

$$Tr\left[(A+B)^n\right] = Tr\left[\sum_{k=0}^{n} \binom{n}{k} A^k B^{n-k}\right] = \sum_{k=0}^{n} \binom{n}{k} Tr\left[A^k B^{n-k}\right] \tag{4.31}$$

Now when we take the last term of the series for $(k = n)$ and develop its trace, we find :

$$Tr\left[A^n\right] = Tr\left[\begin{pmatrix} Q & 0 \\ 0 & Q' \end{pmatrix}^n\right] = Tr\left[Q^n\right] + Tr\left[(Q')^n\right] \tag{4.32}$$

Going back to the general equation of the n-th contribution to the vdW interaction energy between two clusters as demonstrated in **Eq.(4.27)**, combined with the binomial (**Eq.4.31**) and the result found for the last term (**Eq.4.32**). The contribution of the self-energies of the individual clusters is found to vanish with the last term of the binomial series. The n-th order contribution to the total vdW energy is thus found to be:

$$W^n = c_n \left\{ \sum_{k=1}^{n-1} c_{n,k} Tr\left[A^k B^{n-k} \right] + Tr\left[B^n \right] \right\}$$ (4.33)

The energy is thus resulting either from the pure interaction between atoms of different clusters (2nd term) or from the coupling of inter-interactions with intra-interactions which are expressed by the first terms of **Eq.(4.33)**. The trace of the last term is found to vanish $(Tr[B^n] = 0)$ for odd value of n due to the tracelessnes of the matrix in this case, and for even value of n the trace is found as follows:

$$Tr\left[B^n \right] = Tr\left[(MM')^{n/2} + (M'M)^{n/2} \right]$$ (4.34)

The first term is a series of k-th order. The trace of each term of this series has four possible outcomes related to the value of k and n, for n and k both are even or odd the trace of the matrix is given in **Eq.(23)**. For n and k being out of order, (i.e. one is odd and the other is even) the matrix becomes traceless.

$$Tr\left[A^k B^{n-k} \right] = Tr\left[Q^k (MM')^{(n-k)/2} \right] + Tr\left[(Q')^k (M'M)^{(n-k)/2} \right]$$ (4.35)

Since the clusters are identical, and from symmetry we have $(M' = M)$ and $(Q' = Q)$. Considering this assumption and by substituting **Eq.(4.35)** and **Eq.(4.34)** into **Eq.(4.33)**, the n-th contribution to the vdW interaction energy is reduced into the following formula:

$$W^{\,n} = 2 \times c_n \left\{ X_n + Z(n) \times K_n \right\}$$ (4.36)

Where:

$$X_n = \sum_{k=1}^{n-1} c_{n,k} Z(n-k) \times X_{n,k}$$ (4.37)

With Z is a mathematical object proposed to include all vanishing terms in the general equation as contributions of zeros, this mathematical function is defined as follows:

$$Z(n) = \begin{cases} 0 & for \ \ n = 2k+1 \ \ \forall k \in \mathbb{N} \\ 1 & for \ \ n = 2k \ \ \ \ \ \ \forall k \in \mathbb{N} \end{cases}$$ (4.38)

The last term K_n presents the interactions between atoms of the two clusters (intra-interactions), this term when calculated for a couple of atoms presents the results of London. The first series of terms presents the coupling between the interactions between atoms of the same cluster (inter-interactions) and the interactions between atoms of different clusters, with n is the total number of contributions and k is number of contributions inside the cluster. From the multiplication of matrices, we can deduce easily the formulas of the explicit formulas of the contributing K_n and W_n terms involved in **Eq.(4.36)** and **Eq.(4.37)**.

$$\mathrm{K}_n = Tr\left[\left(M\right)^n\right]$$

$$= Tr\left[\sum_{i_1=1}^{N}\sum_{i_2=1}^{N}\sum_{i_3=1}^{N}\cdots\cdots\sum_{i_n=1}^{N}\left(M_{i_1 i_2} M_{i_2 i_3}\cdots\cdots M_{i_n i_1}\right)\right] \qquad (4.39)$$

$$\mathrm{X}_{n,k} = Tr\left[Q^k\left(M\right)^{(n-k)}\right]$$

$$= Tr\left[\sum_{i_1=1}^{N}\cdots\sum_{i_k=1}^{N}\sum_{i_{k+1}=1}^{N}\sum_{i_{k+2}=1}^{N}\cdots\sum_{i_n=1}^{N}\left(\Gamma_{i_1 i_2}\Gamma_{i_2 i_3}\cdots\Gamma_{i_{k-1} i_k}\right.\right.$$

$$\left.\left.\times M_{i_k i_{k+1}} M_{i_{k+1} i_{k+2}}\cdots M_{i_n i_1}\right)\right] \qquad (4.40)$$

The model is now straightforward and informative as it was intended to be, and we can derive the possible many body contributions easily without going through the tedious calculations.

3.1. Presentation of possible interaction modes:

When examining the terms K_n, we notice that the path of the interaction is cyclic and that the number of atoms is even due to the vanishing odd terms owing to the tracelessness of the involved matrices (M_{ij}). To simplify the graphical representation of the interaction modes, a schematic representation **(Fig.4.2)** can be given in an innovative way using the concept of isomorphism of graphs from graph theory [30].
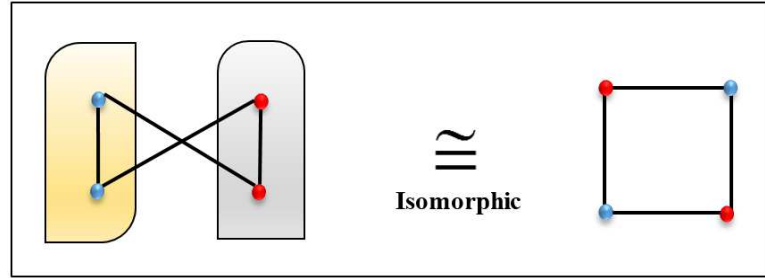
Figure 4.2 : The transformation from ordinary representation to the graph-theory based representation using the isomorphism of graphs.

The representation proposed does not consider distances or boundaries of objects. Only atoms presented by points (vertices) and the interaction matrix (M_{ij}, T_{ij}) expressing the interaction between each two atoms are represented as lines (edges); we distinguish between particles by assigning a different color for particles (vertices) of different clusters (in our case blue and red for the two interacting clusters). **Fig.(4.3)** shows all possible modes for the second term K_n of **Eq.(4.36)** for $n = 2, 4, 6$. **Fig.(4.4)** shows the modes that occur due to the first terms (X_n) of the equations of the n-th order contributions to the total interaction energy (W_n). the inner interactions of atoms of the same object (cluster), which are expressed in terms of the matrices (T_{ij}), are presented as edges with different color than that presenting matrices (M_{ij}).
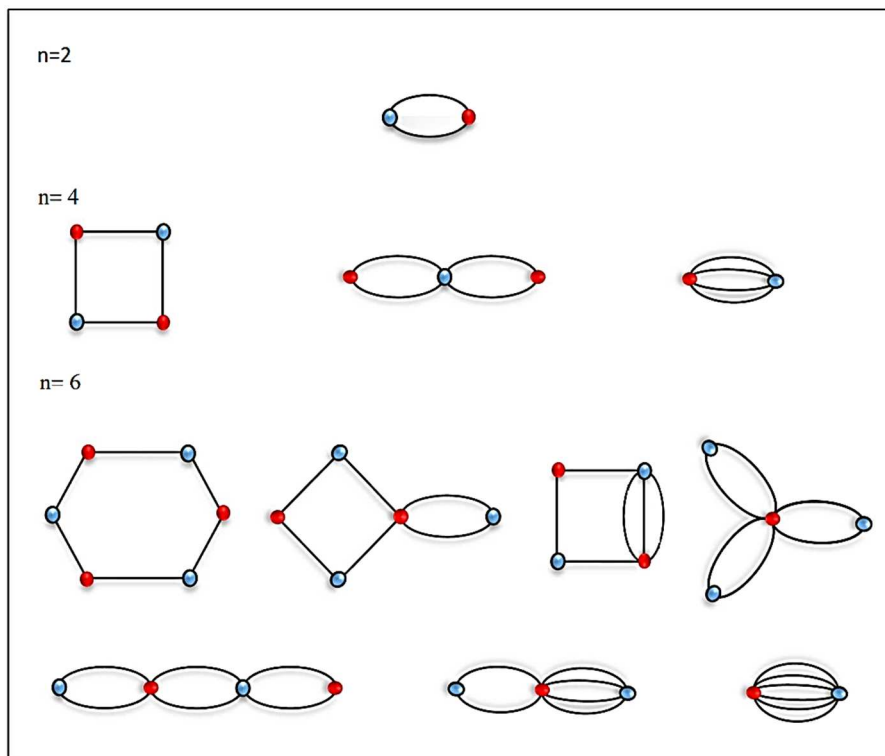
Figure 4.3: Graphical representations of the interaction modes involved in the first K_n terms.
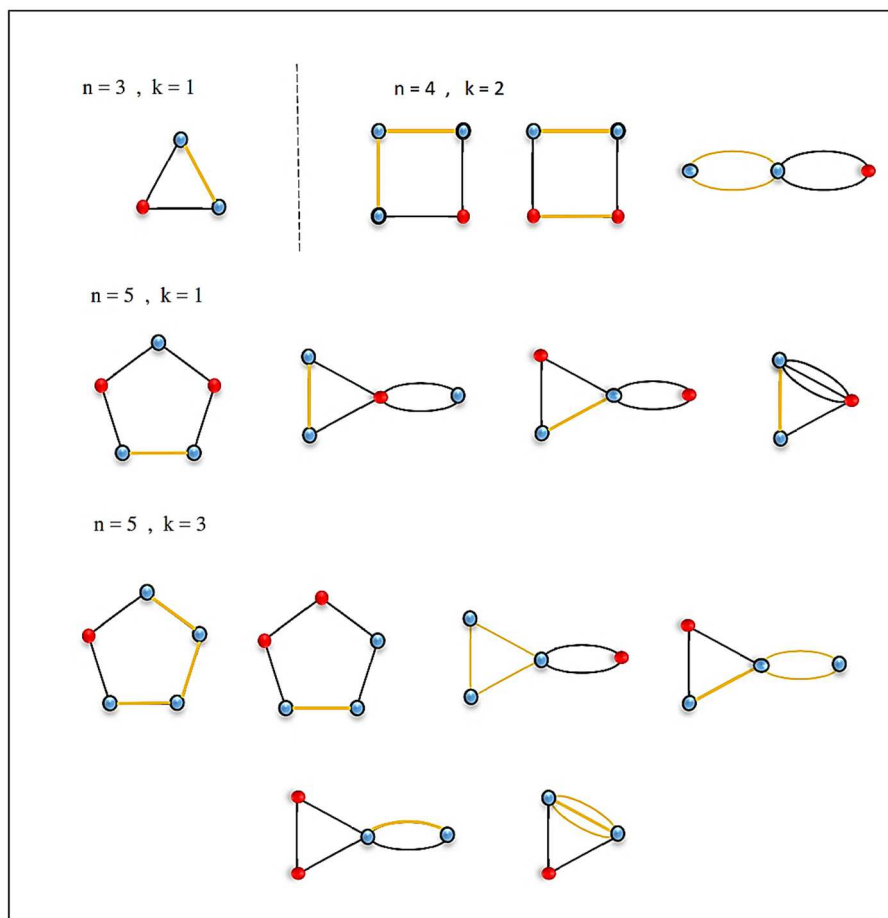
Figure 4.4: Graphical representations of the interaction modes involved in the first X_n terms.

This method of representing the interaction between particles will allow us to find graphically all possible modes of interaction for each n-th order contribution. This investigation of the possible modes would be achieved by conserving the size of the graph (the number of edges; n) and reduce the order of the graph ('m' the number of vertices) by relating non-neighbored vertices of the same color. The operation of graph-reduction is a map (Π) from the set (E^m) of graphs $G(m, n)$ with order 'm' to the set (E^{m-1}) of graphs $G(m-1, n)$ with order 'm-1'. This operation is repeated until the graph is irreducible.

$$\Pi : \ E^m \big[G(m, n) \big] \to E^{m-1} \big[G(m-1, n) \big] \tag{4.41}$$

This type of transformation **(Eq.4.41)** is due to the permutation of labels (i_n), where this permutation allows for cases where two labels coincide, which reduces the number of atoms (n) contributing to interaction and thus reduces the graph. The rules used to produce the graphs of all possible modes exemplified in **Fig.(4.3)** and **Fig.(4.4)**, are inherited from the properties of the equations that these graphs present. For the case of the K_n term, we notice that all modes are reduced to a two-body interaction; the sum of the terms associated to these graphs can be easily demonstrated to be the same as the result calculated from perturbation theory as will be shown later in this thesis.

3.2. Deriving m-body interaction energy:

To calculate m-body interaction energies separately using the model proposed in this work, the representative graphs are used. Each graph is associated with the energy of the interaction which it is representing, thus the m-body interaction energy can be calculated from the sum of the energies of all possible graphs of order (m).
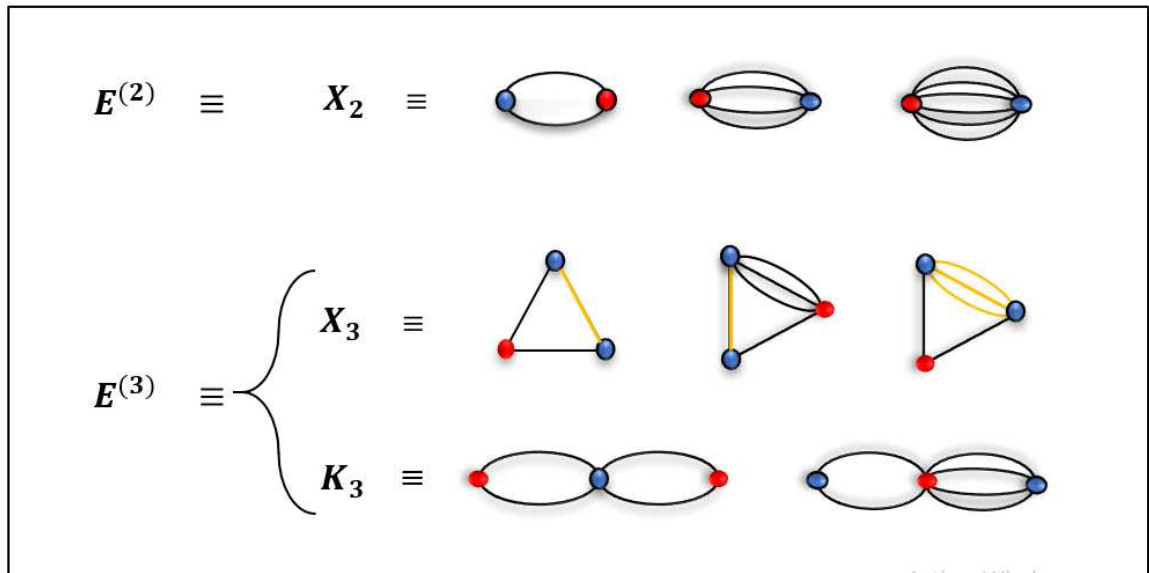
Figure 4.5: Graphical representations of 2-body and 3-body interaction modes.

A simple example would be to deduce the 2-body effect contribution from the model proposed. as can be seen in **Fig.(4.5)**, the 2-body interaction energy is represented by a group of graphs which can be algebraically interpreted as a power series of the form:

$$E^{(2)} = \frac{\hbar\omega_0}{2} c_n \sum_{i=1}^{\infty} Tr\left[M^{2i} \right]$$

(4.42)

By feeding the values of the dipole-dipole tensor elements into the matrices M and Γ, we have these matrices for identical atoms to be given as follows [18]:

$$M_{ij} = T_{ij} = \begin{pmatrix} \alpha_0/r_{ij} & 0 & 0 \\ 0 & \alpha_0/r_{ij} & 0 \\ 0 & 0 & -2\alpha_0/r_{ij} \end{pmatrix}$$

(4.43)

After introducing **Eq.(4.42)** into the derived formula **(Eq.4.41)**, the 2-body interactions for identical particles is therefore found to be given as follows:

$$E^{(2)}(\vec{r}_i, \vec{r}_j) = \sum_{i=1}^{\infty} C_{6i} \cdot r_{ij}^{-6i}$$

(4.44)

Where the dispersion coefficients C_{6i} are defined for identical atoms to be given as:

$$C_{6i} = \frac{c_{2i}\hbar\omega_0}{2}\left(2+(-2)^{2i}\right)\alpha_0^{2i}$$

(4.45)

We notice that the first term of the series (**Eq.4.44**) is exactly the same as the formula proposed by London for 2-body interactions using perturbation theory [31, 32]. We should also recognize that this term is equivalent to the first contribution W^2 to the total interaction energy. This result demonstrates how powerful is this approach in calculating non-retarded dispersion forces. Moreover, from our calculations, the general formula of all dispersion coefficients for identical particles, is found to be written as follows:

$$C_{3i} = \frac{c_i\hbar\omega_0}{2}\left(2+(-2)^i\right)\alpha_0^i \quad with \quad i = 2, 3, .., n$$

(4.46)

The 3-body interaction energy is derived from the graphical presentation also in the same manner, and it is given as follows:

$$E^{(3)}(\vec{r}_i, \vec{r}_j, \vec{r}_k) = \frac{\hbar\omega_0}{2}Tr\left\{\sum_{l=0}^{\infty}\sum_{m=0}^{\infty}\left[\sum_{\delta=0}^{\infty}\Gamma_{ij}^{3l} M_{jk}^{3m}, M_{ki}^{3\delta} + M_{ij}^{2(l+1)}M_{jk'}^{2(m+1)}\right]\right\}$$

(4.47)

The first term of this series presents the Axilrod-Teller-Muto (ATM) potential of the 3-body dispersion interaction energy, where the coefficient C_9 can be calculated from **Eq.(4.37)** and given as $9\hbar\omega_0\alpha_0^3/16$. This term can be calculated in a simple form by considering a system of only three atoms which leaves the interaction matrices Γ and M to be identical, and by taking the first term of sum, we get the following formula which also presents the first graph of the series of graphs given in **Fig.(4.5)**:

$$E_{ATM}^{(3)} = \frac{9\hbar\omega_0}{16} Tr\left[\Gamma_{ij}\Gamma_{jk}\Gamma_{ki} \right] \tag{4.48}$$

By substituting the dipole-dipole tensor elements within this formula we get the energy for identical particles to be:

$$
\begin{aligned}
E_{ATM}^{(3)} &= \frac{9\hbar\omega_0}{16}\left\{\alpha_0^3 T_{ij}T_{jk}T_{ki}\right\} \\
&= \frac{9\hbar\omega_0}{16}\left\{\alpha_0^3 \left(r_{ij}r_{jk}r_{ki}\right)^{-3}\right\} \times \left\{-2 + 3\left(\hat{n}_{ij}\bullet\hat{n}_{jk}\right)^2 + 3\left(\hat{n}_{jk}\bullet\hat{n}_{ki}\right)^2 \right. \\
&\qquad \left. + 3\left(\hat{n}_{ki}\bullet\hat{n}_{ij}\right)^2 - 9\left(\hat{n}_{ij}\bullet\hat{n}_{jk}\right)\left(\hat{n}_{jk}\bullet\hat{n}_{ki}\right)\left(\hat{n}_{ki}\bullet\hat{n}_{ij}\right)\right\}
\end{aligned}
\tag{4.49}
$$

Since we know from basic trigonometry the relation between the scalar product of unit vectors and the angles between those vectors, which are given generally as $(\hat{n}_{ij} \cdot \hat{n}_{jk}) = -\cos\theta_j$. The formula of the 3-body potential energy can be developed and simplified with few lines of trigonometric calculations into the Axilrod-Teller-Muto (ATM) formula:

$$E^{(3)} = \frac{9\hbar\omega_0\alpha_0^3}{16}\frac{\left(1+3\cos\theta_i\cos\theta_j\cos\theta_k\right)}{r_{ij}^3 r_{jk}^3 r_{ki}^3} \tag{4.50}$$

It should be recognized that this term $E_{ATM}^{(3)}$ is equivalent to the second contribution W^3. Using the same method, the series of all n-body interactions can be developed. The model developed here is thus demonstrated to be very efficient in calculating the contributions of n-body interactions separately.

Another aspect of the graphical representation proposed in this is that we can use adjacency matrices to determine the power indices, however in order to accomplish that a whole theory of the dynamics of the proposed graphs have to be developed within the framework of graph theory, a task which is not found in the corpus of this theory and is under construction by us. This unique feature of this representation makes it highly promising more than the diagrammatic representation which was proposed by Jones (2013)[33] although a coupling between the two is needed in future works.

4. Results and discussions

To demonstrate the behavior of many body effects in dispersion interactions between nanoclusters, we study the interaction between two similar chains of atoms. Two configurations are used parallel and collinear with the number of atoms in the chains ranges from 2 atoms to 10 atoms per cluster. **Fig. (4.6)** shows the interaction energy calculated from our model compared with that calculated using the pairwise summation method. We notice that the pairwise summation method underestimates the interaction for small distances and the difference decreases with increasing distance. The difference between the energy calculated from both approaches is far greater for a parallel configuration than that for a collinear one. The

calculations are coded in our own **FORTRAN** code for which the general flow chart is given in "**Appendix II**".
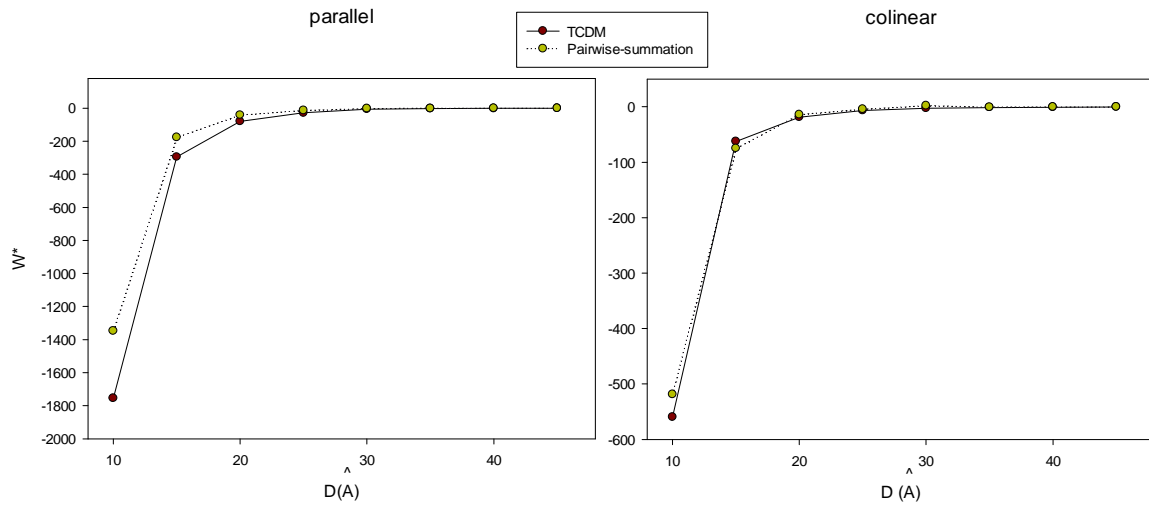
Figure 4.6: The interaction energy between two decamers; a comparison between the results calculated from the pairwise summation approach and that calculated from the TCDM using our derived algebraic formula of the model.

The model proposed is used and the contributions of the two terms (K, X) of this model are compared. **Fig.(4.7)** and **Fig.(4.8)** show the percentage of the contribution of the terms K_n to the total interaction energy for the selected configurations ; parallel and colinear respectively. This study is a preliminary study in which we try to derive some key results concerning the effect of many body interactions on the dispersion energy between identical nanoclusters.
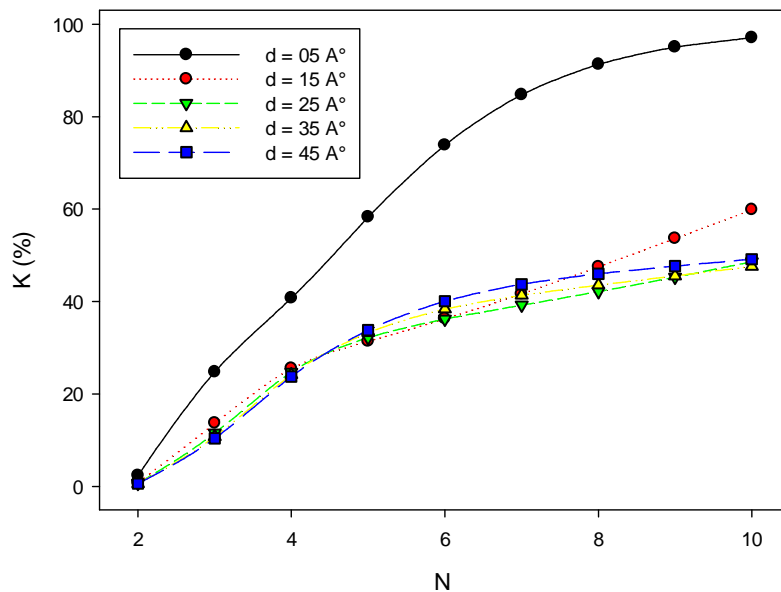
Figure 4.7: The contribution of K (in %) to the total interaction for an interaction between two parallel chains.
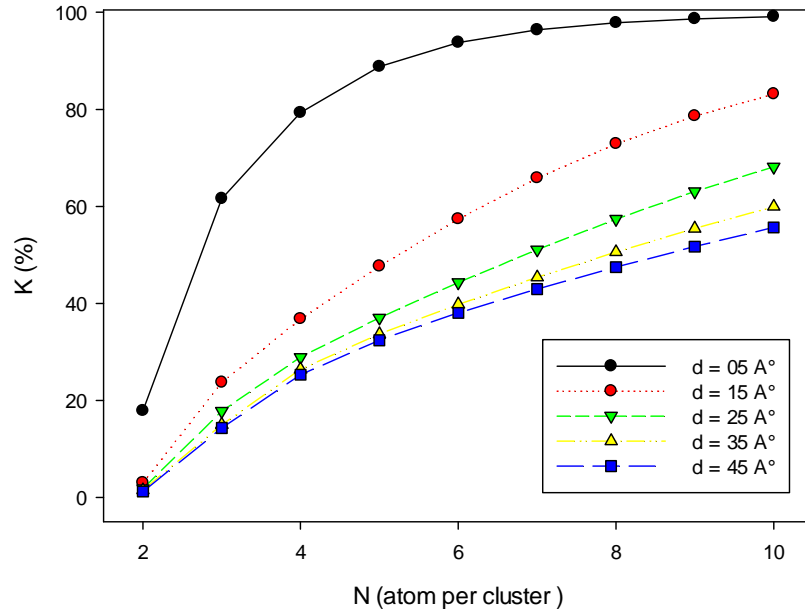
Figure 8: The contribution of K (in %) to the total interaction for an interaction between two collinear chains.

For both geometrical configurations, we notice that the contribution of the K_n terms increases with the increase in the number of atoms constituting the chains, this increase is faster for small distances near the limit of 5 $\hat{A}$. for larger distance the contribution of these terms decreases which means that the many body effects written in the second term X_n have a strong effect on the total interaction energy for these distances (about 50 % of the overall energy). We also recognize that, with increasing distances, there is a difference in the evolution of K_n between the studied configurations. The decrease of the contribution of K_n terms is faster for parallel configuration (**Fig.4.7**) as opposed to the collinear one where this contribution decreases slowly with increasing distances (**Fig.4.8**). This result demonstrates that the effect of many body interactions is far greater in the case of parallel chains of atoms. The amount each contribution W^n is contributing to the system is also studied separately, taking the first three terms W^2 , W^3 and W^4.
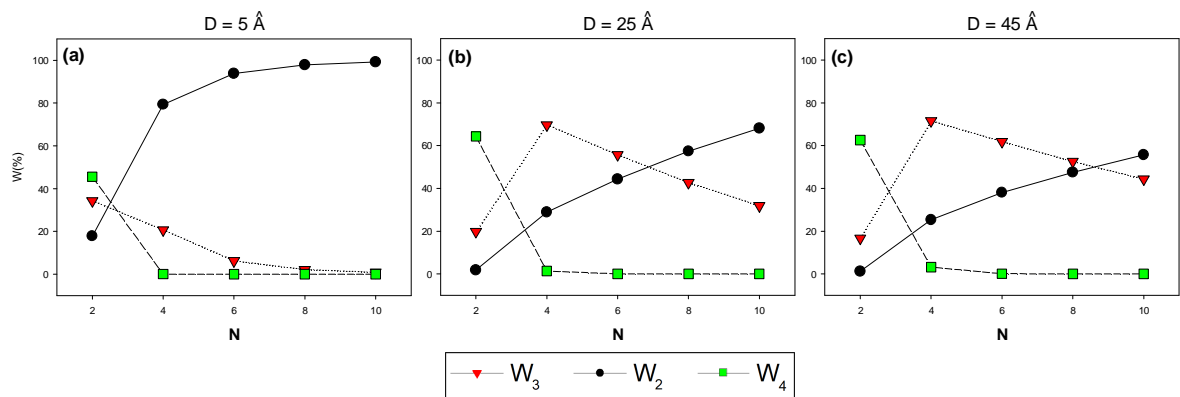
Figure 4.9 : The first three contributions W_2, W_3 and W_4 compared for different distances and different cluster sizes ($N \in [2; 10]$) in the case of collinear configuration.

We notice that for both configurations; parallel (**Fig.4.9**) and collinear (**Fig.4.10**), the first term of the series W^2 is the most dominant for distance less than a nanometer. This result when compared with which was demonstrated from **Fig.(4.7)** and **Fig.(4.8)**, thus we conclude that K_2 which is equivalent to W_2, is the dominant contribution in the second term K. We also notice that for both configurations except for a system of two atoms, the first two contributions W^2 and W^3 are the dominant terms, other terms (W^4 and higher) vanish with increasing number of atoms. Nevertheless, we also notice clearly for parallel configuration that the rate of vanishing of the third term W^2 decreases slightly with increasing distances, this means that the contribution of this term increases for large distances compared to chain size. As the distance increases, we remark slight differences in the behavior of dispersion forces, where the second term W^3 is much more influential on the behavior of the interaction between parallel chains, than it is for collinear ones.
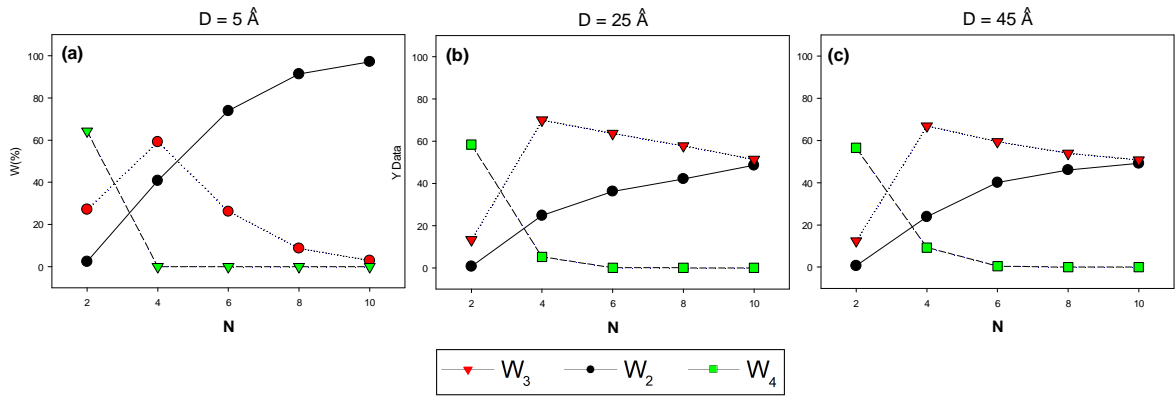
Figure 4.10 : The first three contributions W^2, W^3 and W^4 compared for different distances and different cluster sizes ($N \in [2; 10]$) in the case of a parallel configuration.

The results stated above demonstrates some key findings about the many body effects on dispersion interactions between 1-D nanocluster. These key points are stated as follows:

- Many body interactions have stronger effect for distances larger than clusters dimensions. This result is very interesting since it is not found in literature with this statement, where for most of cases these effects are considered to vanish and only two body interaction are those that survive and effect the interaction between particles. Due to this contrast a more detailed study on the many body effects for long ranges is needed to be conducted at a basic theoretical level using mainly Quantum electrodynamic approaches to either verify or refute the statement claimed here.
- The geometry (configuration in this case) of the interacting clusters has a strong influence on the behavior of many body effects and their contribution to dispersion interactions. Which is found to be stated with various methods in literature [6, 8, 16, 25, 29] although a thorough study on this effect using many body physics is also needed for better understanding of the interactions between nanoparticles.
- For small distances compared to clusters' size, the first two terms are the dominant contributions to the interaction energy.

- Since W^2 and W^3 are equivalent respectively to London's formula for 2-body interactions and the ATM potential for 3-body interactions, we thus conclude that, at close proximities, the dominant many body contributions are the 2-body and 3-body interactions.

This model is very promising although needs more work to be complete, the future prospects of developing this model would be to concentrate on incorporating the retardation effect within this framework and also to include higher multipole interactions. This can be accomplished in our view by examining some of the new features of tensor eigenvalue problem solving theories which are proposed in modern mathematics in the recent years. For this purpose and to develop future works we encourage the exploration of some of the aspects of this side of mathematical methods in order to find a way which we shall investigate to enhance the model. We also propose to follow another line of research in which the CDM method can be coupled with other continuous methods such as the scattering T- Operator theory which is extremely promising [34-37]. This line of research has not been until now investigated which makes it the most interesting prospect of our suggestions**.**

5. **Conclusions:**

In this chapter we have revisited the coupled dipole method, and used the trace-based approach of CDM for solving the problem of dispersion forces between nanoclusters, we further continued with simple algebraic manipulations to derive the explicit formula for the interaction energy between identical nanoclusters. Further, using some concepts of graph theory, we introduced a novel representation of the equations derived. These graphs were used to derive the formula for each m-body contribution in a form of a series which was proven to be equivalent to the results derived from more complicated methods such as perturbation theory in quantum mechanics. We also have studied the interaction between two chains of atoms, with two geometrical configurations parallel and colinear. We have demonstrated that for the studied cases many body interactions have strong effect on dispersion forces at shorter distances, with the dominant contributions are those of 2-body and 3-body interactions. The effect of geometry is also shown to be significant on the behavior of many-body forces and their contribution to dispersion interactions.

References

1.   Salasnich, L.,(2014), *Quantum Physics of Light and Matter: A Modern Introduction to Photons, Atoms and Many-Body Systems*: Springer, Berlin, Germany.
2.   Elrod, M.J. and R.J. Saykally, (1994), *Many-body effects in intermolecular forces.* Chemical Reviews. **94**(7): p. 1975-1997.
3.   Stone, A.,(2013), *The theory of intermolecular forces*: Oxford University Press, Oxford, UK.
4.   Reilly, A.M. and A. Tkatchenko, (2015), *van der Waals dispersion interactions in molecular materials: beyond pairwise additivity.* Chemical science. **6**(6): p. 3289-3301.
5.   Gatica, S.M., M.W. Cole, and D. Velegol, (2005), *Designing van der Waals forces between nanocolloids.* Nano Letters. **5**(1): p. 169-173.

6.   Cole, M.W., et al., (2010), *Many-body van der Waals forces involving chains.* Journal of Nanophotonics. **4**(1): p. 041560.
7.   Donchev, A., (2006), *Many-body effects of dispersion interaction.* The Journal of Chemical Physics. **125**(7): p. 074713.
8.   Jones, A., (2010), *Quantum Drude oscillators for accurate many-body intermolecular forces.*
9.   Shtogun, Y.V. and L.M. Woods, (2010), *Many-body van der Waals interactions between graphitic nanostructures.* The Journal of Physical Chemistry Letters. **1**(9): p. 1356-1362.
10.   Yang, S., et al., (2017), *Many-body dispersion effects on the binding of TCNQ and F4-TCNQ with graphene.* Carbon. **111**: p. 513-518.
11.   Kim, H.-Y., et al., (2006), *van der Waals forces between nanoclusters: Importance of many-body effects.* The Journal of Chemical Physics. **124**(7): p. 074504.
12.   Renne, M. and B. Nijboer, (1967), *Microscopic derivation of macroscopic Van der Waals forces.* Chemical Physics Letters. **1**(8): p. 317-320.
13.   Nijboer, B. and M. Renne, (1968), *Microscopic derivation of macroscopic Van der Waals forces. II.* Chemical Physics Letters. **2**(1): p. 35-38.
14.   Nijboer, B. and M. Renne, (1971), *Van-der-Waals interaction between dielectric media.* Physica Norvegica. **5**(3-4): p. 243-&.
15.   Kim, H.-Y., et al., (2005), *Static polarizabilities of dielectric nanoclusters.* Physical Review A. **72**(5): p. 053201.
16.   Kim, H.-Y., et al., (2007), *Van der Waals dispersion forces between dielectric nanoclusters.* Langmuir. **23**(4): p. 1735-1740.
17.   Phan, A.D., L.M. Woods, and T.-L. Phan, (2013), *Van der Waals interactions between graphitic nanowiggles.* Journal of Applied Physics. **114**(4): p. 044308.
18.   Kim, H.-Y., (2015), *An Efficient Coupled Dipole Method for the Accurate Calculation of van der Waals Interactions at the Nanoscale*, in *Applied Spectroscopy and the Science of Nanomaterials*Springer. p. 85-119.
19.   DiStasio, R.A., O.A. von Lilienfeld, and A. Tkatchenko, (2012), *Collective many-body van der Waals interactions in molecular systems.* Proceedings of the National Academy of Sciences. **109**(37): p. 14791-14795.
20.   Marom, N., et al., (2013), *Many-Body Dispersion Interactions in Molecular Crystal Polymorphism.* Angewandte Chemie International Edition. **52**(26): p. 6629-6632.
21.   Tkatchenko, A., A. Ambrosetti, and R.A. DiStasio, Jr., (2013), *Interatomic methods for the dispersion energy derived from the adiabatic connection fluctuation-dissipation theorem.* Journal of Chemical Physics. **138**(7): p. 074106.
22.   DiStasio Jr, R.A., V.V. Gobre, and A. Tkatchenko, (2014), *Many-body van der Waals interactions in molecules and condensed matter.* Journal of Physics: Condensed Matter. **26**(21): p. 213202.
23.   Hermann, J., R.A. DiStasio Jr, and A. Tkatchenko, (2017), *First-principles models for van der Waals interactions in molecules and materials: concepts, theory, and applications.*
24.   Tkatchenko, A., (2015), *Current understanding of van der Waals effects in realistic materials.* Advanced Functional Materials. **25**(13): p. 2054-2061.
25.   Verdult, M., (2010), *A microscopic approach to van-der-Waals interactions between nanoclusters: The coupled dipole method*, MS thesis, Utrecht University, 2010. Google Scholar.

26. Yang, W.H., G.C. Schatz, and R.P. Van Duyne, (1995), *Discrete dipole approximation for calculating extinction and Raman intensities for small particles with arbitrary shapes.* The Journal of Chemical Physics. **103**(3): p. 869-875.

27. Misra, P.,(2014), *Applied Spectroscopy and the Science of nanomaterials*. Vol. 2. Springer, Berlin, Germany.

28. Salam, A.,(2010), *Molecular quantum electrodynamics: long-range intermolecular interactions*: John Wiley & Sons.

29. Cole, M.W., et al., (2009), *Nanoscale van der Waals interactions.* Molecular Simulation. **35**(10-11): p. 849-866.

30. West, D.B.,(2001), *Introduction to graph theory*. Vol. 2. Prentice hall/Upper Saddle River, New Jersey, USA.

31. London, F., (1937), *The general theory of molecular forces.* Transactions of the Faraday Society. **33**: p. 8b-26.

32. Milonni, P.W.,(2013), *The quantum vacuum: an introduction to quantum electrodynamics*: Academic press, Cambridge, Massachusetts.

33. Jones, A.P., et al., (2013), *Quantum Drude oscillator model of atoms and molecules: Many-body polarization and dispersion interactions for atomistic simulation.* Physical Review B. **87**(14): p. 144103.

34. Kenneth, O. and I. Klich, (2008), *Casimir forces in a T-operator approach.* Physical Review B. **78**(1): p. 014103.

35. Rahi, S.J., et al., (2009), *Scattering theory approach to electrodynamic Casimir forces.* Physical Review D. **80**(8).

36. Ingold, G.-L. and A. Lambrecht, (2015), *Casimir effect from a scattering approach.* American Journal of Physics. **83**(2): p. 156-162.

37. Venkataram, P.S., et al., (2017), *Unifying Microscopic and Continuum Treatments of van der Waals and Casimir Interactions.* Physical Review Letters. **118**(26): p. 266802.

Conclusions

We have examined in this work dispersion forces between nanoparticles and demonstrated the basic concepts of the theoretical modelling process of these Quantum interactions between both microscopic particles (molecules/atoms) and macroscopic objects, focusing on nanosized particles. At first, we have used models developed using the pairwise summation approach of Hamaker to study the effect of geometry using three basic geometries (cubic, cylindrical and spherical) and demonstrated that the effect of geometry is crucial at small distances, generally less than 20 % of particles' size.

Regarding the retardation effect, similarly, we have used this method both by comparing the existing models or by numerical atomic calculations, and we established that, for nanoparticles, this effect is crucially dependent on particle size and shape as well as the distance, and propose a correction to an existing model in order to be applied for the case of such particles this modified model can be used to incorporate dispersion interactions in studying the behaviour of nanoparticles in order to predict the formation of agglomeration, which is a critical factor in assessing the toxicology of these particles to the human body or the behaviour of nanoparticulate materials such as powders aerosols and colloids. Nevertheless, we urge the need for developing a new model based on a more complete theory which can predict and calculate accurately and efficiently the magnitude and behaviour of these interactions at the nanoscale.

For the purpose of developed a model of nanosized particles, in the last segment of this work we have studied and formulate the Coupled Dipole Method in its simplest forms, and used and demonstrated the Trace-based approach of the CDM to the problem. We further continued our calculations in the same mathematical spirit of the TCDM by applying some algebraic manipulations, and thus we derived the solution to the CDM problem, and demonstrated the explicit formula of the interaction energy between identical nanoclusters.

Further, we used the concepts of graph theory coupled with the derived model and introduced a novel representation of those equations, where these graphs generate all possible modes using simple logical rules, and each of them can be retranslated into a mathematical formula of the corresponding interaction energy of those modes. Therefore, these each m-body contribution we derived from all graphs of m degree, and the interaction energy was written thus in a form of a series which was confirmed to be equivalent to the results derived from perturbation theory. We thus emphasize the need to further pursue and develop this graphical representation and its mathematical theory, since it can offer a new aspect of many body physics that can lead for many applications and simplifications of the existing theories and models.

Additionally, using our model, we have studied these interactions between two (parallel and colinear) chains of atoms, and demonstrated that many body interactions have critical effect on dispersion forces at shorter distances, with the dominant contributions are the 2-body and 3-body interactions. The effect of geometry is also shown to be noteworthy on the magnitude of contribution of many-body forces to the total interaction.

The Coupled Dipole method is very promising approach as demonstrated in this work and others, nevertheless there are more work that has to be done in order for this model to be complete. For this purpose, we propose that the future work on the subject should concentrate on incorporating the retardation effect within this framework and also to include higher multipole interactions and solve the problem using the new tensor eigenvalue problem solving techniques or others, depending on the problem at hand when incorporating these contributions. We also propose the coupling of this method with other methods such as the scattering T- matrix approach which is extremely promising, or even many-body Quantum electrodynamics.

It should be recognized that this work and the efforts of modeling the interactions between nanoparticles and nanoclusters which has been undertaken by us or other researchers, are very important to better predict the magnitude of dispersion forces acting between these materials, which in turn would lead to a better understanding of the behavior and ultimately the control of that behavior of nanoparticles used for technological applications such as those stated in Chapter 1.

In the end, we reemphasize the importance of this work both as a slightly different representation and study of the problem of dispersion interactions between nanoparticles, and also as an initiation of the author to the subject with many potentials of future works, which opens the door for a life work in both theoretical and applied side of physics.

Appendices

Appendix I: Flow chart for calculating the retardation using the atomistic method.

```
   ┌─────────┐       ╱─────────────────╱      ┌──┬────────────────┬──┐
   │  Start  │─────▶ ╱ Define variables╱ ────▶│  │ Generate cluster│  │
   └─────────┘      ╱─────────────────╱       │  │    geometry     │  │
                                               └──┴────────────────┴──┘
                                                         │
                                                         ▼
   ┌──┬──────────────────┬──┐                   ┌──────────────────────────┐
   │  │ Label particles i, j│  │──────────────▶ │ i=0 ; j=0 ; E=0 ; E^Rt=0 │
   └──┴──────────────────┴──┘                   └──────────────────────────┘
                                                         │
                                                         ▼
         ╱◇╲                                        ┌────────┐
        ◇ For i≤N ◇ ◀──────────────────────────────│ i=i+1  │◀─────────┐
         ╲◇╱                                        └────────┘          │
          │                                                             │
          ▼                                                             │
   ┌──────────┐              ╱◇╲                                        │
   │ T=E^Rt/E │             ◇ For j≤N ◇ ◀─────────────────────┐         │
   └──────────┘              ╲◇╱                               │         │
          │                   │                          ┌────────┐     │
          ▼                   ▼                          │ j=j+1  │     │
   ╱──────────╱      ┌──┬──────────────┬──┐              └────────┘     │
  ╱  Print    ╱      │  │  Calculate    │  │                  ▲          │
 ╱  (T,f)    ╱       │  │ distance r(i,j)│  │                 │          │
 ╱──────────╱        └──┴──────────────┴──┘                  │          │
          │                   │                              │          │
          │          ┌────────┴────────┐                     │          │
          │          ▼                 ▼                      │          │
          │  ┌──────────────┐  ┌──────────────┐              │          │
          │  │ Calculate     │  │ Calculate     │             │          │
          │  │ (E (r(i,j)))  │  │ E^Rt (r(i,j)) │             │          │
          │  └──────────────┘  └──────────────┘              │          │
          │          │                 │                      │          │
          │          ▼                 ▼                      │          │
          │  ┌──────────────┐  ┌──────────────────────┐      │          │
          │  │ E= E+ E(r(i,j))│ │ E^Rt= E^Rt+ E^Rt(r(i,j))│  │          │
          │  └──────────────┘  └──────────────────────┘      │          │
          │          │                 │                      │          │
          ▼          └─────────────────┴──────────────────────┘          │
   ┌─────────┐                                                           │
   │   End   │                                                           │
   └─────────┘                                                           │
```
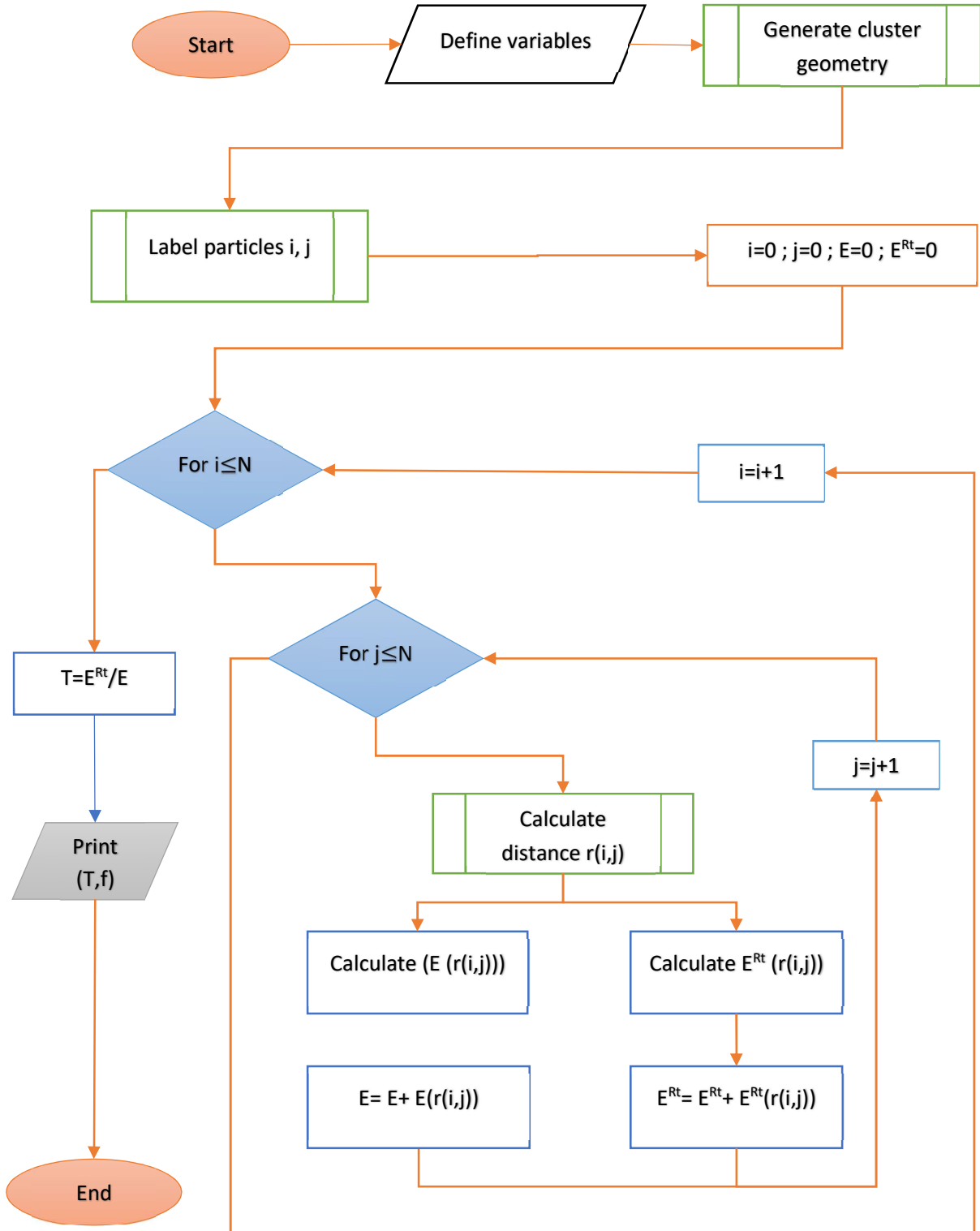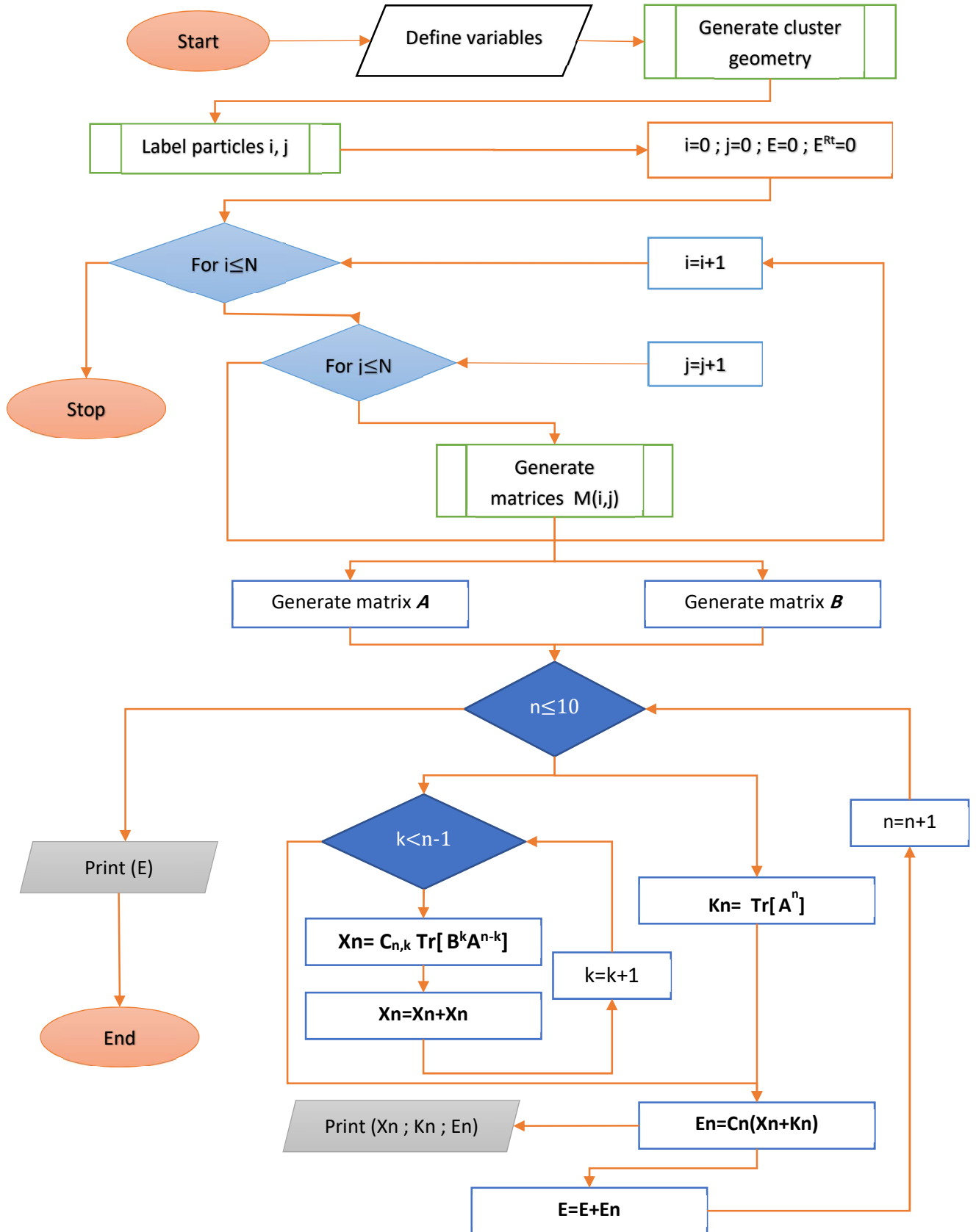
Appendix II : flow chart of the model derived from the CDM approach.

Résumé :

Dans ce travail, les interactions de dispersion entre les nanoparticules et les effets de différents paramètres (taille, géométrie, distance, retardation et l'effets à N-corps) ont été étudiés. L'effet de la géométrie des particules est étudié en comparant trois formes de base: cubique, cylindrique et sphérique. Les résultats montrent que l'effet de la géométrie est significante pour des distances inter-particulaires inférieures à 20% du rayon des particules. L'énergie d'interaction retardée de van der Waals est également étudiée et il a été montré que cet effet dépend fortement de la taille et de la forme des particules, ainsi que de la distance. Un modèle modifié est proposé pour les nanoparticules extrêmement petites (R ~ 10 nm). Nous avons utilisé la méthode des dipôles couplés puis, à partir du formalisme de Trace de ce modèle, nous avons introduit une nouvelle formule algébrique de l'énergie d'interaction entre des nano-clusters identiques. En outre, une nouvelle représentation utilisant la théorie des graphes est également utilisée pour représenter chaque mode d'interaction dérivé du nouveau formalisme. Ces graphiques ont été utilisés pour calculer la formule de l'énergie d'interaction m-corps sous la forme d'une série qui s'est avérée équivalente aux résultats développés à partir de méthodes plus complexes telles que la théorie des perturbations en mécanique quantique. Nous avons également étudié l'interaction entre deux chaînes d'atomes, avec deux configurations géométriques parallèle et colinéaire. Lorsque nous comparons notre résultat à celui qui a été calculé à partir de la méthode de sommation par paire, nous constatons que de nombreuses interactons corporelles ont un effet significatif sur l'interaction globale.

Mots clés: Interactions de dispersion; forces van der Waals; forces à plusieurs corps; Méthode dipolaire couplée; Nanoparticules

ملخص:

في العمل الحالي ، تم التحقيق في تفاعلات التشتت بين الجسيمات النانوية والتأثيرات المختلفة للمعايير (الحجم ، الهندسة ، المسافة بين الجسيمات ، التخلف و تأثير الأجسام المتعددة). يتم دراسة تأثير هندسة الجسيمات عن طريق مقارنة ثلاثة أشكال أساسية: مكعب ، أسطواني وكروي. تظهر النتائج أن تأثير الهندسة مهم في□الة المسافات بين الجسيمات أقل من 20٪ من نصف قطر الجسيمات. كما تم التحقق من طاقة تفاعل فان فالز المتخلفة، وتبين أن هذا التأثير يعتمد بشكل كبير على □جم وشكل الجسيمات وكذلك المسافة. تم اقتراح نموذج معدل للجسيمات النانوية الصغيرة نانومتر(10 ~ R) .استخدمنا الأسلوب ثنائي القطب المزدوج ثم من الصيغة التصحيحية لهذا النموذج، نقدم صيغة جبرية جديدة للطاقة التفاعل بين العناقيد النانوية المتطابقة. علاوة على ذلك، يستخدم التمثيل الجديد بتطبيق نظرية الرسم البياني لتمثيل كل طريقة تفاعل مشتقة من الصيغة الجديدة. تم استخدام هذه الرسوم البيانية لاشتقاق صيغة طاقة تفاعل الجسم في شكل سلسلة أثبتت أنها مكافئة للنتائج التي تم تطويرها من طرق أكثر تعقيدًا مثل نظرية الاضطراب في ميكانيكا الكم. لقد درسنا أيضًا التفاعل بين سلسلتين من الذرات ، مع تكوينين هندسيين متوازيين وخطين. عند مقارنة نتائجنا بما تم□سابه من طريقة الجمع الزوجي ، نجد أن العديد من تفاعلات الأجسام المتعددة لها تأثير كبير على التفاعل الكلي.

كلمات مفتاحية : قوات فان دير فالس ؛ تأثير الأجسام المتعددة ؛ طريقة ثنائي القطب مقترن ؛ النانوية.